ARCTIC RESPONSE TECHNOLOGY
OIL SPILL PREPAREDNESS

15 October 2013

Thomas Puestow , *(C-CORE)*
Lance Parsons, *(C-CORE)*
Igor Zakharov, *(C-CORE)*
Neil Cater, *(C-CORE)*
Pradeep Bobby, *(C-CORE)*
Mark Fuglem, *(C-CORE)*
Grant Parr, *(C-CORE)*
Awantha Jayasiri, *(C-CORE)*
Sherry Warren, *(C-CORE)*
Greg Warbanski, *(Emergency Spill and Consulting Inc.)*

OIL SPILL DETECTION AND MAPPING IN LOW VISIBILITY AND ICE: SURFACE REMOTE SENSING

FINAL REPORT 5.1

Report from Joint Industry Programme to define the state-of-the-art for surface remote sensing technologies to monitor oil under varying conditions of ice and visibility.

ABOUT THE JIP

Over the past four decades, the oil and gas industry has made significant advances in being able to detect, contain and clean up spills in Arctic environments. To further build on existing research, increase understanding of potential impacts of oil on the Arctic marine environment, and improve the technologies and methodologies for oil spill response, in January 2012, the international oil and gas industry launched a collaborative four-year effort – the **Arctic Oil Spill Response Technology Joint Industry Programme (JIP)**.

Over the course of the programme, the JIP will carry out a series of advanced research projects on six key areas: dispersants, environmental effects, trajectory modeling, remote sensing, mechanical recovery and in situ burning. Expert technical working groups for each project are populated by the top researchers from each of the member companies.

JIP MEMBERS

The JIP is managed under the auspices of the International Association of Oil and Gas Producers (OGP) and is supported by nine international oil and gas companies – BP, Chevron, ConocoPhillips, Eni, ExxonMobil, North Caspian Operating Company (NCOC), Shell, Statoil, and Total – making it the largest pan-industry programme dedicated to this area of research and development.

LIST OF ACRONYMS

ACR	Area Coverage Rate
AHS	Airborne Hyperspectral Scanner
AIS	Automatic Identification System
ATMARIL-3	ATMospheric and MARine LIDAR
AUV	Autonomous Underwater Vehicle
BAOAC	Bonn Agreement Oil Appearance Code
CIS	Canadian Ice Service
DMC	Disaster Monitoring Constellation
DMI	Danish Meteorological Institute
ECS	Electronic Chart System
EM	Electromagnetic
EMSA	European Maritime Safety Agency
ERMA	Environmental Response Management Application
FLIR	Forward-Looking Infrared
FMCW	Frequency Modulated Continuous Wave
GIS	Geographic Information System
GPR	Ground Penetrating Radar
GUI	Graphical User Interface
HF	High Frequency
INTA	Instituto Nacional de Técnica Aerospacial
IR	InfraRed
ISTOP	Integrated Surveillance and Tracking Of Pollution
JIP	Joint Industry Program
LDI	Laser Diagnostic Instruments
LED	Light-Emitting Diode
LFS	Laser Fluorosensor
LIDAR	LIght Detection and Ranging
LOS	Line-of-Sight
LURSOT	Laser-Ultrasonic Remote Sensing of Oil Thickness
MF	Medium Frequency
MMS	U.S. Department of the Interior, Minerals Management Service
MSS	Maritime Satellite Surveillance
MWIR	Mid-Wavelength InfraRed
MWRs	Microwave Radiometers
NIR	Near-InfraRed
NMR	Nuclear Magnetic Resonance
NOAA	National Oceanic and Atmospheric Administration
NOFO	Norwegian Clean Seas Association for Operating Companies
NRT	Near Real-Time
OI	Ocean Imaging
OSSAS	Oil Spill Scene Analysis System
ppb	parts-per-billion
RCM	RADARSAT Constellation Mission
RMS	Root Mean Square
ROV	Remotely Operated Vehicle
SAR	Synthetic Aperture Radar
SLAR	Side-Looking Airborne Radar
SNR	Signal-to-Noise Ratio
SWIR	Short Wave InfraRed
TDLS	Tunable Diode Laser Spectroscopy
TIR	Thermal InfraRed
UAV	Unmanned Aerial Vehicle
UV	UltraViolet
VHF	Very High Frequency
VIS	Visible
VNIR	Visible and Near InfraRed
VV	Vertical transmit and Vertical receive

EXECUTIVE SUMMARY

This study was conducted under the Remote Sensing Technical Working Group of the recently formed Arctic Oil Spill Response Technology Joint Industry Program. The primary objective is to define the state-of-the-art for surface remote sensing technologies to monitor oil under varying conditions of ice and visibility. A review of current and emerging technologies with a documented ability to detect oil on water was conducted, their potential for application in ice-affected waters assessed and near term recommendations for Research and Development (R&D) priorities assigned. Performance parameters in ice and low visibility were defined to evaluate technologies. Many imaging systems are available that can be used from helicopters, fixed-wing aircraft, vessels and drilling platforms.

Recent studies demonstrate the utility of hyperspectral imagery, although at present the interpretation of hyperspectral datasets requires specialized expertise. Automating the information extraction process used will make it easier to integrate hyperspectral sensor output into operations. Optical (visible, multispectral (MS) and ultraviolet (UV)) and thermal infrared (TIR) sensors are routinely used in oil spill monitoring, and visual interpretation from still and video cameras remain an important element of operational surveillance. Oil can be confused with other phenomena, especially if the interpretation is not made by trained operators. A significant body of knowledge exists to describe the use of visual instruments to map and characterize oil on water, but there is little validated information available to describe their use in ice conditions. A weakness of optical systems is their reliance on good visibility, which is limited in Arctic conditions, while TIR is less restricted.

Airborne Laser Fluorosensors (LFS) have the unique ability to detect oil with a high degree of certainty, classify oil type and determine the thickness of thin slicks. Despite this, LFS systems are not widely used for oil spill monitoring. LFS instruments require dedicated aircraft and due to power limitations of the laser their use is restricted to relatively low altitudes and correspondingly narrows spatial coverage. In the context of spill response, LFS sensors may be useful. Non-UV LIDAR sensors have also shown promise for detecting oil, with generally lower costs and increased availability compared with LFS systems.

Ongoing research supports Ground Penetration Radar (GPR) and Nuclear Magnetic Resonance (NMR) technologies for detecting oil in ice and snow. Present GPR work is focused on developing airborne-based systems for detecting oil covered by snow or under ice, but more work is required for unambiguous detection of oil under varying ice conditions and validation of the technology for operational use. NMR advances to detect oil in ice from helicopters is focused on improving several factors: reducing weight of the loop antenna to make it more convenient for aerial deployment; reducing signal collection time; and increasing the signal-to-noise ratio to reduce false alarms. Arctic field testing and validation with a full-scale prototype are expected within the next two years.

Although radar sensors are being used to detect and monitor oil spills on water, their utility for detecting oil under ice has not been extensively studied. However, satellite, airborne and field-based radar are extremely useful in characterizing and mapping the general ice environment, tracking the movement of ice and guiding deployment of surveillance equipment. In addition, they do not rely on solar illumination to operate, and in the case of satellite-based imagery, dependence on weather conditions is minimal. Radar sensors should be considered a component of any suite of sensing technologies deployed for spill response in ice-affected waters.

This review of remote sensing technologies for oil in ice detection recommends near term priorities for research and development. Potential technologies were analyzed to address their utility in various ice scenarios and in conditions of low visibility. In addition to ongoing research on GPR and NMR, recommended actions include validating technologies, such as hyperspectral (including infrared (IR) spectral range), laser based systems, and microwave radiometers for oil in ice detection that are currently in use to detect oil in open water conditions. It is recommended to conduct research in two steps:

i. *Specialized facilities or field testing are necessary to understand the underlying physical mechanisms for oil detection in different ice regimes as well as other conditions encountered in Arctic. The results will be used as a baseline for analysis of off-the-shelf sensors (e.g., UV, visible, infrared) to determine operational performance.*
ii. *Testing and estimating the capabilities of suitable sensors in different scenarios in the field, including oil in varying concentrations of pack ice as well as on fast ice or large ice floes, oil on ice and snow, oil between ice floes, and other scenarios. The performance of optical (UV, visible, and hyperspectral) and IR sensors, laser based systems (LFS and LIDAR) and microwave radiometers for detecting oil in slush, brash ice and encapsulated in ice is unknown.*

Recommendations include programmes for embedding trained oil observers in ongoing operations, developing and implementing integrated multi-sensor systems with automated data analysis and working towards standardized products and processes for remote sensing of oil in ice environments.

TABLE OF CONTENTS

LIST OF TABLES

LIST OF FIGURES

CHAPTER 1. INTRODUCTION

In 2012, a Joint Industry Program (JIP) was established to build on past research for spill response in ice-affected waters and advance knowledge and capabilities in several areas including dispersants, environmental effects, trajectory modeling, remote sensing, mechanical recovery and in situ burning. The work reported herein was conducted under the JIP Remote Sensing Working Group. This report provides a review and evaluation of surface remote sensing technologies for detecting and monitoring oil in the presence of ice and under conditions of low visibility.

The current understanding of oil behavior and fate in ice-affected environments stems from research conducted by various groups within Canada, the US and Norway over the last 40 years. A number of intensive studies were done throughout the 70s and early 80s during the initial surge of interest in oil and gas exploration of the North. Work consisted of field tests, laboratory experiments, analytical calculations and observations of relatively small Arctic spills which, in many cases, had emanated from ruptured storage tanks. One of the largest field experiments during this period was completed by NORCOR in 1974-75 (NORCOR, 1975). This test involved the release of various crude oils under sea-ice in the Beaufort Sea. Another set of large-scale field experiments was conducted to simulate an oil and gas blowout under landfast ice in McKinley Bay, Northwest Territories, Canada (Dickins and Buist, 1981). Additionally, field experiments were undertaken to study the behavior of oil in broken ice. These were conducted off the coast of Eastern Canada (Ross and Dickins, 1987) and Norway (Vefsnmo and Johannessen, 1994).

Renewed interest in Arctic oil and gas over the past decade has brought renewed interest in Arctic oil spill clean-up and monitoring. Furthermore, large-scale spills, including the Godafoss ship spill in Norway and the Runner 4 ship spill in the Gulf of Finland highlight gaps in knowledge and practices.

Most recently, a substantial four-year (2006 to 2009) research program was led by SINTEF to study the behavior of oil in an Arctic setting and assess the effectiveness of various spill countermeasures including mechanical recovery, in situ burning, chemical dispersion and remote sensing, not including oil spills under ice (Sorstrom et. al., 2010). The project “Remote Sensing Technology Review and Screening” of Oil-in-Ice JIP (Dickins and Andersen, 2009) evaluated off-the-shelf technologies and sensors to detect oil in the presence of ice. The report analyzed airborne systems with multiple sensors, satellite systems, dogs for surface oil detection, methane sensors, ground penetrating radar (GPR) and shipborne sensors. The project (Dickins and Andersen, 2010) evaluating airborne systems represents a detailed overview of the current state of knowledge. It focuses on demonstrated and expected potential of different airborne sensors to detect oil and map the contaminated boundaries through analyzing various oil and ice scenarios and investigating the likely behavior of slicks in different ice concentrations.

The program consisted of a series of laboratory experiments and field tests together with two large-scale field tests in the Barents Sea near the Norwegian coast. It was found that sea ice had a significant effect on the spill, with the oil forming relatively thick layers between ice floes and in undulations under solid ice sheets.

1.1 Oil in the Arctic Marine Environment

Ice-affected regions with significant oil and gas deposits that may be of interest to the JIP partners include Northern regions such as the Canadian Archipelago, offshore Labrador and the

Grand Banks, Beaufort Sea, Greenland Sea, Baffin Bay and others. Additionally, areas along potential or existing pipeline and shuttle tanker routes in Arctic regions are considered to be of interest.

In the event of an oil spill in ice-affected waters, the effectiveness of clean-up counter measures, including detection, will be subject to the ice and environmental conditions. In particular, ice conditions vary considerably from region to region, so necessary oil treatment and removal operations may also vary. Furthermore, the behaviour and fate of the oil will be dictated by ice and environmental conditions. The role of a surface remote sensing technology may be considered within two broad categories: (a) direct detection and monitoring of spills and (b) monitoring the surrounding environmental and ice conditions.

1.1.1 Oil Spill in Open Water

For a spill on open water, as would be the case for an Arctic marine spill during late summer, the oil spreads into a relatively thin slick on the surface. The thickness of the slick depends on the type of oil, with heavy oils forming thicker slicks (on the order of a few millimeters). The movement and thinning of the slick are affected by sea state with the oil being moved along the surface by the surface currents and wind (Fingas, 2011).

If oil emanates from a subsurface leak or blowout, it migrates up through the water column. The movement of oil through the water can be quite complex, depending on physical properties including oil and water densities, water depth, ocean currents, and the molecular composition of the oil (Yapa and Zheng, 1997). In the case of a pipeline rupture or a blowout, the oil is introduced into the ambient water as a jet. It may be accompanied by natural gas which will also affect the nature of the spill. As the jet propagates up through the water column, it entrains the denser seawater which increases the density of the jet/plume.

Depending on the stratification and depth of the water the plume may become neutrally buoyant before reaching the surface. Under these circumstances the oil will form small, millimeter-sized droplets and eventually float to the surface (Yapa et al, 1999). In this instance, however, it is possible that oil may become entrapped between the stratified water layers, remaining suspended in the water column (Adalsteinsson et al., 2011). For typical ocean conditions most of the oil makes it to the surface. Once on the surface, oil spreads horizontally forming a thin slick. Under the influence of ocean currents, the slick will experience a lateral displacement from the initial release point.

Weathering processes such as evaporation, water-in-oil emulsification and natural dispersion in the water column are subject to environmental conditions, such as temperature and sea state, as well as the physical properties of the released oil. For an Arctic spill on open water in late summer, which is influenced by tidal mixing and relatively high temperatures, weathering rates can be significant (Payne et al., 1991, Fingas, 2011). Weathering of an open water spill can greatly reduce the effectiveness of spill clean-up countermeasures, making it crucial that countermeasures be deployed quickly before the oil emulsifies.

1.1.2 Oil Spill on and under a Solid Ice Sheet

The fate and behavior of an oil spill in ice-affected water can differ significantly from a spill in open water. Snow and ice tend to reduce the spreading and weathering. Figure 1 illustrates possible scenarios for the presence of oil in ice and snow.

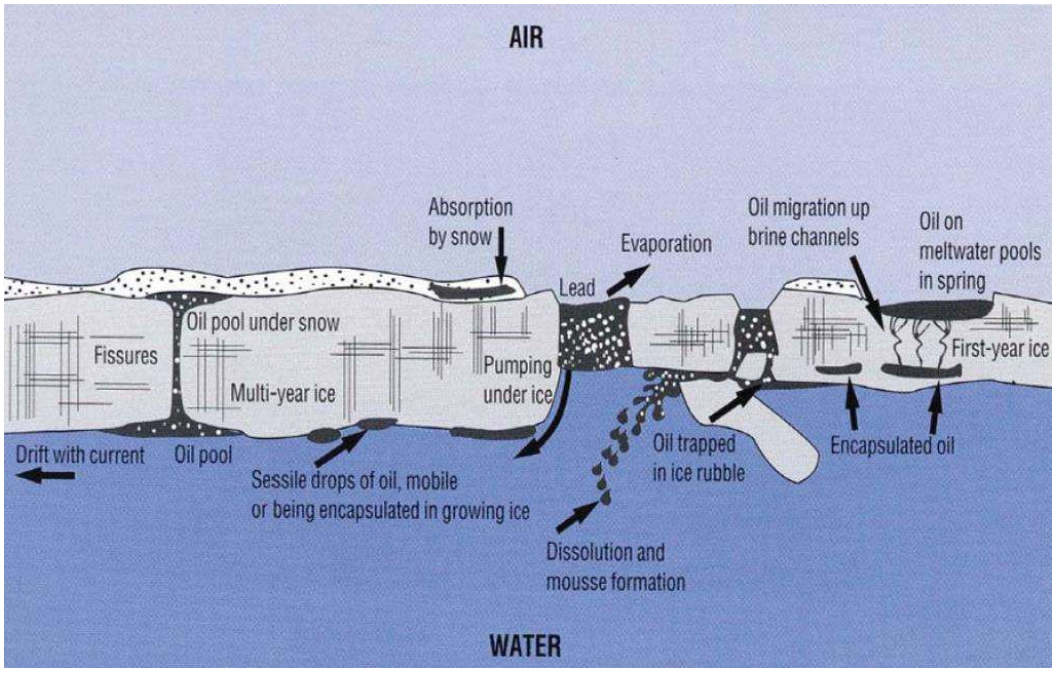

Figure 1. Oil behavior in ice-affected water (from Bobra and Fingas (1986) adopted Allen, 2008)

Under lower temperatures, oils become highly viscous and do not spread as easily resulting in thicker oil being present. Snow and ice impede oil movement and the oil may become encapsulated as ice cover grows (Bobra and Fingas, 1986). For oil spills on or under ice, the movement of the spill is largely dictated by the roughness of the ice interface, with oil pooling in undulations. Furthermore, oil weathering rates are slower due to lower evaporation losses and, for oil spilled under sea ice, a decrease in the rate of emulsification stemming from reduced wave-action compared to open-water conditions. Overall, the way oil spreads and weathers is subject to the ice and snow conditions, thus, is influenced by the time of year and the geographic region. In the case of oil trapped under ice, it can be tracked using the buoys deployed on the ice floes (Goodman, 1978).

Like spills on land, the fate of oil on ice is largely dependent on the nature of the surface with large amounts of oil being retained in depressions and irregularities in the ice (Fingas, 2011). The resulting oil layer is typically approximately 2 cm thick, but can be over 30 cm thick in areas where the oil is contained by ice deformation features such as rafting and pressure ridges (Dickins and Buist, 1999; Fingas and Hollebone, 2003). Additionally, if ice is covered by snow, oil may spread along the ice-snow interface. For dry snow, approximately 25% of the oil may be absorbed into the snow cover. Under high wind conditions the oil-snow mixture may be distributed over large distances.

For a subsurface leak under ice, the nature and fate of the oil depends on ice conditions at the surface. In the case of solid ice coverage, the oil forms a relatively thick layer (on the order of a few centimeters) which pools in undulations on the underside of the ice. The oil movement is impeded by the interface roughness and, therefore, may remain relatively localized. Studies have found that a current with an approximate speed of 0.5 m/s is required to force the oil out of undulations (Dickins and Buist, 1999; Fingas and Hollebone, 2003). Additionally, if the oil is accompanied by an abundance of natural gas, the buoyant force resulting from gas build-up may crack the ice cover allowing oil to flow onto the ice surface (Fingas and Hollebone, 2003).

If the leak occurs during winter freeze-up, pooled oil becomes encapsulated in the growing ice sheet. Studies have shown that the time for encapsulation is on the order of two days (Buist et al., 1983), occurring more quickly under first-year ice than under multi-year ice. Oil remains trapped until spring when the ice warms and brine channels open, at which time oil migrates to the surface (Potter et al., 2012). Once at the surface, the oil floats on the melt pools and, due to the low rate of weathering, the exposed oil is relatively "fresh".

For spills on and under solid ice cover, the ultimate fate of the oil is dictated by ice behavior. If the ice breaks up, the oil will be carried along with the floes (Deslauriers et al., 1977). The oil may then be distributed into the water through tidal action on the broken ice.

1.1.3 Oil Spill with Moving Pack Ice

Not surprisingly, the behavior and fate of oil in pack ice is heavily influenced by the concentration of ice cover. The presence of close-pack ice (i.e., an ice-to-surface ratio greater than 6/10) reduces the spread of oil and the spill will be thicker. This contained oil moves with the ice floes. As ice concentration decreases the oil behavior changes, approaching that of an open-water spill for ice concentrations less than 3/10. Oil spreads more freely as ice concentration decreases (Dickins and Buist, 1999).

The spreading of oil between broken ice is influenced by the presence of slush and brash ice. While light hydrocarbon components surface to the water-air interface, heavier components will incorporate into the slush and brash ice (Dickins, 2011). In turn, lighter hydrocarbons are more readily evaporated than the heavier components, which are suspended in the slush.

There have been a number of experiments conducted to determine the behavior of oil in ice leads. As suggested by MacNeill and Goodman (1987), lead closures redistribute the oil. In particular, at low closure rates, oil is pushed under the ice surface while at high closure rates (i.e., above 12 cm/s) oil is pushed up onto the ice surface. Further field analysis found that the lead closure rates under normal conditions were insufficient to push oil onto the ice. In fact, this mechanism of "lead pumping" may only be encountered in the case of ice closing behind ships (Fingas and Hollebone, 2003). Consequently, this may be important for oil spills from ice-bound vessels.

1.2 Low Visibility

Visibility in the Arctic can be reduced by several factors:

- clouds and fog;
- precipitation;
- blowing snow; and
- darkness and Polar Night.

These factors primarily affect passive optical sensors. Low visibility can be defined as the combination of above mentioned factors, which limits the range of operation for certain sensors.

1.2.1 Clouds

In general, much of the Arctic sky is covered by low (up to 2 km high) stratus and stratocumulus clouds (NSIDC, 2012). Total cloud cover combines low, middle (2-8 km), and high clouds (8-15 km). Low cloud cover is more common and uniform and increases over the Arctic Ocean. The increase reflects the dominance of low-level stratus, which forms as warm air masses moving over the ocean are chilled by the cold, melting sea ice. Total cloud cover extent is lowest in December and January (65-80%). Starting in May, cloudiness is within 73-78% with average 75% (Wang et al., 2012). Autumn months exhibit cloud cover in the range from 72-84%. For

certain Arctic regions these numbers are even higher; a 10 year record from National Oceanic and Atmospheric Administration (NOAA) Barrow Observatory in Alaska, for example, showed annual average of 76% cloud coverage with 80-90% from May to October (Dong et. al., 2010).

Low level stratus clouds form and persist through the spring and summer due to the presence of warm air over the water adjacent to ice, frequent temperature inversions, and fog. Evaporation fog, called Arctic sea smoke, is produced when air above open water within Arctic ice is stable and relatively cold. Arctic haze in Arctic regions reduces horizontal and slant visibility and which may extend to a height of about 10 km.

1.2.2 Precipitation and wind

Precipitation, such as rain, snow, hail, dew and hoar frost, is an important component of the hydrological cycle. Precipitation is low over much of the Arctic (NSIDC, 2013). Some areas are referred to as polar deserts and receive as little precipitation as the Sahara desert. However, the Atlantic sector of the Arctic between Greenland and Scandinavia receive higher precipitation due to winter storms originating in the Atlantic Ocean.

Almost all precipitation in the central Arctic and over land falls as snow in winter. More than half of the precipitation events at the North Pole are snowfall. Over the Atlantic sector, snow is very rare in summer. However, rain can occur on rare occasions during winter in the central Arctic Ocean when warm air is transported into this region.

Wind speeds over the Arctic Basin and the western Canadian Archipelago average 14 and 22 kilometers per hour, respectively, in all seasons. Stronger winds are present in these areas during storms with wind speeds up to 90 km/h. During all seasons, the strongest average winds are found in the North-Atlantic seas, Baffin Bay, Bering Sea and Chukchi Seas, where cyclone activity is most common. On the Atlantic side, the winds are strongest in winter, averaging 25 to 43 km/h, and weakest in summer, averaging 18 to 25 km/h. On the Pacific side they average 22 to 32 km/h year round. Maximum wind speeds in the Atlantic region can approach 180 km/h in winter (Przybylak 2003).

Blowing snow accompanied by high wind (above 30 km/h) reduces visibility to 800 m or less and to less than 400 m for wind speeds of 40 km/h (Environment Canada, 2013). Sensors operating in ultraviolet (UV), visible, and near-infrared (NIR) bands have decreased effectiveness in blowing snow.

1.2.3 Polar night

By definition, Polar night means that it is absolutely dark and occurs between November to January when the sun is below the horizon. On a clear day, however, the sky is often illuminated by flares of northern lights. During Polar night active remote sensing systems which illuminate the observed scene are preferred.

1.3 Remote Sensing Platforms

Several platforms can be used to deploy sensors for detecting and monitoring oil. Those considered in this report are situated on or above the surface. Table 1 summarizes type of platform, distance from the surface, typical sensor spatial coverage and resolution. The distance from the surface is an important consideration since it indicates whether information must be collected in situ or not. For example, airborne platforms can provide coverage up to 1000 km2 with a resolution on the order of meters or better depending on the system and its distance from the surface. These platforms are capable of carrying a range of relevant sensors and decisions must be made regarding trade-offs between resolution, coverage and reliability of detection.

Table 1. Remote sensing platforms

Platform	Distance from the Surface	Sensor Spatial Coverage	Sensor Spatial Resolution
Satellite	Several hundred kilometers	~100-10000 km2	From 0.5 to >250 m
Airborne (helicopter, airplane, Unmanned Airborne Vehicle, aerostat)	From tens meters to kilometers	up to 1000 km2	From centimeters to meters
In the field (e.g., ship, rigs)	Centimeters to meters	Up to km 10s km2	From centimeters to meters
Contacted, on the surface (water, oil or ice).	N/A	Point measurement	From millimeters to meters

A number of remote sensing platforms have proven effective for detection and monitoring oil spills on open water. For example, a new compact aerostat system “Ocean Eye” can carry a high resolution camera and IR sensor to monitor spills from altitudes up to 150 m (Jensen et al., 2012). Both airborne and space-borne sensors, including Synthetic Aperture Radar (SAR), Side-Looking Airborne Radar (SLAR), infrared- and visible-range imaging, microwave radiometers, and laser fluorosensors, can be used (Fingas and Brown, 1997; Jha et al., 2008). The various sensors use different physical attributes of the oil and the surrounding environment to detect the presence of oil. The applicability of a given detector depends on such factors as the size of the spill, ambient weather conditions, time of day, and accessibility of the geographic region. Overall, remote sensing has been an effective surveillance technique for oil spills on open water.

Various technologies have been developed and tested for application to remote sensing of oil under ice and snow. Satellite-based sensors, such as SAR, are less effective for direct detection of such spills since the returned signal does not have a distinct signature when oil is present. Contact based methods (e.g., acoustic) require deployment of instruments on the clean snow or ice surface; therefore, it is reasonable to consider if these methods offer an advantage compared to drilling a hole in ice. As described by Goodman (2009), using mechanical equipment to drill a hole in the ice and visually detect oil is the only proven technology. There have been very few oil spills under ice in the past few years, thus little opportunity to test new technologies. Some sensors mounted on surface and aerial platforms, including ground-penetrating radar, acoustic sensors, as well as laser-based systems that measure either a fluorescence signature or thermal emission from the trapped oil were experimentally tested. There are a number of extensive reviews of this early work (Dickins, 2000; Fingas and Brown, 2000).

1.4 Objectives

The primary objective of this work is to identify the state-of-the-art of surface remote sensing technologies to monitor oil under varying conditions of ice and visibility. To this end, a review of current and emerging technologies with a documented ability to detect oil on water was conducted, and their potential for application in ice-affected waters was assessed. A series of performance parameters was defined to evaluate the technologies according to their respective

strengths and limitations. Based on the results of this evaluation, recommendations for research and development in the near future (18-24 months) were formulated.

CHAPTER 2. OPTICAL SENSORS

Optical sensors are passive imaging devices sensitive in the UV, visible and near-infrared (NIR) spectral region. They exploit differences in reflectance as the primary mechanism for detecting oil on water. Optical sensors include hyperspectral sensors, multispectral imaging systems, still and video cameras, UV and NIR sensors.

2.1 Cameras and Multispectral Sensors

The visual interpretation of oil spills by trained operators remains an important method for detecting oil on water (Bonn Agreement, 2009). The primary sensors include digital still or video cameras mounted on aircraft, vessels or rigs (Jha et al., 2008) which are sensitive to reflected visible light (i.e., corresponding to wavelengths ranging from 400 to 700 nm) as well as the near-infrared range (i.e., from 700 to ~1000 nm) (Campbell and Wynne, 2011). Figure 2 shows an aerial photograph in which oiled and clean water are discernible.

Figure 2. An aerial photo of an oil sheen and slick observed during the Deepwater Horizon blowout (from Leifer et. al., 2012)

Since the amount of oil is a critical parameter to guide response actions, it is important for operators to relate the visual appearance of oil to layer thickness and volume. An example of the appearance of oil on different types of water is presented in Figure 3. The letters were assigned by NOAA (2012) according to modified Bonn Agreement Oil Appearance Code (BAOAC), represented in Table 2 as an interpretation key to relate the brightness and colour of oil on water to layer thickness.

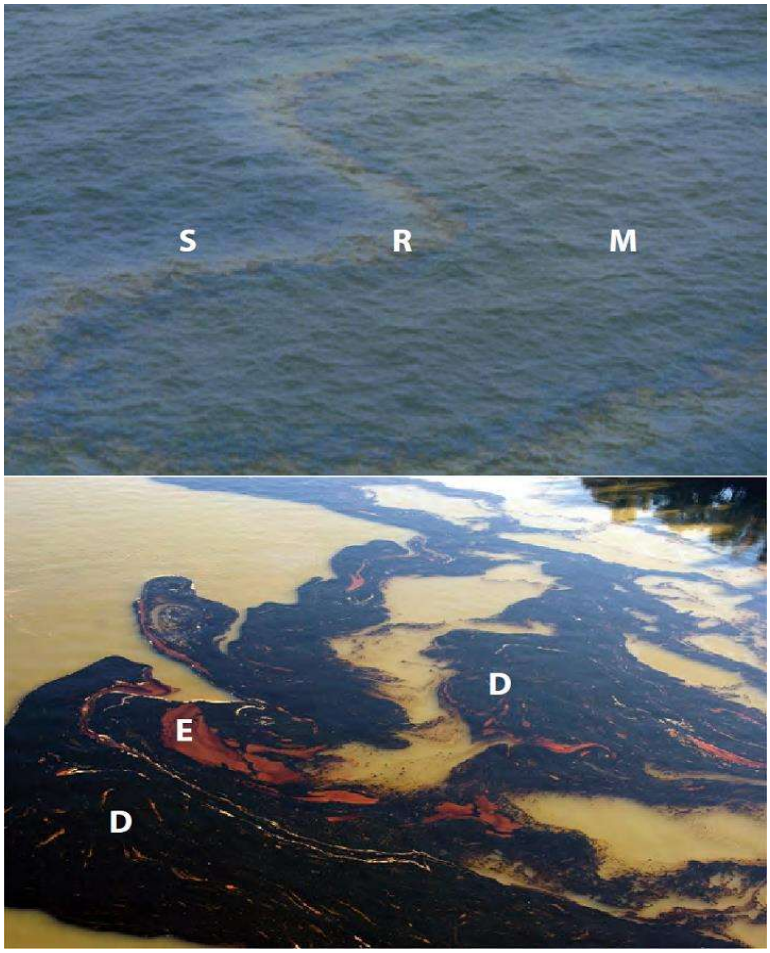

Figure 3: Aerial digital photography of oil spilled on (top) the ocean and (bottom) the Mississippi River. S: silver/gray; R: rainbow; M: metallic; D: dark or true color; E: emulsified (from NOAA, 2012)

Table 2. Relationship between oil thickness and appearance (from Bonn Agreement, 2009)

Code	Appearance	Layer Thickness (□m)
1	Silvery/gray sheen	0.04 to 0.30
2	Rainbow	0.30 to 5.0
3	Metallic	5.0 to 50
4	Discontinuous true oil colour	50 to 200
5	Continuous true oil colour	200 to >200

Silver/gray and rainbow sheens are due to optical interference effects over the thin oil film, while the metallic appearance is caused by the reflection of skylight. For thick layers, the true colour of the oil dominates (Bonn Agreement, 2009; Leifer et al., 2012). In addition to colour, shape, size, contrast and context are used to interpret oil on open water (NOAA, 2012).

Since oil does not have specific absorption bands in the visible and NIR spectral ranges, detecting oil on water relies on differences in contrast between the oil and the surrounding oil-free water. The difference in reflectance between oil and water increases for shorter wavelengths and the contrast may be enhanced by filtering out any response above 450 nm and by using cameras positioned at the Brewster angle of water (i.e., at an incidence angle of 53□) in conjunction with a horizontal polarizing filter (O'Neil et al., 1983; Ahmed et al., 2006; Fingas and Brown, 2011). Recent work by Svejkovsky and Muskat (2009) and Svejkovsky et al. (2012) used multispectral airborne imagery to map oil on water and characterize oil thickness. The approach relied on a priori knowledge of reflectance properties over varying oil thicknesses as presented in Figure 4.

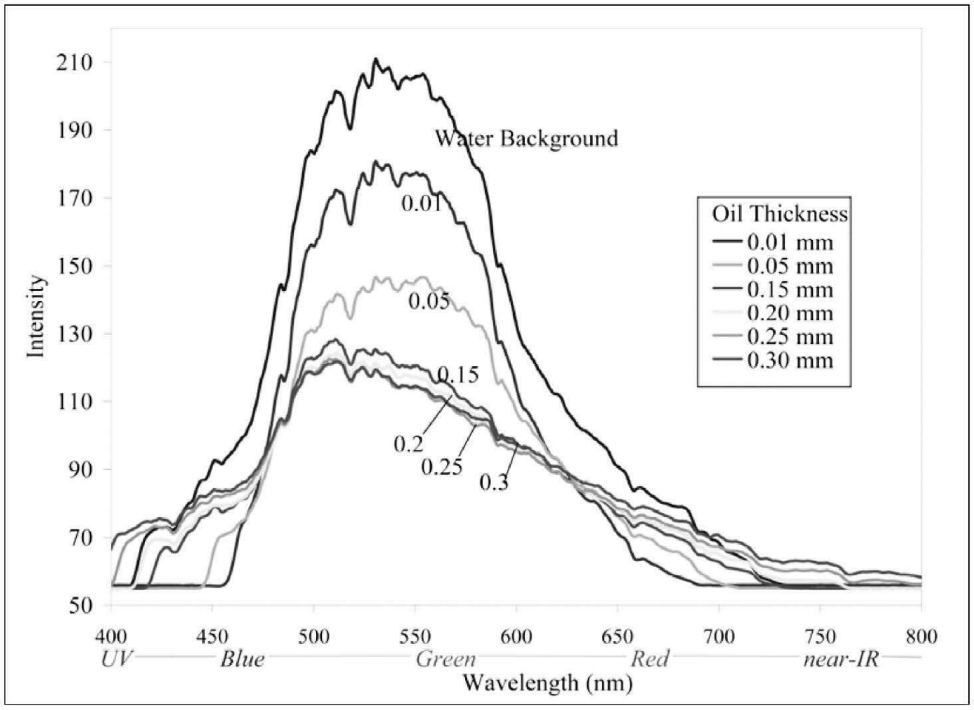

Figure 4. Thickness dependence of the visible-NIR range reflectance of Alaska North Slope crude oil (from Svejkovsky et al., 2012)

Using a portable spectrometer with four spectral channels, oil slicks were categorized into different thickness classes in two stages. A neural network algorithm was used to replicate the visual interpretation process based on contrast and shape parameters to classify oil and oil-free water. A second step used the reflectance ratios between water and oil pixels to extract thickness classes, from which volume estimates can be derived.

2.1.1 Operational Performance in Open Water

Visible sensors, such as still and video cameras, are widely used for aerial reconnaissance of open water spills as they are readily available, inexpensive and easy to use. However, visible imaging of oiled water is affected by false alarms. Oil sheens can be confused with sun glint and wind sheens, while biogenic materials such as seaweed, sunken kelp beds and fish sperm can be confused with thicker oil slicks (Jha et al., 2008; Fingas and Brown, 1997; Fingas and Brown, 2011). While typical camera systems are limited to use during sunlight hours, visible-range detection of spills may be extended into dark and low light conditions using night-vision

technology. However, the capabilities of the current low-light systems for detecting oil on water have not been thoroughly documented (Brown et al., 2005).

Optical satellite imaging has also been used to monitor and map oil slicks on water. However, the dependence on cloud cover, infrequent revisit and low spatial resolution makes optical satellite imagery an ancillary rather than a primary data source. Interpretation of satellite data requires specialized expertise and may take too long in tactical situations (Fingas and Brown, 2011). Liefer et al. (2012) completed a comprehensive review of spaceborne and airborne sensors for oil spill monitoring. An overview of operational optical satellite systems is presented in Table 3.

Table 3. Operational optical satellite systems

Instrument	Resolution (m)	Swath (km)	Revisit (days)
LANDSAT 5, 7, 8	15 - 30 (MS) and 120 (TIR)	185	16
MODIS	250 to 1000	2330	1-2
MISR	275 to 1100	360	2-9
DMC	20 to 30	600	Near daily
SENTINEL-2	10 to 60	290	Near daily; to be launched 2014
QuickBird	0.6-2.4	16.4	1-3.5 days
Worldview-1/2	0.5-1.8	16.4	Near daily
Geoeye	0.41-1.35(MS)	15.2	2.1 days

Despite limitations, optical satellite surveillance has been used successfully in conjunction with radar-based oil spill monitoring to identify areas of algal blooms and remove them as sources of false alarms from SAR images (e.g., Brekke and Solberg, 2005; ASL, 2012). Image products from MODIS, MERIS and LANDSAT were generated every few days to support cleanup efforts of the Deepwater Horizon spill (Leifer et al., 2012). Given the size of the spill, which covered a surface area on the order of 104 km2, the oil was readily discernible in relatively low spatial resolution data (i.e., >30 m). A true color image of the Deepwater Horizon spill collected by MODIS is shown in Figure 5.

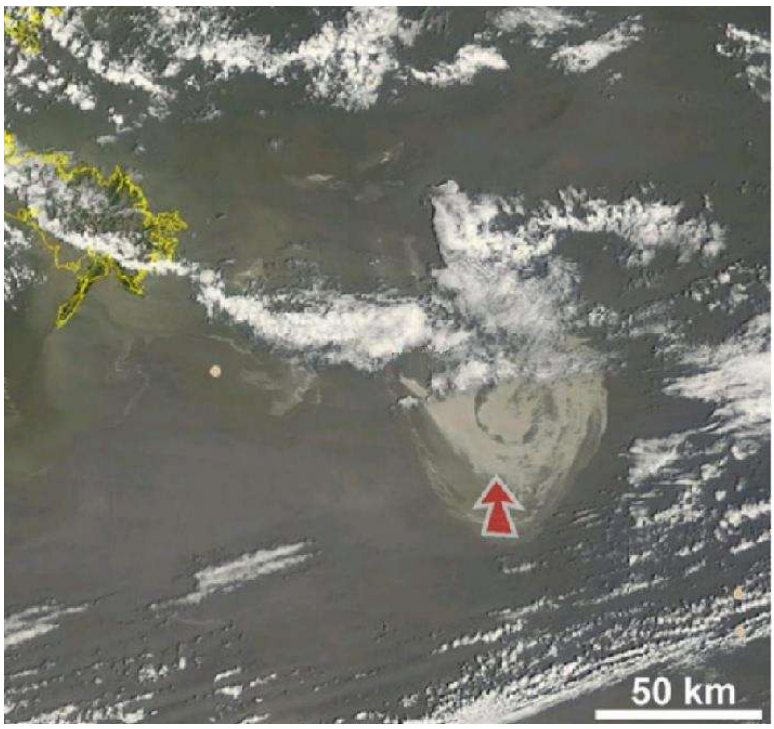

Figure 5. MODIS true color image of the Deepwater Horizon spill collected on May 8, 2010. The red arrow denotes the position of the spill (from Leifer et al., 2012)

Given the high rate of false positives from sun glint, kelp beds, jellyfish, cloud shadows and changes in water depth (NOAA, 2012), the need for specially-trained, experienced personnel is essential. Due to the relatively long imaging and data processing time required for both aerial and satellite-based sensors, observations by trained personnel will probably remain more timely and cost effective for rapid surveys of large spills (Svejkovsky et al., 2012).

2.1.2 Application in Ice-Affected Water

Optical detection methods are hindered when ice is present. Optical signals are attenuated in ice and snow making passive optical sensors ineffective for characterizing oil encapsulated in ice and under snow or ice (Fingas and Brown, 2000). Dark melt pools as well as sediment and dirt on ice during the break-up season can be confused with oil on the ice (Dickins and Andersen, 2009). Even with oil on snow or bare ice, visible detection may be difficult due to synoptic conditions in Arctic regions, including the presence of fog, marine layer, low cloud ceiling and long periods of darkness (Potter et al., 2012). Newly formed ice may also be misinterpreted as oil (Dickins and Andersen, 2009). In relatively high ice concentrations, the oil is contained within the ice and remains fairly localized. Under these conditions, the equilibrium thickness of the oil can be quite thick (i.e., on the order of millimeters) and, in accordance with Table 2, the oil has a true colour appearance. An example is presented in Figure 6, where the oil is clearly visible through its colour contrast with ice and water.

Figure 6. Photograph showing oil being released between ice floes during the SINTEF JIP field experiments carried out in 2009 (from Dickins, 2010)

In the case of open ice (<3/10 concentration), the oil spreads more freely and the oil sheen may appear similar to that expected in open water conditions (Wang et al., 2008). A small experimental spill near the ice edge is shown in Figure 7.

The limitations of optical systems are most severe for satellite-based systems, whereas aerial and ship-borne systems may be operated in cloudy conditions. Due to these restrictions optical sensors need to be combined with other technologies to offset their limitations. To this end, currently available optical sensors and processing methods should be subjected to a thorough performance evaluation and validation in a range of representative ice conditions and spill scenarios. Training oil observers specifically in the interpretation of optical imagery in ice conditions should also be considered.

Figure 7. Aerial photograph showing oil being released into ice-affected water during the SINTEF JIP field experiments carried out in 2008 (from Dickins, 2010)

2.2 Ultraviolet Sensors

The ultraviolet (300 nm to 400 nm) reflectance of oil is greater than that of water (Hurford and Buchanan, 1989). Aerial passive UV scanners have been engineered to collect and analyze UV sunlight reflected from the water surface and discriminate oiled water from oil-free water through observed variations in the electromagnetic intensity. UV sensors have detected sheens as thin as 0.1 □m (Fingas and Brown, 2011; Jha et. al., 2008).

2.2.1 Operational Performance in Open Water

The level of expertise required to operate a UV detector is comparable to that of a Thermal InfraRed (TIR) system, although the technology is not as well developed as TIR or visible-range sensors (Fingas and Brown, 2011). Due to the high attenuation of UV light by fog and clouds, oil spill detection with UV requires clear atmospheric conditions (Jha et al., 2008) and the need for ambient sunlight further limits use of the system to daylight hours. UV-based oil spill detection is also susceptible to false alarms caused by sun glints, wind slicks, and biogenic material (Fingas and Brown, 1997).

UV and TIR sensors are frequently used together to assess thinner and thicker parts of an oil slick (Jha et al., 2008). In addition, the false positives observed in TIR images are often different from those for UV images and the results obtained from using both offsets individual limitations (Fingas and Brown, 1997). An example of concurrently acquired UV and TIR data is presented in

Figure 8.

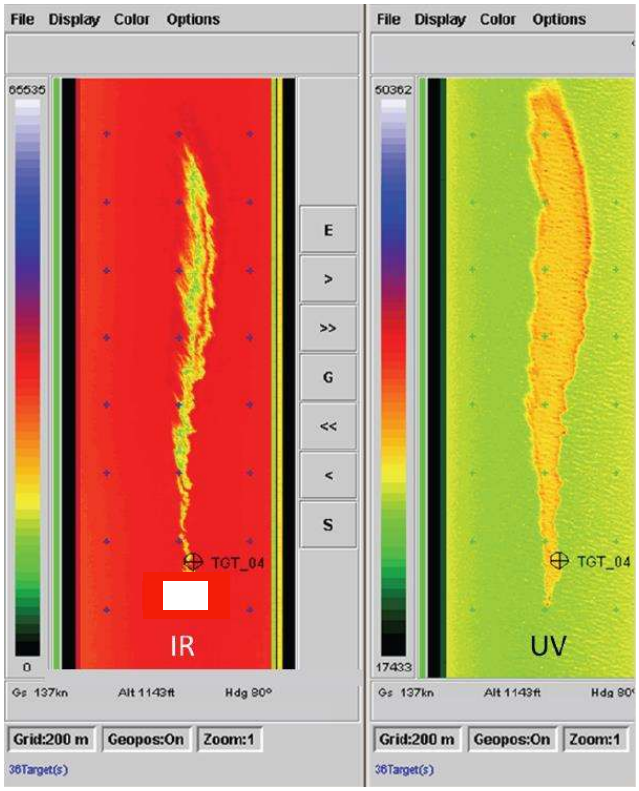

Figure 8. Concurrent aerial Thermal Infra-Red (TIR) and UV images of a slick (Robbe, 2012).

2.2.2 Application in Ice-Affected Water

The effectiveness of airborne UV sensors for detecting oil in ice-affected water is not well understood, and assumptions have been made about their capabilities in such situations based on how they performed in open water spills. UV imaging could be useful for detecting thin oil layers on melt ponds as well as oil between floes (Dickins and Andersen, 2009). Attempts were made to test an aerial UV/IR line scanner during the SINTEF JIP field experiment, but poor weather and fog over the test site did not allow these measurements to be taken (Dickins, 2010). Weather is a significant factor that must be considered in sensor selection. The performance of UV sensors for detecting oil in slush and brash ice is also unknown. Additional testing under field conditions is required to determine the capabilities of UV sensors for detecting oil in a variety of ice conditions (i.e., oil on ice and snow, oil between ice floes, etc.).

2.3 Hyperspectral Sensors

Hyperspectral sensors registering reflected electromagnetic radiation over tens or hundreds of spectral bands have been used to detect oil on water (Salem and Kafatos, 2001; Plaza et al., 2005; Leifer et al., 2012). Hyperspectral sensors typically operate from the UV to the mid-infrared part of the electromagnetic spectrum (i.e., ~2500 nm). A number of hyperspectral sensors are commercially available, such as the MEIS, CASI, AVIRIS, CAESAR and AISA systems (O'Neil et al., 1983; Salem et al., 2002; Wang and Stout, 2006; Clark et al., 2010). It should be noted that there are hyperspectral sensors which also provide coverage of the infrared spectral range. The Airborne Hyperspectral Scanner (AHS) instrument has 80 spectral bands covering the Visible and Near InfraRed (VNIR), Short Wave InfraRed (SWIR), Mid-Wavelength InfraRed (MWIR) and TIR spectral range. The instrument is operated by Instituto

Nacional de Técnica Aerospacial (INTA) and it has been involved in several field campaigns since 2004 (Sobrino et al., 2009). HyMap, another airborne hyperspectral sensors developed in Australia, has contiguous spectral coverage of visible (VIS), NIR, SWIR, MWIR, and TIR spectral regions with a spectral bandwidth of 10-20 nm and spatial resolution of 2-10 m (Cocks et al., 1998).

2.3.1 Active Hyperspectral Systems

Most hyperspectral imaging systems operate in the visible through NIR wavelengths and rely on solar illumination which may limit their use in an Arctic environment. Actively illuminating the scene of interest offers a way to address these limitations while providing additional advantages (Nishan et al., 2003). The benefits of active illumination with spectral imaging for a variety of applications were demonstrated in a laboratory. The setup included multispectral and hyperspectral sensors used in conjunction with several laser illumination sources including a broadband white-light laser (Figure 9).

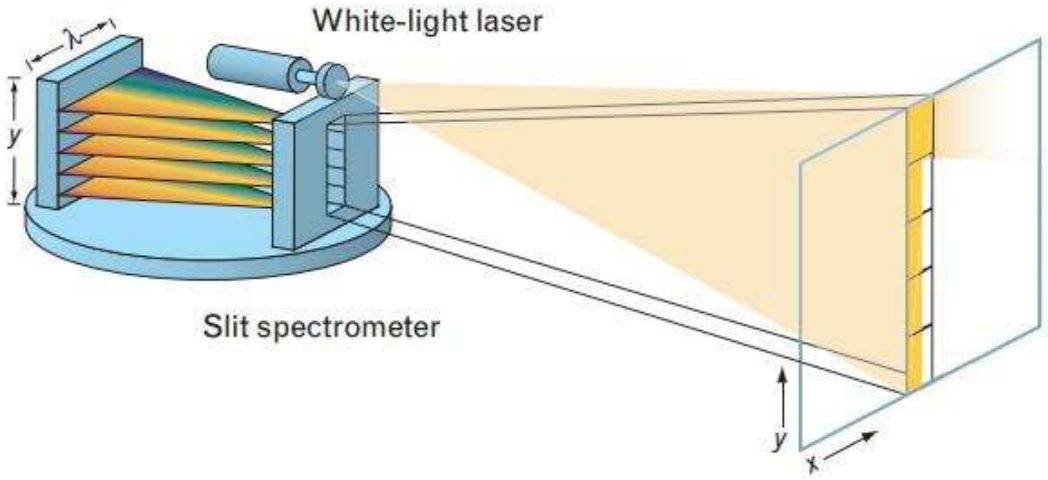

Figure 9. Visible and NIR hyperspectral imager for acquisition of a spectral signature for every pixel in y (vertical slit field of view of the imager) and wavelength λ (from Nishan et. al., 2003).

Adding active spectral imaging to spectral reflectance, fluorescence, and polarization measurements have been used under laboratory and field conditions during day and night. Laboratory and outdoor tests (Johnson et al., 1999) have shown that using an active illumination source can improve target detection performance while reducing false alarm rates for both multispectral and hyperspectral imagers. The improved performance is important for applying the system in automated or semi-automated mode and for oil monitoring in darkness.

2.3.2 Operational Performance in Open Water

The higher spectral resolution of hyperspectral imagers allows them to assess spectral signatures specific to oil. For example, the NIR portion of the spectrum is sensitive to oil thickness and the water-to-oil ratio in an emulsion (Clark et al., 2010). An example of laboratory spectra of oil emulsions sampled during the Deepwater Horizon spill is presented in Figure 10. The emulsion exhibits clearly defined spectral features in the NIR, and the shape of the spectrum depends on emulsion thickness. The black lines/arrows highlight spectral regions corresponding to the absorption bands in the oil.

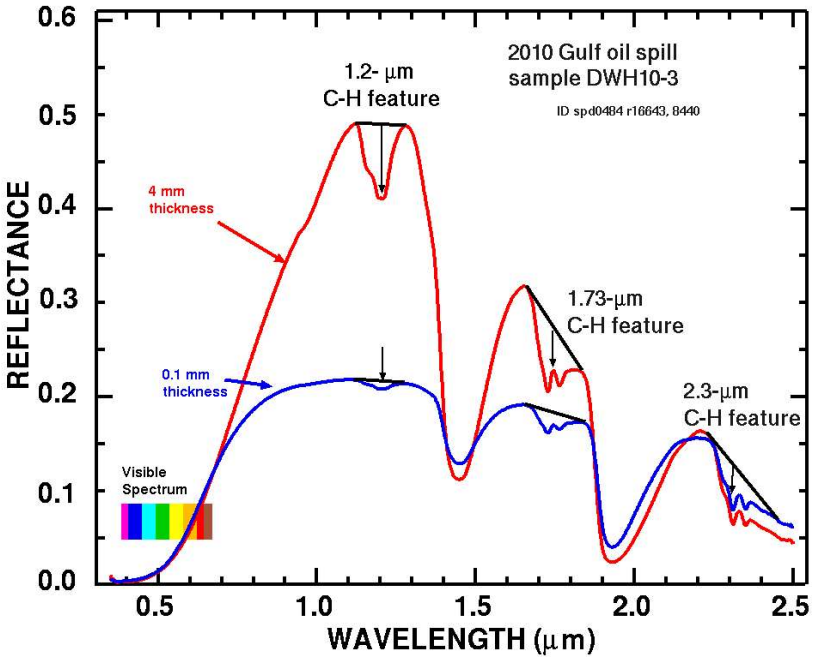

Figure 10. Laboratory spectra collected from a sample of oil emulsion (from Clark et al., 2010)

Analysis of field data collected over the Deepwater Horizon spill using the Airborne Visible Infrared Imaging Spectrometer (AVIRIS) provided quantitative values for oil thickness and oil-water ratio (Leifer et al., 2012). Clark et al., (2010) generated maps of oil thickness and emulsion ratio (as shown in Figure 11) using emulsion ratios of oil absorption bands. This information was subsequently used to estimate oil volume.

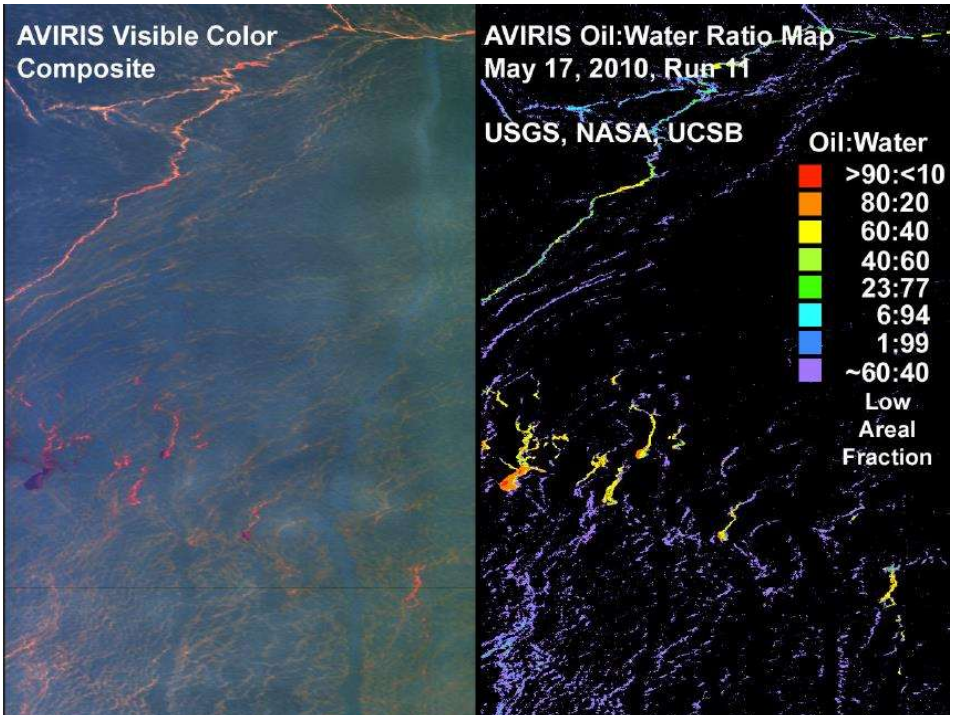

Figure 11. Colour composite and corresponding oil-water ratio map generated with AVIRIS (from Clark et al., 2010)

Other field experiments suggest hyperspectral measurements could be used to differentiate between light and heavy oils (Salem and Kafatos, 2001). While the products resulting from hyperspectral measurements can be generated relatively quickly when compared to optical satellite products, the analysis can be quite complex. The raw hyperspectral image is typically processed using spectral unmixing algorithms and the spectra deduced from each image pixel is compared to a spectra library to classify the surface material composition (Plaza et al., 2005). Classifying the surface material (i.e., in this case, oil on water) requires a priori knowledge of the spectral response of the material being probed, which means that in-situ field measurements must be taken before classification can be carried out. In contrast to the preceding sensors, operators require a higher level of expertise to use and interpret hyperspectral measurements. Additionally, these detectors can be quite large and are not readily deployed.

An oil spill determination system using airborne/spaceborne hyperspectral sensors for detecting oil spills and other contaminants on a water surface is described in Alawadi (2011). Such systems consist of a moderate resolution imaging spectrometer (e.g., MODIS for satellites) and provide high radiometric sensitivity in two spectral bands (i.e., one in the NIR and the other outside of the NIR) within the wavelength range of 0.4 micron to 14.4 micron. Maximum and minimum spectral radiance values are 649 nm and 869 nm, respectively, corresponding to MODIS bands 1 and 2 of the 250 m product. Oil spills are assessed based on the calculation of the spectral contrast shift between two bands. A cloud mask is required for satellite data, but not for data collected from aerial platforms.

2.3.3 Application in Ice-Affected Water

Hyperspectral imaging of oil in ice-affected waters has not been field tested. Given the high spectral resolution and approximately 1 m spatial resolution it is expected that this sensor would be at least as effective as a low spatial resolution, multispectral visible range camera for

detecting oil around ice. Analysis of hyperspectral data can be complicated. Future operational applications will need to consider automation to generate products that can be easily interpreted in near real-time (NRT) for tactical spill response.

Similar to the approach taken for oil spill detection in open water, there is a potential to use hyperspectral measurements to quantify oil spill characteristics (e.g., thickness, oil-to-water ratio, etc.). In order for this technology to be a viable method for oil-in-ice detection, spectral libraries corresponding to the applicable surface conditions need to be developed. The necessary reflectance spectra will depend on the oil, the ice conditions (e.g., is the oil mixed with brash ice), visibility and atmospheric state.

Upcoming hyperspectral satellite missions may provide useful information in the context of spill response and should be evaluated for their possible contributions. Planned missions to be launched within the next five years are presented in Table 4.

Table 4. Future hyperspectral satellite missions

Instrument	Spectral Range (nm)	Number of Bands	Spatial Resolution (m)
ENMAP	420-2450	155	30
HYSPIRI	380-2500	213	60
PRISMA	400-2500	211	20 - 30

CHAPTER 3. INFRARED SENSORS AND RADIOMETERS

Passive remote sensing instruments operating at IR and radar frequencies detect radiation emitted from the earth's surface.

3.1 Thermal Infrared Sensors

The nature of energy radiated from an object is dependent on its temperature and TIR sensors are sensitive to the radiant energy emitted by objects according to their kinetic temperature. Absorption in the atmosphere affects most of the TIR spectrum except for atmospheric windows from 3 to 5 µm and 8 to 14 µm where most TIR sensors are designed to operate.

Oil and water have different emissivities causing a thermal contrast that can be identified using TIR sensors (Goodman, 1989; Salisbury et al., 1993; Fingas and Brown, 1997). During daylight thick spills appear warmer than the surrounding water since they absorb solar radiation faster (Fingas and Brown, 2011). By contrast, thin films tend to appear cooler than oil-free water. The apparent decreased temperature of a thin slick is not well understood but it may be due to electromagnetic interference effects over the oil film (Fingas et al., 1999). For night-time TIR imagery this pattern is reversed, with thin slicks appearing warmer than the water background and thicker oil acting as a thermal insulator thus appearing cooler (Goodman, 1989). While TIR imagery does not rely on solar illumination, Dickins (2010) reports that the contrast between oil and water tends to be higher during daylight hours.

Many TIR sensors used in maritime oil spill detection operate in the 8 to 14 µm spectrum since past research suggests that the 3 to 5 µm atmospheric window is of limited utility (Salisbury et. al., 1993; Fingas and Brown, 2000). Hover and Plourde (1994) evaluated the day and night imaging capabilities of ship-mounted TIR sensors operating in 8 to 15 µm range, as well as hand-held sensors exploiting the 3 to 5 µm interval and found both types of systems useful in the identification of oil slicks, although the performance of individual sensors depended on environmental conditions and sensor tuning. The 3 to 5 µm spectral range is also used by operational TIR sensors embedded in APTOMAR's SECurus system (FLIR, n. d.; see Section 7.1).

TIR sensors are available as cooled (cryogenic) or more recently, un-cooled systems. Older cooled systems required liquid nitrogen which limited the period of operation to several hours. Newer systems use cooling based on gas expansion (Fingas and Brown, 2011). More recently, un-cooled systems have become available that are smaller and more easily operated and maintained (Svejkovsky et al., 2012). Cooled systems, however, have a lower noise floor and greater sensitivity to detect thermal contrast, resulting in longer operating ranges and higher spatial resolution compared to un-cooled systems (Veprik et al., 2012).

3.1.1 Operational Performance in Open Water

TIR sensors are relatively inexpensive, easy to deploy and commercially available as handheld or airborne units. TIR sensors are used widely for oil spill detection and response as they can operate day or night and provide information on relative slick thickness (Fingas and Brown, 2011). Svejkovsky et al., (2012) confirmed the quantitative extraction of oil thickness up to 2 mm based on the correlation of oil thickness and measured radiant temperature. TIR sensors can be paired with UV sensors to capture slicks thicker than 20 µm, while UV scanners are used to map thinner accumulations of oil.

Although TIR sensors do not rely on solar illumination, they are adversely affected by fog, poor weather and rough water. TIR imagery may also generate false positives from aquatic vegetation, shoreline and oceanographic phenomena (e.g., fronts). Early research suggested

that TIR systems were not able to identify emulsions due to reduced thermal contrast with surrounding oil-free water. However, Svejkovsky et al., (2012) were able to successfully map emulsions with a water content of 60% using an un-cooled microbolometer. Figure 12 shows an example of emulsified oil captured by thermal and multispectral imagery.

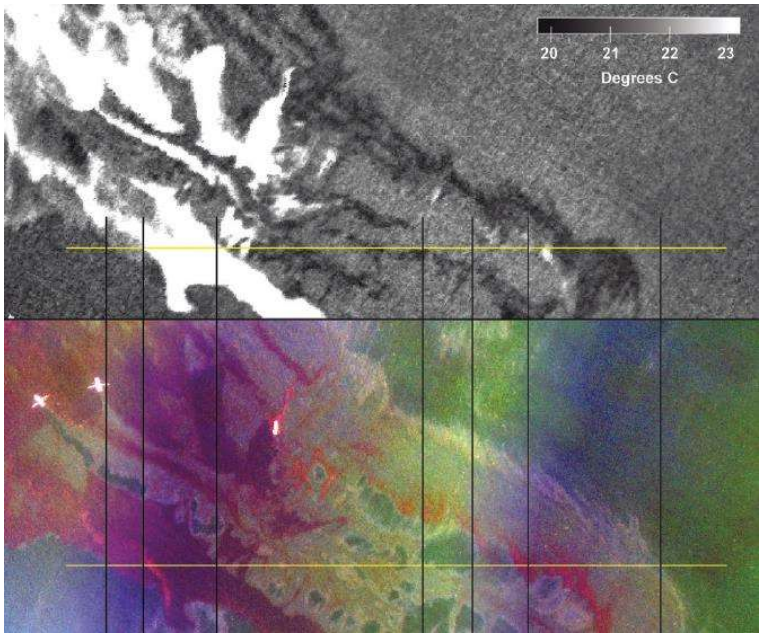

Figure 12. Emulsified oil of the Deepwater Horizon spill captured by thermal (top) and multispectral (bottom) sensors (from Svejkovsky et al., 2012)

In addition to nadir-viewing line scanners, forward-looking infrared (FLIR) is frequently used in aerial oil spill surveillance (e.g., Trieschmann et al., 2001). FLIR sensors perform similarly to TIR scanners, although varying viewing angles make area and distance measurements less feasible (Potter et al., 2012). FLIR systems are also routinely used in other maritime surveillance applications, such as vessel detection and search and rescue missions. An example of a FLIR image integrated within the Maritime Satellite Surveillance (MSS) 6000 airborne surveillance system (see Section 7.1) is presented in

Figure 13.

Figure 13. Example of FLIR image of oil spill (from Domargård, 2012).

3.1.2 Application in Ice-Affected Water

Since the emissivities of ice and water are similar over much of the TIR spectrum (SL Ross et al., 2010), it is expected that TIR will be suitable for detecting oil in ice-affected waters. The results of a recent study undertaken to evaluate the performance of several remote sensing systems in ice conditions suggest that TIR sensors are promising tools for detecting oil on water between ice floes (Dickins et al., 2010). However, TIR sensors will likely not be effective in detecting oil in ice or under snow since the radiation emitted by the oil is absorbed during its passage through the overlaying ice and snow.

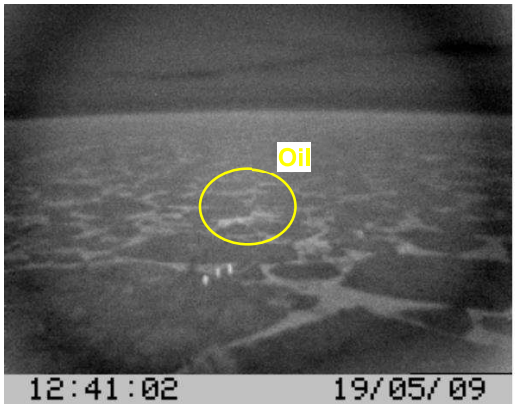

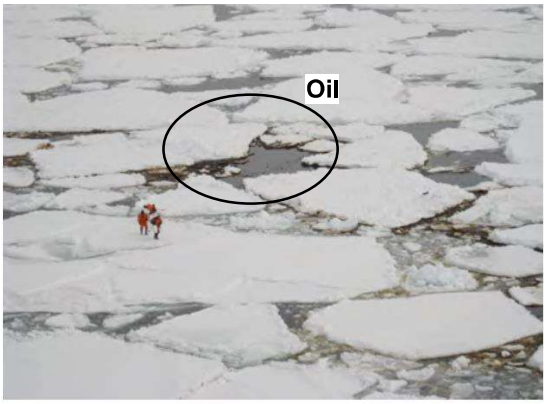

Figure 14 shows images of a hand-held TIR sensor (left) and an optical camera (right), with oil from a controlled release clearly visible in both images.

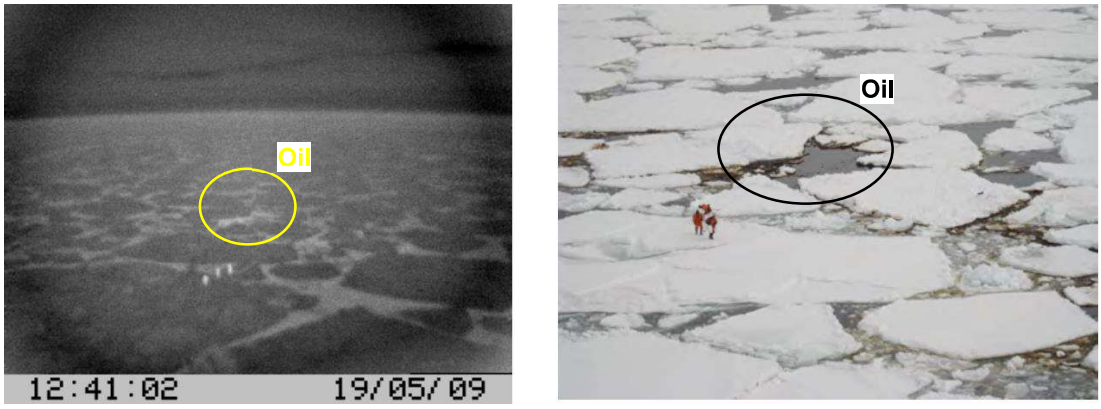

Figure 14. Oil between ice floes imaged by TIR (left) and optical camera (right) (adapted from Dickins, 2010)

Additional research is required to fully test and validate the performance of TIR imaging systems in different ice conditions, such as brash and grease ice. The detection of oil on ice as well as on surface melt ponds should also be investigated. These investigations may include sensors mounted on vessels or platforms, as well as airborne TIR scanners and FLIR systems.

Satellite-based TIR sensors are unlikely to provide valuable tactical information for detecting oil in ice environments due to their limited spatial resolution (e.g., 30 m for LANDSAT, 1-2 km for MODIS and AVHRR).

3.2 Microwave Radiometers

Microwave radiometers (MWRs) measure emitted radiation with wavelengths in the range of millimeters. As with TIR detection, observed differences in the surface microwave emissivity facilitate discrimination between different surface materials in a scene. In the microwave range oil has a higher emissivity than water (Fingas and Brown, 2011) and can appear brighter than oil-free water in MWR images (Jha et al., 2008). Microwave emission from oil slicks can be influenced by interference over the oil layer and is greatest when the round-trip electromagnetic phase difference over the oil layer is equal to a multiple of π (Jha et al., 2008). The brightness measured by the MWR sensor can theoretically be related to estimates of oil slick thickness. In practice, signal ambiguities have been reported as a result of the cyclic nature of the constructive interference condition and the resulting thickness estimation (Lääperi and Nyfors, 1983; Skou, 1986; Goodman, 1994). Attempts to resolve this issue include the use of multi-frequency scanning radiometers (McMahon et al., 1997) and relating oil thickness to variations in polarization of the microwave signal (Pelyushenko, 1995).

3.2.1 Operational Performance in Open Water

Although not in widespread use, multi-frequency MWR sensors are used for operational pollution surveillance in Germany (Trieschmann et al., 2001; Dickins and Andersen, 2009). OPTIMARE's MWR is capable of detecting, measuring, and mapping oil layers with thicknesses in the range from 0.05 to 3 millimeters (OPTIMARE Product Sheet, 2013). Trieschmann et al., (2001) reports that MWR instruments enable oil film thickness measurement in the range of 0.05 to 2.5 mm when flying at an altitude of 300 m. MWR systems operating at 18, 36 and 89 GHz, provide complementary information at varying spatial resolutions as follows:

- 18 GHz: sensitive to thicker films, spatial resolution is 22 m;
- 36 GHz: compromise regarding spatial resolution (11 m) and all-weather capability; and
- 89 GHz: sensitive to thin films, spatial resolution is 5 m.

An example of an oil slick imaged by multi-frequency MWR as well as TIR and UV instruments is presented in

Figure 15.

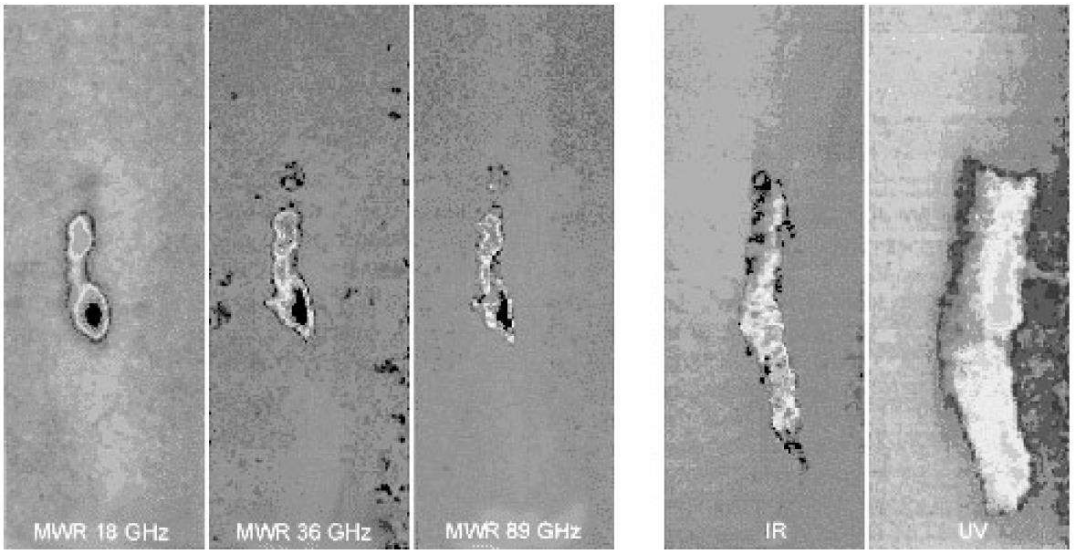

Figure 15. Oil spill on water imaged by three-frequency MWR, IR and UV sensors (from Trieschmann et al., 2001)

Microwave radiometers can operate in conditions of low visibility (e.g., fog, rain and night), although false positives can be generated by waters of different temperatures, seaweed and biogenic material (Pelyushenko, 1995; Fingas and Brown, 2011). MWR systems can be costly and require a dedicated aircraft to accommodate a special antenna (Jha et al., 2008).

3.2.2 Application in Ice-Affected Water

MWR systems have not been tested or validated in ice conditions, and their potential for characterizing oil in ice-affected waters remains unknown. Research on utilization of MWR sensors in ice environments, especially in low ice concentrations (<3/10), can be useful to evaluate capabilities of this technology for operational application.

CHAPTER 4. RADAR SENSORS

Radar sensors are active systems and include SLAR, SAR, marine radar and GPR.

4.1 SLAR and SAR Systems

Radar systems operate in the microwave spectrum, are largely weather-independent, can acquire images day and night and are available on airborne and satellite platforms. Radar backscatter signal depends on the parameters of the imaged surface such as target material and conductivity and system characteristics, such as wavelength, incidence angle and polarization (Campbell and Wynne, 2011). Radars use an antenna to emit and collect the microwave signal and spatial resolution improves as the length of the antenna increases (Van Zyl and Kim, 2011).

Due to the large antenna size, SLAR is restricted to aerial platforms, typically fixed-wing planes. SAR by contrast, uses the forward motion of the sensor platform, while taking into account Doppler shift of the collected signal to synthetically increase antenna aperture (Gade et al., 1996). Imaging satellite radars rely on SAR, although airborne SAR sensors are also used. SAR satellite sensors are emerging as the predominant means of ice surveillance over large areas and are widely used by national ice centers around the world.

Oil slicks on water are detectable by radar imagery because of the dampened capillary waves which correspondingly reduces backscatter compared with the surrounding oil-free water (Solberg et al., 1999). Oil on water appears as dark patches on radar images (Topouzelis, 2008). Capillary waves are also reduced by other phenomena (see Section 4.1.1) and verification by other means is required to identify oil unambiguously.

Most current radars operate in C-Band (wavelength ~5 cm) or X-Band (wavelength ~3 cm), although L-band (15 to 30 cm) and P-Band (30 to 100 cm) systems have been used on airborne and satellite platforms. Radars can be configured to transmit and receive horizontally or vertically polarized radiation and vertical antenna polarizations for both transmission and reception (VV) have been shown to yield better results than other configurations for oil detection (Brekke and Solberg, 2005).

4.1.1 Operational Performance in Open Water

Wind speed is a major factor in detection of oil with radar. At low wind speeds, there is relatively little wave activity and almost no Bragg scattering from the ocean surface, minimizing the contrast between oil-affected and oil-free areas (Solberg et al., 1999). On the other hand, at very high wind speeds the larger waves are substantial enough to overcome damping effects caused by the oil. Again, under these conditions the brightness contrast between the oil and surrounding water is diminished, and the presence of oil cannot be detected. In general, wind conditions between approximately 3 and 10 ms-1 are favorable for detecting oil on open water using SLAR or SAR sensors (Gade et al., 1996; Solberg et al., 1999; Brekke and Solberg, 2005; Babiker et. al., 2010).

False alarms are possible from areas of low wind, biogenic slicks, fresh water inclusions, grease ice, shear zones and internal waves, all of which may have a radar signature similar to oil on water (e.g., Fingas and Brown, 1997; Solberg, 2012). Discriminating oil from the water background typically relies on analysis of local image contrast as well as shape and distribution of observed dark patches (Brekke and Solberg, 2005; Topouzelis, 2008).

In the last decade, satellite-based oil spill monitoring has become an integral part of national pollution control programs in Europe and Canada (Ferraro et al., 2010). In Europe, the

European Maritime Safety Agency (EMSA) administers satellite-based monitoring through a network of service providers, while in Canada the Integrated Surveillance and Tracking Of Pollution (ISTOP) program is executed through the Canadian Ice Service (CIS).

Figure 16 shows an example of a satellite SAR image with oil and ship signatures acquired and analyzed by CIS.

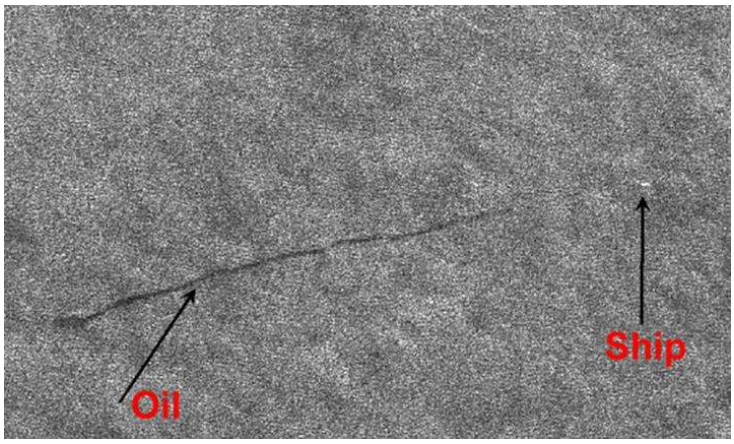

Figure 16. Satellite SAR image acquired on January 30, 2009 in Cabot Strait, Canada with oil and ship signatures (from http://www.ec.gc.ca/glaces-ice/default.asp?lang=En&n=C5EE0C9F-1)

The approaches and algorithms used to extract potential oil slicks are typically divided into two major stages. In the first stage areas of low backscatter are identified in the image either through manual interpretation or automated segmentation. In the second stage the characteristics of the low-backscatter areas are evaluated to determine if it is likely an oil slick. Classes of features used in this context are slick geometry and structure, appearance of the edges, brightness contrast to surrounding areas, known sea state, known presence of algae blooms and locations of ships or platforms (Brekke and Solberg, 2005; Solberg et al., 2007; ASL, 2012).

The presence of oil slick look-alikes remains a constant issue, with false alarm rates ranging from 15 to 85% (Tarchi, 2005), however, recent research indicates that automated algorithms are increasingly able to differentiate between oil slicks and look-alikes, with classification accuracies ranging from 73% to 92% (Brekke and Solberg, 2005; Bogdanov et al., 2005; ASL, 2012). Present operational oil spill monitoring using satellite SAR is based on manual or semi-automatic interpretation with significant input from operators (Ferraro et al., 2010), suggesting that automated algorithms may not yet be able to fully take account of environmental conditions, look-alikes and slick characteristics encountered in the routine surveillance of large areas.

Fully-polarimetric SAR has been recently investigated for characterizing oil slicks. Minchew et al. (2012) examined polarimetric SAR imagery acquired with an unmanned aerial vehicle (UAV) over the Deepwater Horizon spill. The results show that radar backscatter from both clean water and oil in the slick is predominantly due to single bounce surface scatter. The most reliable indicator for slick detection was found to be the major eigenvalue ($\lambda 1$) of the coherency matrix, which is approximately equal to the total backscatter power for both oil and oil-free water see (Figure 17).

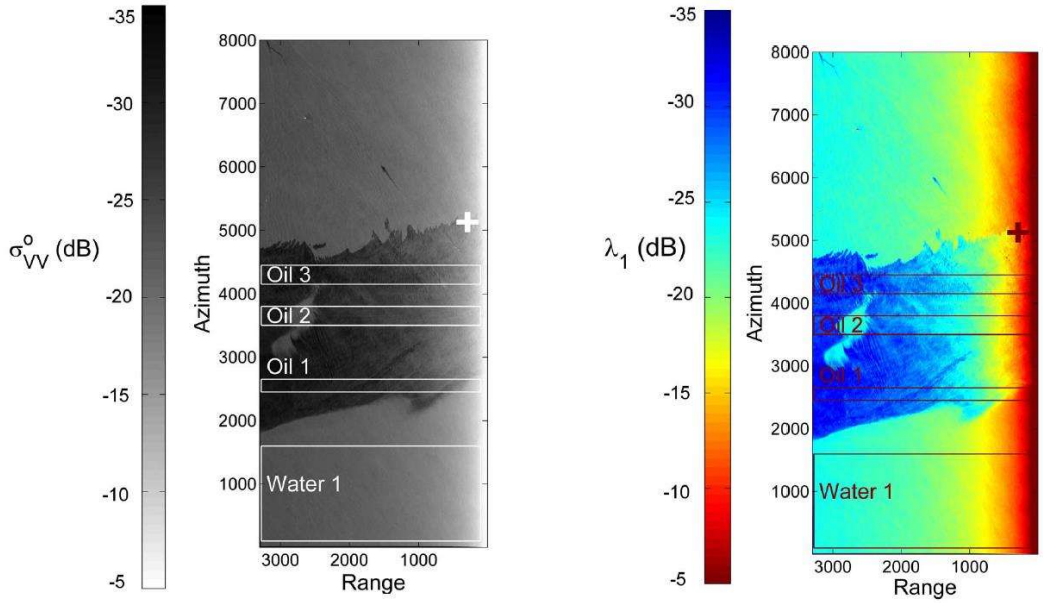

Figure 17. Vertical co-polarized normalized radar cross section, σVV, image (left) and major eigenvalue (λ1) images (right) of oil spill (from Minchew et al., 2012)

Other polarimetric parameters studied in the context of oil slick characterization include the circular polarization coherence, the co-polarized phase difference standard deviation, polarimetric entropy and anisotropy, among others (Solberg, 2012). Recent work has indicated that polarimetric entropy is a promising area to consider (ASL, 2012). An overview of current and future SAR satellites is provided in Table 5.

Table 5. Current and future SAR satellites

Sensor	Band	Polarizations	Spatial Resolution [m]	Swath Width [km]	Revisit Frequency	Status
RADARSAT-1	C	HH	10 to 100	50 to 500	2 to 3 days	Safe Mode*
RADARSAT-2	C	HH, VV, HV, VH	1 to 100	50 to 500	2 to 3 days	Operational
COSMO-SKYMED	X	HH, VV, HV, VH	1 to 100	10 to 200	2 days	Operational
TERRASAR-X	X	HH, VV, HH/VV, HH, HV, VV, VH	1 to 18	10 to 150	3- 4 days	Operational
SENTINEL-1	C	HH, VV, HH/VV, HH, HV, VV, VH	20	250	1 to 3 days	Launch in 2013
RCM	C	HH, VV, HV, VH	1 to 100	50 to 500	Daily	Launch in 2018

* RADARSAT-1 stopped accepting new tasking requests in April 2013, but may become operational again

4.1.2 Application in Ice-Affected Water

Reduced wave activity in areas filled with broken ice limits the utility of radar for detecting oil spills within moving pack-ice. Recent studies found that SAR or SLAR were not able to detect

oil contained between close-pack ice (Dickins et al., 2010). While it was suggested that radar may be useful for imaging spills in open pack ice, where the ocean wave behavior is closer to that of open water conditions, this assertion has not been validated in the field. Additionally, new ice may dampen ocean waves in a fashion similar to that of oil, resulting in potential ambiguities in spill assignment when analyzing radar images, especially with single-band SAR data (Babiker et al., 2010).

SAR cannot penetrate thick ice cover due to the high attenuation of saline ice. The ice thickness is particularly critical when operating at high SAR frequencies (e.g., X-band, 8-12GHz), as the attenuation coefficient increases with frequency (Fingas and Brown, 2000). While attempts to detect oil within high ice concentration during the SINTEF JIP project were unsuccessful, it was suggested that there was no technical reason why such sensors could not detect oil in open ice (1/10 to 3/10) (Dickins, 2010). Further work is required to determine the full capabilities of SAR and SLAR systems in ice.

4.2 Marine Radar

In the last decade there has been an effort to develop and utilize ship-based marine radar to detect the presence of oil in ice. The approach taken to date is to use shipboard marine radar to supplement aerial and satellite sensors (Egset and Nøst, 2007). SLAR and SAR typically operate at steep incidence angles that are more conducive to ocean backscatter, but the relatively low elevation of the marine radar on a ship's superstructure means that it must operate at much shallower angles of incidence. Consequently, there is less backscatter, making discrimination between individual objects in the scene more challenging. To compensate for this, commercially available marine radars integrate successive radar images to produce stable images of potential targets. The integration is possible since marine radar is able to dwell on an area of interest for many revolutions of the antenna and improve the ability to discriminate between different objects in the scene. Present commercially available integrate up to 128 images. For typical marine radar scanners that operate in the range of 20 - 30 RPM this necessitates a dwell time in the order of four to six minutes to create a stable image.

There are several commercially available scan averaging radar systems including SeaDarq, Rutter Sigma S6, Miros OSD and Consilium and are offered as an add-on to standard marine X-Band radars. An example of vessel-based Rutter Sigma S6 marine radar output is provided in Figure 18.

Figure 18: Vessel-based oil spill surveillance using Rutter Sigma S6 (from Safer, 2011)

The range of ship-borne radar is limited, largely by the height of the antenna, from eight to 30 km. Ship radars can be adjusted to reduce the effect of sea clutter. During trials in the Baltic Sea ship-borne radar successfully detected a surface slick at a distance of 8 km and during a trial off the coast of Canada slicks were detected at a maximum range of 17 km (Tennyson, 1985). During the Prestige spill a Netherlands vessel successfully used this technique to guide a recovery vessel into slicks. The technique is, however, very limited by sea state and, in all cases where it was used, the presence and location of the slick were already known or suspected; ship radars will provide little forensic evidence. Gangeskar (2004) proposed an automated system that could be mounted on oil-drilling platforms and use the standard X-band ship navigation unit to provide an alert if an oil spill is present. The system includes an extensive post-processing system to provide both a user-friendly graphical user interface (GUI) and an automatic detection and alert system.

4.2.1 Application in Ice-Affected Water

As is the case with SAR and SLAR, the ability of marine radars to detect oil in the presence of ice has not been validated yet, but it is expected that the ability to detect oil reliably will deteriorate with increasing ice concentration. Further validation is required to identify the window of opportunity within which oil can be detected in sea ice.

4.3 Ground-Penetrating Radar

GPR uses electromagnetic waves in the microwave region (typically 250 MHz to 1 GHz) to probe the subsurface of an area. An electromagnetic pulse is produced and directed into material below the GPR. Through analysis of the resulting backscattered signal, information about the composition of the underlying material structure is obtained. The collected data consists of a collection of return pulses corresponding to reflections at interfaces where the dielectric permittivity or electrical conductivity change.

4.3.1 Application in Ice-Affected Water

This technique has been used to characterize ice and snow structures in the Arctic. Recent studies have shown that GPR can detect oil spills under snow (Bradford et al., 2010) and ice (Bradford et al., 2008). The dielectric permittivity ratio between sea ice and sea water is much larger than the corresponding ratio between sea ice and oil (Bradford et al., 2008). Therefore, GPR has potential for imaging an oil layer within ice and snow. The large difference of permittivity at the ice/water interface compared to that of the ice/oil interface, however, poses problems in both signal strength and sensitivity range and requires that the GPR receiver have a large dynamic range (Goodman, 2008).

A limitation to GPR to probe for oil under ice stems from the strong signal attenuation in ice. In contrast to electromagnetic propagation in dry snow, electromagnetic signals are highly attenuated in sea ice, thus limiting signal penetration. In cold ice, GPR can penetrate the full ice thickness (i.e., approximately 2 m). Signal penetration is decreased in thick warm ice (more than -5 oC). Given this, 500 MHz is considered the optimal operating frequency for oil detection under ice (Bradford et al., 2008), while 1000 MHz has been used to detect oil under snow (Bradford et al., 2010).

Oil located between snow and ice or between ice and sea water manifests as a change in the amplitude, phase, and frequency of the collected return pulses. While phase and frequency are susceptible to uncertainty due to noise, the reflection amplitude is fairly robust. The reflection amplitude of an oil/ice interface is less than that of a snow/ice interface, while the reflection amplitude of an oil/water interface is greater than that of an ice/water interface. For spills between snow and ice, oiled regions correspond to dark patches on the GPR images (Bradford et al., 2010).

Figure 19 shows cross-sections of GPR data before and after oil placement. Bradford et al. (2008) suggest a topographic high is visible along x=8 m, where the oil reached the greatest thickness, with a phase reversal after oil placement. The irregular ice/water interface is visible before oil placement along y=8 m.

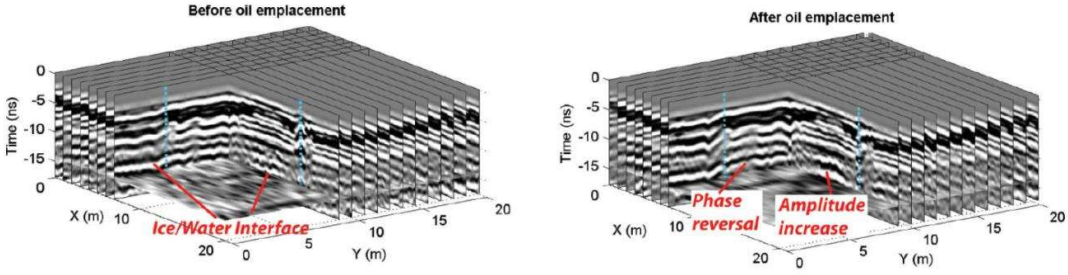

Figure 19. GPR images before (left) and after (right) oil emplacement in ice (from Bradford et al., 2008)

Although this technology has potential for detecting oil under ice and snow, obtaining quantitatively meaningful values for properties such as oil type is a difficult problem. The scattering process can be quite complex and analysis of the collected reflection signal can be plagued by ambiguities. Variations in the snow and ice structure, such as stratification in snow as well as deformations at the ice interfaces, can lead to observable changes in the amplitude. Hence, the GPR response to an oil spill is not-unique and is similar to the response from ice layers and channels in the snow. Therefore, an important task is to develop semi-automated classification algorithms and software to help analyze the GPR signal (Dickens, per. comm., 2013).

Between 2003 and 2008 the U.S. Department of the Interior, Minerals Management Service (MMS) initiated four international JIP's to develop GPR into a functional remote monitoring sensor (MMS, 2009). The GPR system currently available is capable of detecting and mapping oil in ice over a broad operational time window from early to late winter, typically November to April, in the Arctic. This window of opportunity covers approximately 70% of the near shore fast ice season in most years. The current generation GPR is capable of mapping oil under or trapped within growing winter ice from 30 to 210 cm (one to seven feet thick) provided that the oil thickness is at least 2 cm (MMS, 2009).

A controlled field experiment (Bradford, et.al., 2010) using a helicopter based, 1000 MHz GPR system, was able to detect a 2 cm thick oil film trapped between snow and sea ice based on a 51% decrease in reflection strength. The results indicate that GPR has the potential for oil spill characterization.

Ongoing work is focused on developing and testing airborne radar systems based on Frequency Modulated Continuous Wave (FMCW) architecture (CRREL, 2012). The recent prototype of the mobile two-horn antenna (25-30kg) combined with a variable frequency (500 MHz to 2 GHz) system achieves signal extraction with improved signal-to-noise ratio (SNR) (Dickins, pers. comm., 2013).

CHAPTER 5. LASER AND FLUOROSENSORS

Existing airborne laser remote sensing systems for oil pollution monitoring can be divided into several groups: multispectral, hyperspectral, and laser-ultrasound (LURSOT) (Samberg, 2007). Active lasers and fluorosenor technologies have been widely tested for oil spill monitoring. A hyperspectral LIDAR was discussed in the section on active hyperspectral remote sensing system (2.3.1).

5.1 Fluorosensors

Certain hydrocarbons have fluorescent properties. For these materials, when ultraviolet light (typically between 300 nm to 400 nm) is incident on an oil sample visible light within the range of 500 nm to 600 nm is produced through a sequence of energy transitions in the hydrocarbon molecules. Figure 20 shows a typical fluorescence spectra collected from crude oil over a period of several days. This fluorescence signal is unique to oil and can be used to differentiate a probed oil sample from materials such as chlorophyll, kelp, water, ice, and snow (Fingas and Brown, 2000). In fact, the fluorescence peak is unique for each oil sample and can be used to classify oil (Turner Designs, 2012). For thin slicks on water (i.e., approximately 1 micrometer thick), information on the oil thickness can be deduced through intensity analysis of the Raman spectral peak observed from the water beneath the oil. As the oil thickness increases, the intensity of the Raman peak (stemming from inelastic light scattering in the water) decreases (Brown, 2011).

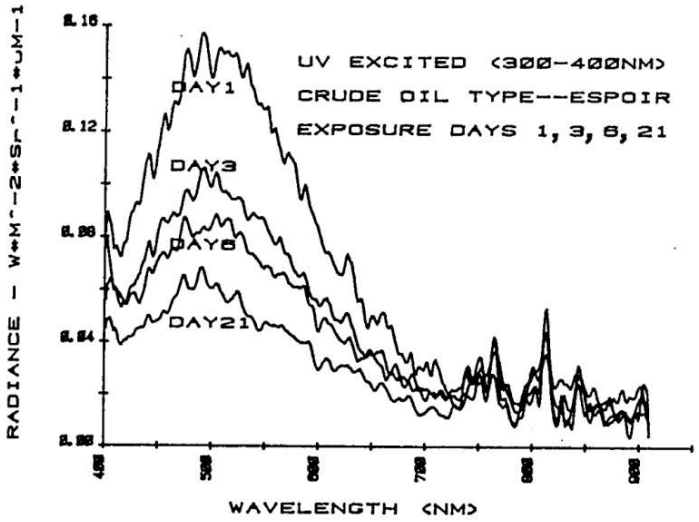

Figure 20. Fluorescence response of crude oil when illuminated by UV light. From Knoll (1985).

5.1.1 Operational Performance in Open Water

Fluorosensors can be deployed from aircraft or the surface. For the former, a UV laser pulse is emitted from the bottom of an aerial platform (typically a plane). The laser is scanned across the flight track to cover a horizontal swath of land (see Figure 21). The visible-range spectral response is monitored and a spectral peak between 400 nm to 600 nm clearly indicates the presence of oil. This spectral analysis may be done in real-time on the aircraft (Brown, 2011).

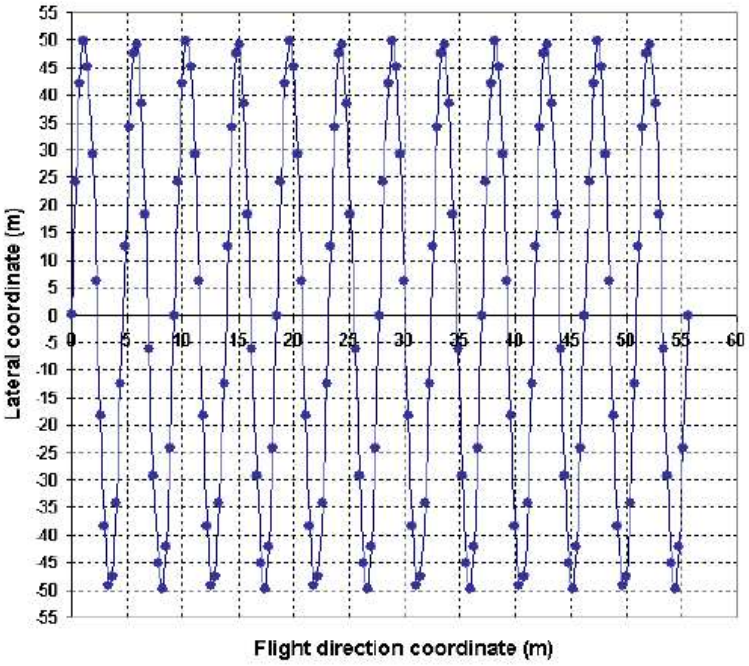

Figure 21. Surface footprint of an aerially deployed laser fluorosensor. From Jha et al. (2008).

While fluorosensors can be used to detect oil on a variety of backgrounds, the relatively high attenuation of UV light in water renders the system ineffective in fog, low cloud-ceiling, and inclement weather. The system requires a dedicated aircraft with an open belly hatch and depressurized cabin (Fingas, 2011).

There are only a small number of airborne laser fluorosensors in routine operation due to the difficulty of operation as well as the relatively high cost to maintain the system. Systems are being operated in Germany and Estonia (Trieschmann et al., 2001; Babichenko, 2008) and Environment Canada (2007) has a long history in developing and operating a laser fluorosensor (LFS), but this program has been discontinued (Fingas, per. comm., 2012).

Recent field-tests using an airborne Raman laser spectroscopy system reported that methane and hydrogen sulfide leaks could be detected with concentrations as low as six parts-per-billion (ppb) and two ppb, respectively (Alimov et al., 2009). The system was based on a pulsed UV laser, however, the authors suggest that it may be modified to be integrated with a fluorosensor.

5.1.2 Application in Ice-affected Water

Fluorosensors operating in the UV spectrum are not suitable for detecting oil under snow since light in the UV to visible range is highly attenuated in snow. The attenuation in ice is not as high over this spectral range suggesting that fluorosensors may be able to penetrate ice covers. Past research suggests that this approach works well with snow-free ice up to about 1 m thick (Goodman, 2008).

In 1992 Environment Canada conducted a field test to evaluate the capabilities of laser fluorosensors to detect oil in various environments including vegetation, water, ice and snow (Dick et. al. 1992). The results demonstrated that LFS were capable of detecting oil on different surface types (Figure 22). While LFS would be ineffective for detecting oil under ice and/or snow, they have future potential for discriminating between oiled and un-oiled surfaces.

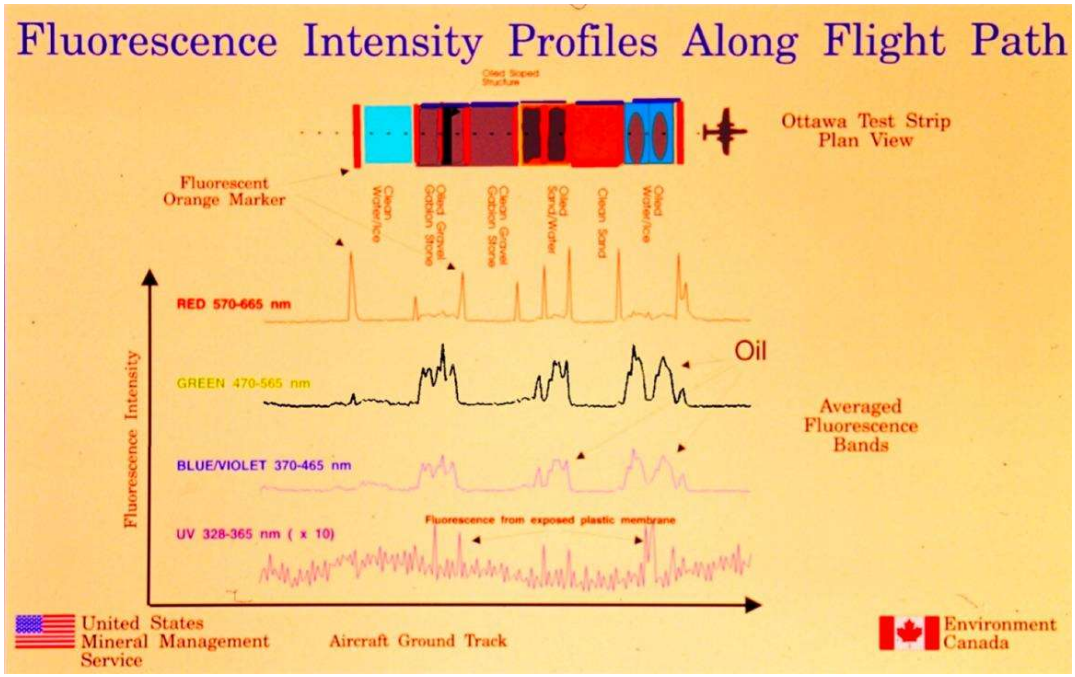

Figure 22. Oil detection using fluorosensor (Environment Canada, 1992).

Surface-based fluorosensors have lower power requirements and compact continuous-wave UV lasers or Xenon lamps have been used as the active source (Turner Designs, 2012; Goodman, 2008). These detectors have been used to detect oil on the ground, in water, on snow and on ice. Research been conducted to implement laser-based fluorosensors from vessels (Brown and Fingas, 2003a), but the utility of these systems is not well understood.

5.2 Tunable Diode Laser Systems

Ethane/methane gas sensors based on the principle of Tunable Diode Laser Spectroscopy (TDLS) have been used to measure hydrocarbon mass flux rates generated by oil under ice in the laboratory and the field (Dickins, 2005; Brandvik and Johansen, 2007; Brobronikov et al., 2008). The atmospheric concentration of the gas can be deduced using a tunable diode laser to scan the absorption bands specific to methane and ethane. Concentrations less than one ppb are detectable. Since there are several sources that result in methane gas, ethane is a more unique marker for oil. Ethane detection should have a lower false alarm rate for oil than methane detection.

5.2.1 Application in Ice-Affected Water

Early tank tests with the Shell LightTouch system for detecting oil under ice determined that the ethane concentrations in the air above the oil was only approximately 0.7 ppb above the ambient concentration of around 100 ppb (Dickins, 2005). The measurements were challenging to take and required placing a bubble flux chamber on the ice in order to isolate the ethane emitted the ice from that in the test room. The calculated ethane flux was 3.0 x 10^{-3} (kg hr^{-1} km^{-2}), three orders of magnitude lower than the value that Shell states can be reasonably detected from several kilometers away (i.e., 1 kg hr^{-1} km^{-2}). These results suggest that practical application of TDLS sensors for detecting spills of unknown location is limited.

There have been challenges in preparing airborne TDLS-based sensors for detecting and mapping ethane and methane from oil under ice and snow. This is due to the cold weather as well as the relatively long collection times, with measurements taking several minutes to complete (Goodman, 2008). Furthermore, data interpretation can be challenging as observed signal and system performance is sensitive to changes with wind direction and the release of fumes from nearby machinery (Dickins, 2010).

Initial field tests using a TDLS sensor for detecting methane emissions from oil in ice-affected water were conducted at Svea (Hirst and O'Connor, 2007). These tests used a Boreal Line-of-Sight path-integrated methane sensor. The results suggested that the emission of light hydrocarbons during a large spill would be sufficient to be detected by Shell's sophisticated LightTouch system at distances of several kilometers. These findings were later contested in a response given by Brandvik and Johansen (2007). Brandvik and Johansen (2007) stated that the ethane and methane would be released from the oil within 10 minutes after the spill occurred, rendering the TDLS sensor ineffective for detecting an actual spill due to the short window of opportunity. TDLS sensors are most appropriate during blowouts where there is a continuous supply of fresh oil. In this case, however, the position of the leak would probably already be known. Additionally, since oil trapped under ice weathers much more slowly, TDLS may be useful for detecting oil concealed in ice (Dickins, 2005). Further work must be done to determine the corresponding ethane emission rates.

5.3 Laser-Ultrasonic Remote Sensing of Oil Thickness

The Laser-Ultrasonic Remote Sensing of Oil Thickness (LURSOT) is an aerially-deployed three laser airborne system for determining absolute thickness of an oil spill. Measurements are based on the excitation and detection of an acoustic pulse in the oil. Since the acoustic wave velocity of oil is known, oil thickness can be deduced from the acoustic wave time-of-flight (Brown and Fingas, 2003b).

This technique requires two lasers in a pump-probe configuration. An infrared CO2 pulsed laser is used to cause a rapid thermal expansion of the oil and thus excite (i.e., pump) an acoustic pulse in the material. A second laser probes the acoustic pulse reflected back from the oil-water interface. Upon reaching the oil-air interface, the reflected acoustic pulse causes a measurable Doppler shift in the frequency of the reflected probe laser signal. Consequently, the time delay between the initial CO_2 laser pulse and the measured frequency shift in the probe laser is related to the acoustic wave time-of-flight across the oil film. Finally, a continuous-wave HeNe laser is used to monitor the material surface, triggering the pump-probe system when the surface geometry is appropriate for oil thickness measurements (Brown and Fingas, 2003b).

5.3.1 Operational Performance in Open Water

Oil thickness has been successfully determined in both laboratory and small-scale field tests with this sensor (Brown and Fingas, 2003b; Environment Canada, 2007; Fingas, pers. comm., 2012), however, the performance of this technique in an ice environment is unknown. Due to the high attenuation of lasers in ice and snow, LURSOT would be impractical for characterizing oil under ice cover. On the other hand, there may be potential to determine oil thickness for spills in broken ice when oil is contained between floes. If oil is mixed with brash ice and slush, however, oil thickness measurements could have systematic errors due to the influence of ice on the acoustic pulse propagation and, thus, the deduced time-of-flight reading. The LURSOT system is expensive to maintain and requires a dedicated plane (Fingas, pers. comm., 2012). There is no LURSOT system currently in operation.

5.3.2 Application in Ice-Affected Water

The system has never been applied to ice conditions, and the testing of the system was discontinued. Therefore, LURSOT is not considered a priority for research and evaluation in ice conditions in the near term.

5.4 LIDAR

LIght Detection and Ranging (LIDAR) systems are based on laser technology (similar to fluorescence sensors). A number of airborne and ship-based LIDAR systems which operate in visible (i.e., non-UV) and IR ranges using CO2 lasers were developed and tested in USSR (Kozintsev et al., 2002).

5.4.1 Operational Performance in Open Water

The results indicate that it is possible to detect oil on the water by analyzing the backscattered LIDAR signal (Figure 23). Oil is easily detected on lakes and rivers provided that wave heights are low, which suggests that the system may function in ice covered water where there are no waves. Experiments in the Baltic Sea in high winds (up to 50 km/hour) have demonstrated that ship-based LIDAR systems using a CO_2 laser are effective (Kozintsev et al., 2002). Figure 24 shows signal scatter from a diesel fuel spill and sea water with winds about 1-5 km/hour.

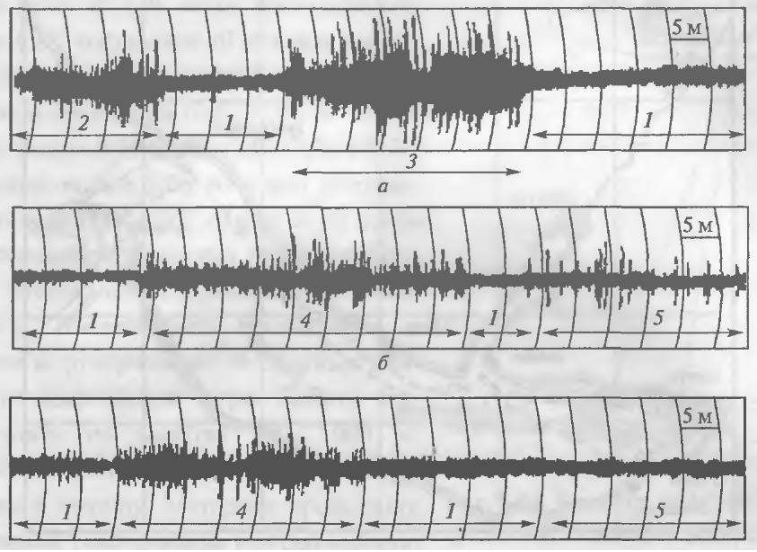

Figure 23. Recorded signal of optical LIDAR acquired on the test sites: river (top), lake (middle and bottom). Section of the signal: 1 - clear water, 2 and 4 – oil film with thickness of 0.2-0.5 micron, 3 - oil slick 3 micron, 5 – biological film (from Kozintsev et al., 2002).

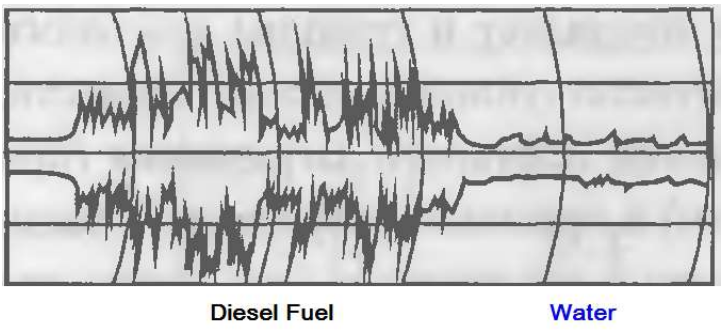

Figure 24. Backscatter from CO_2 LIDAR for the Baltic Sea (from Kozintsev et al., 2002)

5.4.2 LED Based Detector

Lumex (2012) has developed an active IR sensor for environmental monitoring and detection of oil pollution on water. The KRAB-1 detector is based on three infrared Light-Emitting Diodes (LEDs) to generate light beams (similar to laser) and a single channel receiver system. Signal processing capabilities are built into the microprocessor of the unit and the detection of oil on water is based on the difference in the coefficients of light reflection for oil and water. The device can be calibrated for different environmental conditions to reduce the impact of wind waves and background light on the measurement results. The instrument can be mounted on vessels or platforms and detect oil slicks with thicknesses greater than 0.5 μm over distances up to 25 meters. The instrument supports the generation and transmission of information products in real-time using wireless communications. The KRAB-1 sensor is shown in Figure 25.

Figure 25. KRAB-1 detector of oil film on the water surface (from Lumex, 2012)

5.4.3 Atmospheric and Marine LIDAR

The experimental LIDAR system, called ATMospheric and MARine LIDAR (ATMARIL-3), was developed for atmospheric-optical and hydro-optical measurements from the carrier platform (e.g., aircraft, vessel, etc.). This LIDAR is capable of revealing an oil film on the water surface and chlorophyll/phytoplankton in the water. The laser locator exploits the phenomenon that when short laser radiation pulses enter the water they are dispersed and illuminate various heterogeneities (e.g., polluting hydrosols, fishes). The optical signal reflected from the heterogeneities is received, detected and processed by various algorithms. The LIDAR consists of an opto-mechanical transmitter-receiver, a laser with power supply and cooling systems, an analog-digital converter and a computer (Figure 26). The system makes it possible to account for the influence of above-water atmosphere, including atmospheric precipitations, to reduce the effect of mirror glares resulting from micro-roughness and to adjust the LIDAR parameters to changing conditions and different tasks.

Figure 26. ATMARIL-3 on-board LIDAR. From the pamphlet of the Institute of Atmospheric Optics SB RAS, Russia, http://www.sbras.nsc.ru/dvlp/eng/pdf/059.pdf

5.4.4 LFS LIDAR

FUGRO operates an airborne (pod-mounted) spectral fluorescence/reflectance LIDAR that can be flown on both fixed wing aircraft and helicopters (Ed Saade, FUGRO, pers. comm., 2012) (see Figure 27).

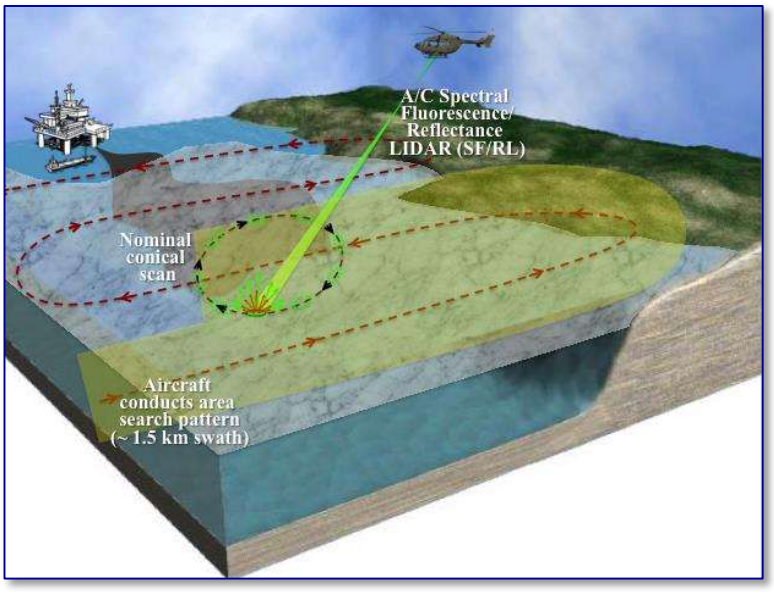

Figure 27. Fugro LFS LIDAR system

The nominal altitude of operation is between 500 and 3,000 ft. with ground-speed ranging from 50 to 250 kts. As the aircraft flies forward along its track, the LFS LIDAR continuously scans the surface (i.e., snow, ice or water) generating a georeferenced ice-thickness map (see Figure 27).

For aircraft altitude of 2,000 ft, ground speed of 125 kts and a scan angle of ±50° (i.e., a 1.5 km swath width), the Area Coverage Rate (ACR) is ~ 336 km^2/hr (with 30 m spatial sampling). For a 10 W laser transmitter pulsing at 750 Hz, the model predicts robust detection (i.e., 36 dB signal to noise ratio (SNR)) through four inches of snow (average) and eight feet of Arctic ice. Although not currently used for oil spill detection, it may be adapted to monitor and map oil in ice under appropriate conditions.

5.4.5 Application in Ice-Affected Water

Although there is no documented performance for detecting oil in ice conditions associated with the reviewed LIDAR technologies, adaptation to oil-in-ice scenarios may be feasible since the longer wavelengths are less attenuated by ice. In cases where LIDAR applications would be advantageous, further research could be considered as an alternative to LFS systems.

CHAPTER 6. EXPERIMENTAL SENSORS

There are a number of remote sensing approaches that have undergone limited laboratory or experimental testing, but do not have a documented history of operational application to oil spills. Several are discussed in this section.

6.1 Acoustic Sensors

Acoustic detectors use sonic and ultrasonic waves to probe the subsurface of an area. Seismic frequencies above 200 kHz can penetrate sea ice and are reflected from the ice/water or ice/oil interface (Dickins et al., 2006). Unlike electromagnetic energy in GPR, acoustic signals are not highly attenuated in ice allowing acoustic sensors to penetrate thick ice layers. Moreover, acoustic sensors are capable of imaging with shorter wavelengths enabling oil thickness to be deduced (Liberty et al, 2006).

Oil is an impurity in the ice and results in anomalies in the amplitude of the acoustic signal, which is used to differentiate oiled ice from oil free ice (Liberty et al, 2006). The difference in the elastic impedance between oil and water gives rise to a difference in the acoustic reflectance at the ice/water and ice/oil interfaces. As the variability of the ice structure results in variability in the collected acoustic signal, the acoustic reflection amplitude alone may not be sufficient to reliably differentiate oil from water at the base of the sea ice.

Exploiting the semi-solid properties of oil may provide an alternative method for acoustic-based detection of a spill under ice. At relatively high acoustic frequencies oil behaves as a semi-solid and can support both shear and compressive waves. The presence of oil at the ice-water interface is thus uniquely identified by the detection of two return peaks due to the compressive and shear waves (Goodman, 2008). By comparison only the compressive wave is returned at the ice/water interface. Since the shear wave and compressive wave in oil have velocities of approximately 1.9 km/s and 4.0 km/s, respectively, the detection process can be carried out in the time domain.

While acoustic sensors can be used to detect oil under ice, there are several challenges for deployment. The acoustic sensor (i.e., transducer) must be directly coupled to the ice surface due to the relatively high attenuation of sound in air. This may be achieved by freezing the sensor into the ice surface or by coupling the transducer to the ice through a layer of liquid (seawater or anti-freeze) (Dickins, 2006) and the ice must also be snow free. When operated above the ice surface acoustic sensors are strictly surface-based systems and cannot be deployed from vessels or aircraft.

6.2 Nuclear Magnetic Resonance Spectroscopy

Nuclear Magnetic Resonance (NMR) spectroscopy is a technique used to characterize the magnetic properties of a materials system. When a material is placed in a well-defined magnetic field, the magnetic dipoles in the specimen are aligned along a known direction. Subjecting the material to an electromagnetic pulse perturbs the magnetic dipoles away from equilibrium. Once the electromagnetic pulse ends, the dipoles return to equilibrium, producing a measurable electromagnetic signal in the process. This electromagnetic response is partially dependent on the material allowing NMR to image materials based on their magnetic properties (Kudryavtsev and Linert, 1996).

The earth's magnetic field is highly uniform and can be used for NMR with exciting and emitted electromagnetic pulses in the radio frequency range (Robinson et al., 2006). At these frequencies the electromagnetic fields can penetrate rock, soil and ice. The penetration depth depends on the dimensions of the loop antenna used to produce and receive the

electromagnetic signal and the material properties. Penetration depths of one to two meters require a loop antenna with a diameter of approximately 5 meters. This technique has been used successfully to detect subsurface water aquifers, which is unsurprising since water exhibits a strong NMR response (Legchenko et al., 1995).

Preliminary work has been done to assess the potential for using aerially-deployed earth field NMR for detecting oil under ice in experimental conditions (Nedwed et al., 2008) using a loop antenna slung from a helicopter. Initial findings suggest that the electromagnetic response obtained from oil is sufficiently different from water to allow oil detection. Furthermore, the relatively high rigidity of ice and snow results in NMR responses over much shorter timescales than those of oil and water and, thus, do not interfere with spill detection.

NMR imaging requires sophisticated computer control of the NMR phase and timing parameters and complex processing techniques, such as multi-dimensional Fourier transform (Robinson et al, 2006). Halse et al. (2006) demonstrated that the acquisition time in imaging mode is long, with imaging times for small objects in a laboratory setting ranging from 90 minutes to more than three hours. Much shorter integration times are required for the system to be operationally feasible. Accordingly, recent work has focused on improving antenna portability to facilitate aerial deployment, removing dead time between individual measurements to shorten the overall imaging time and improving the SNR to reduce the probability of false alarms. It is anticipated that a total imaging time of less than 10 minutes is achievable under operational conditions. Arctic field testing and validation with a full-scale prototype are expected within the next two years (Nedwed, pers. comm. 2013).

6.3 Trained Dogs

Recent studies have shown that trained dogs are effective for locating oil spills in soil (Huppunen et al., 2012) as well as in ice and snow (Brandvik and Buvik, 2009). After six months of training, GPS-tracked canines were able to locate oil based on the fumes which emanated through the snow. The dogs involved in the field tests, a Dachshund and two Border Collies, were able to pinpoint small test spills (approximately 400 mL) which were placed in a snow-covered hole in ice for one week. Using triangulation of the detected oil plume, a large 400 L spill was located.

In this initial field study the dogs detected oil 5 km from the source. This did not appear to be the upper limit for the range of detection and further study has been recommended (Dickins, 2010). All the experimental oil spills involved oil between ice and snow and a follow-up study would be useful to test the dogs' capabilities for locating oil under ice.

Dogs will likely be limited in an offshore spill response scenario. In addition to logistical challenges and safety concerns with deploying personnel on sea ice, there is currently no evidence that dogs can reliably detect oil embedded in or under ice. By contrast, trained dogs have considerable potential for application on landfast ice and large ice floes, and they should be considered for detecting oil covered by sediment or snow on shorelines. In the context of Arctic shoreline response, dogs may also contribute positively to the engagement of local stakeholders, since dogs constitute an important element of the social and economic fabric of northern communities.

CHAPTER 7. MULTI-SENSOR DATA INTEGRATION

The concurrent use of multiple sensors with complementary characteristics can minimize uncertainties associated with single sensors and facilitate the generation of enhanced, comprehensive information products, while allowing visual interpretation of imagery to remain a central element of oil spill surveillance (Fingas and Brown, 2011). Leifer et al., (2012) reports the importance of trained observers during early stages of a spill to deploy clean-up resources in the most effective and efficient manner. Visual analysis and interpretation by a trained operator implicitly integrates information from different sources according to the cognitive abilities and experience of the observer.

While visual interpretation works well for extracting qualitative information, generating quantitative information from diverse data sources and their dissemination to downstream users requires the use of automated systems. Data fusion provides a useful framework for integrating observations from multiple remote sensors (Pohl et al., 1998). Fusing information from various sources generates meaningful information products of higher quality than could be obtained from single data sources only and requires a range of methods to accurately integrate co-registered or geocoded image data sets at pixel, feature and decision levels (Solberg, 2006; Zhang, 2010).

7.1 Operational Multi-Sensor Systems

Integrated systems of multiple sensors are increasingly used for operational monitoring of oil spills and discharges. Specially equipped and dedicated aircraft using a combination of SLAR, UV/IR, FLIR, photo cameras, and video have emerged as a typical payload for maritime monitoring (Brown and Fingas, 2005; Baschek, 2007; Armstrong et al., 2008). In some cases, the basic sensor suite is extended by LFS and MWR systems, and the integration of other datasets, such as satellite imagery and Automatic Identification System (AIS) data, is increasingly enabled (Bonn Agreement, 2009).

In Germany, maritime oil spill surveillance in the North Sea and the Baltic Sea is accomplished using two dedicated and specially equipped Dornier Do 228 aircraft (Tufte et al., 2004; Robbe and Hengstermann, 2008). Equipped with OPTIMARE's MEDUSA maritime surveillance system, the sensor suite comprises SLAR, UV/IR, FLIR, MWR and LFS, together with FLIR and digital still and video cameras (Robbe and Zielinski, 2004; Gade and Baschek, 2013). In this configuration, the SLAR is used for far-range detection of potential slicks with a swath width of 60 km, while the other sensors are used in the near range to describe the slick and extract oil properties, including classification and thickness with swath widths of 500 m (UV/IR, MWR) and 150 m (LFS), respectively. The data streams are displayed on a central operating console, which is the primary interface with the operator for data manipulation and product generation.

An example of an oil slick captured by the five different sensors is presented in

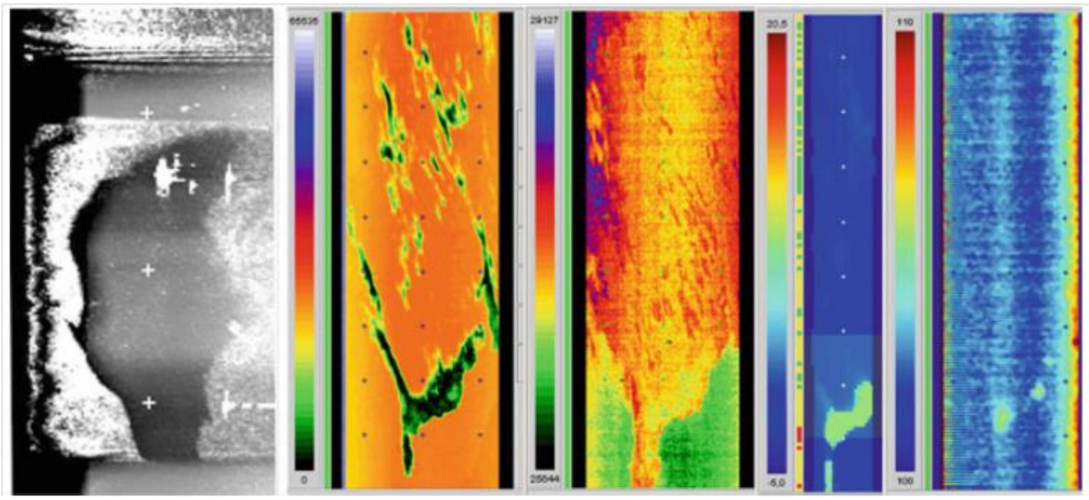

Figure 28.

To prevent operators from being overwhelmed by incoming multi-sensor data streams, the MEDUSA system's automated oil spill scene analysis system (OSSAS) module automatically generates a range of information products including raw UV/IR imagery, area of the oil spill, maps showing intermediate and thick areas within an oil slick, the centre of its area and specific size parameters (Robbe and Hengstermann, 2008). OSSAS also generates higher-order oil thickness products by merging UV/IR and LFS data. In this case, the UV signal is correlated with LFS-derived optical thickness and scaling-up is performed from the narrower LFS swath (150 m) to the spatial coverage of the UV sensor (500 m) (Robbe and Zielinski; Bogdanov et al., 2005). Figure 29 shows an example of the fused UV/IR and LFS data, with extrapolated optical thickness as a measure of oil film thickness and UV and IR spill contours.

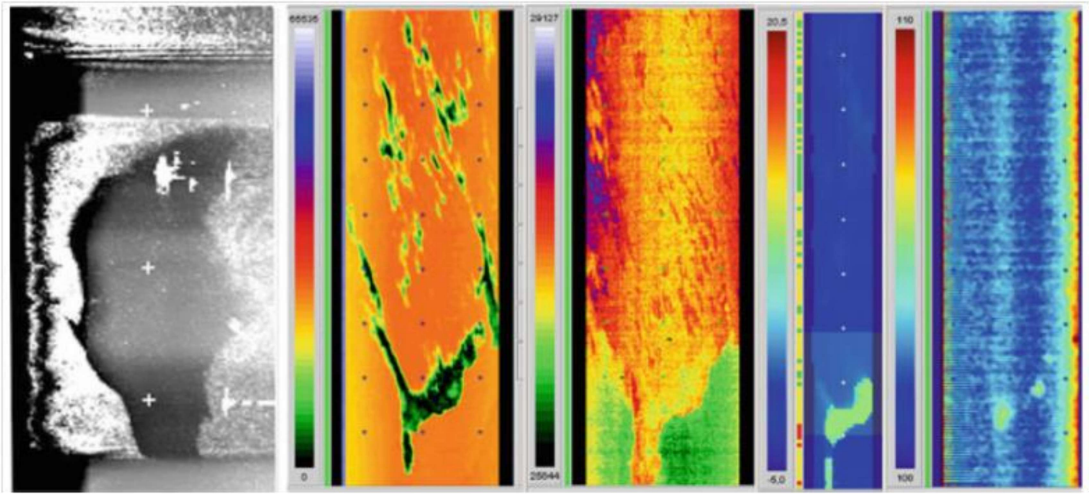

Figure 28. Oil pollution event observed using the MEDUSA system with concurrent acquisition of SLAR, IR, UV, LFS and MWR imagery (Gade and Baschek, 2013).

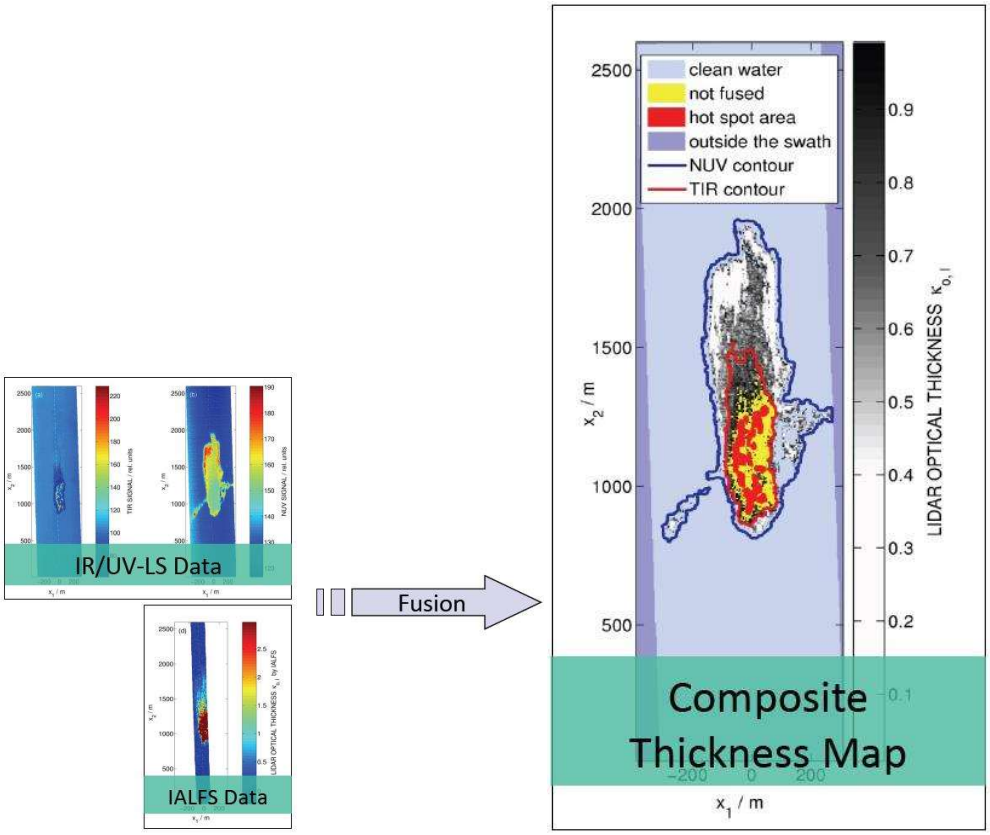

Figure 29. MEDUSA composite thickness map generated with OSSAS (from Robbe, 2012)

The Swedish Space Corporation has developed and installed more than 80 operational aerial monitoring suites since 1976 (Domargård, 2012). The latest MSS 6000 comprises a combination of SLAR, FLIR, IR/UV-LS, as well as still and video cameras. Data flows from imaging sensors and other equipment, including direction finder, search radar and AIS, are accessible to the operator via a dual operator console (Armstrong et al, 2008). The system further supports the integration of digital nautical charts and satellite SAR images. Depending on user requirements, information products can be generated in a variety of formats, including reports, map products, image maps and video feeds. All information generated can be disseminated in real-time to command centers and ground crews using high-speed INMARSAT communication. In addition to oil slick products, MSS 6000 supports vessel tracking and identification. An example of different data streams integrated within the MSS 6000 operator

console is presented in

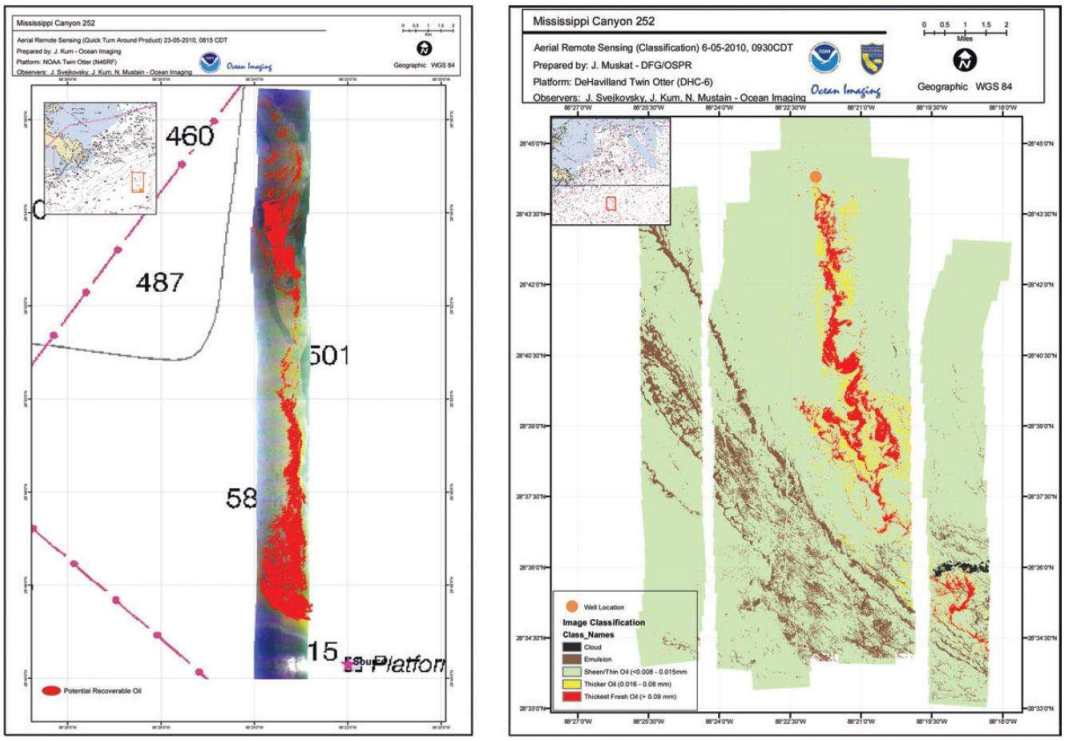

Figure 30.

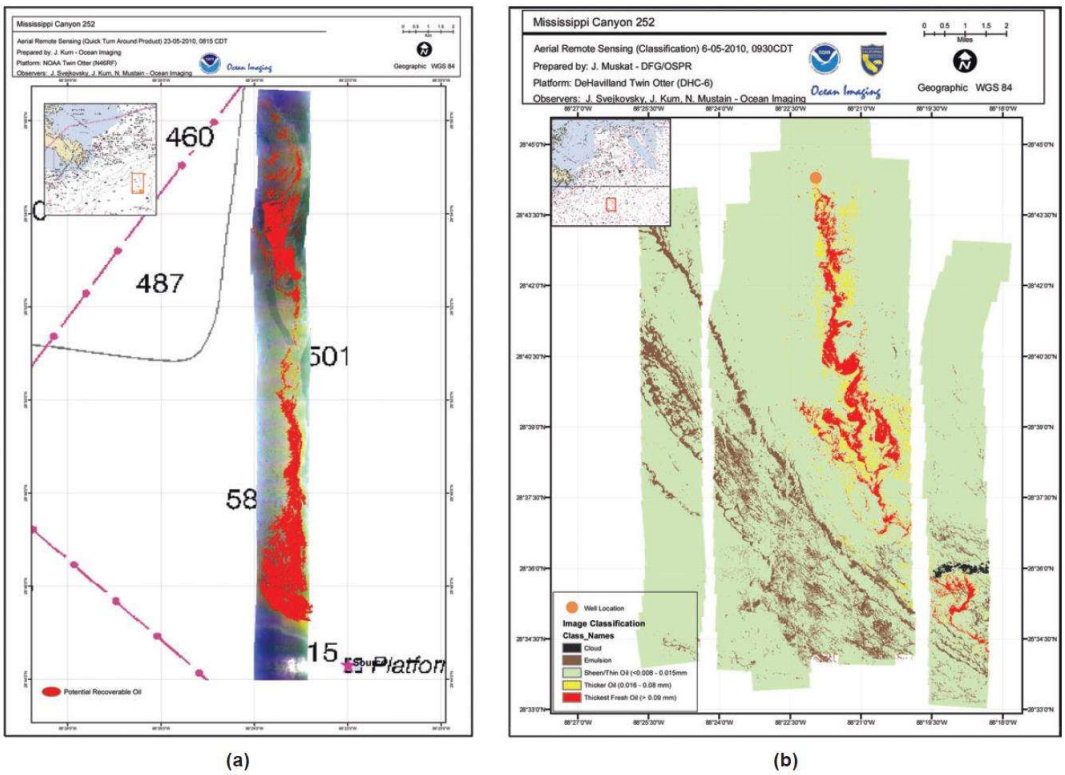

Figure 30. MSS 6000 Integrated system (from Domargård, 2012)

While MEDUSA and MSS 6000 are examples of permanent installations on dedicated aircraft, Svejkovsky et al. (2012) describe a mobile system by Ocean Imaging (OI) that combines multispectral and TIR sensors and can be mounted on aircraft of opportunity. The system consists of a DMSC MK2 progressive-scan CCD camera with four selectable narrow (10 nm) spectral bands within the spectral range of 400 to 950 nm, together with an IR-TCM640 uncooled micro-bolometer measuring emitted radiation from 7.5 to 14 µm. The spatial integration of the two sensors is based on a combined differential GPS and inertial measurement unit with a circular positional error of 2 m, resulting in an RMS error of less than 6 m. At an altitude of 3800 m, the ground resolutions are 2 m (multispectral) and 4 m (TIR), with a swath width of 2048 m.

Building on established principles of visual interpretation, the system uses a two-tiered process to generate oil spill information products with up to six oil thickness classes. In a first stage, a neural network is used to differentiate oil and water, while a second step involves extracting oil thickness classes using a fuzzy ratio-based classification. Field and experimental validation results confirm that the combination of multispectral and TIR imagery enables characterization of oil thickness of up to 2 mm (Sveikovski and Muskat, 2009).

Figure 31 shows example products generated in-flight (a) and post-flight (b) during the Deepwater Horizon spill. The generation of detailed thickness classes requires additional calibration and operator input, and the final product includes a series of thickness classes as well as areas covered by emulsion. By contrast, the in-flight product, generated in NRT, shows only areas of thicker oil that are likely recoverable.

Figure 31. In-flight product for rapid turn-around (a) and fully processed post-flight product (b) with detailed oil thickness classification (from Svejkovsky et al., 2012)

OI information products are fully compatible with GIS typically used in oil spill response, such as NOAA's Environmental Response Management Application (ERMA) online mapping tool

(noaaerma.org). During the Deepwater Horizon response, repeat coverage with the OI system was also used to provide situational awareness with respect to vessels in the spill area, verify the effectiveness of sub-surface dispersant application and assess the impact of aerial dispersant application and the mapping of beached oil.

APTOMAR's SECurus system is a ship-mounted situational awareness and decision support tool comprising TIR and digital video sensors installed on a stabilized pointing unit that allows for images to be collected in all weather conditions (Hänninen and Sassi, 2010; Skjelten et al., 2011; Buffagni et al., 2012). A xenon searchlight is synchronized to point in the same direction as the cameras. The TIR camera uses a cooled mercury-cadmium-telluride (MCT) detector with a resolution of 640 x 512 pixels and operates in the spectral range of 3 to 5 µm (FLIR n. d.). At a sensitivity of 18 mK, the TIR camera generates estimates of relative oil thickness at distances of up to two nautical miles to support response measures. The video and TIR data streams are georeferenced and integrated into an electronic chart system (ECS) and displayed on a touch-input bridge console operated by a dedicated high-speed processor (see Figure 32).

Figure 32. View of bridge console depicting spill location on ECS, digital video and TIR imagery

An open sensor communication interface allows for the integration of inputs, such as radar-based oil spill detection systems and AIS and information can be generated and shared with other stakeholders in real-time. System performance was validated through planned exercises in collaboration with The Norwegian Clean Seas Association for Operating Companies (NOFO), and the system complies with NOFO requirements for oil recovery vessels on the Norwegian continental shelf (NOFO, 2009). In addition to spill response, the SECurus system is applicable to maritime surveillance and search and rescue operations.

7.2 Conceptual Systems

Yarovenko et al. (2011) describe a prototype shipborne pollution detection system based on the FLS-SUV fluorescent LIDAR system designed by Laser Diagnostic Instruments (LDI). The

system consists of a UV excimer laser and a hyper-spectral detector. A series of five field tests were carried out in 2010 using rhodamine and fluorescein dyes to simulate pollutants in water and an automated, two-tiered algorithm was implemented to detect and identify pollution. In the first step, a support vector machine was used to differentiate between unpolluted water and anomalies. In the second, a minimum distance classifier assigned detected anomalies to pollutant categories. The products were generated in real-time and disseminated via a dedicated web page. The process is presented in Figure 33.

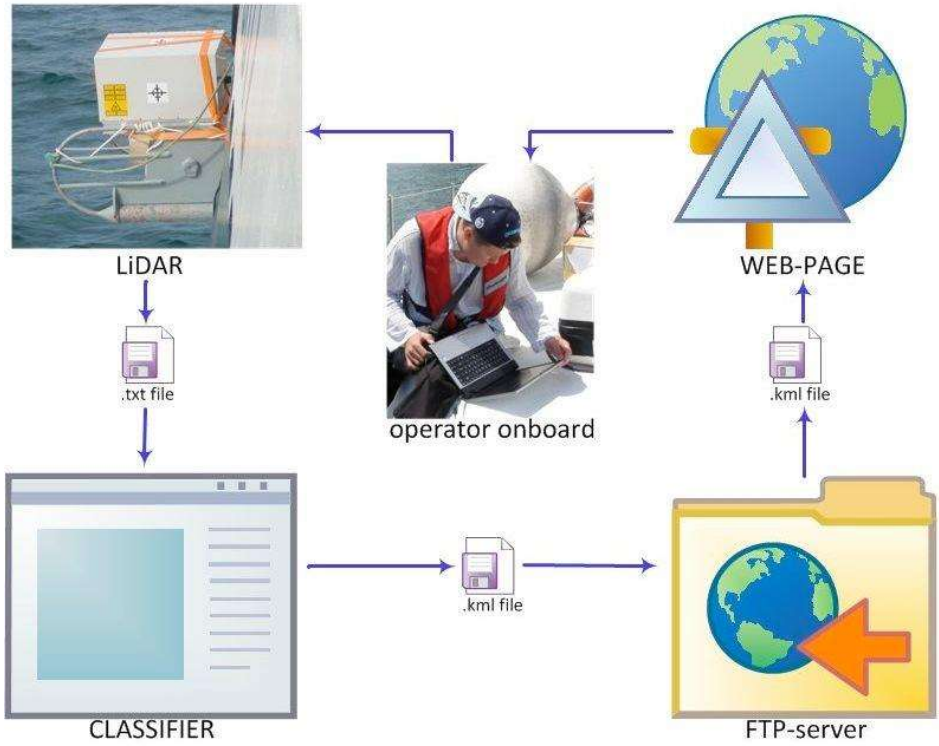

Figure 33. Process flow for real-time pollution detection and product dissemination using the FLS-SUV fluorescent LIDAR system (from Yarovenko et al., 2011)

Emphasizing an automated subsystem for marine oil spill monitoring, Lobkovsky et al., (2009) analyzed various components for an integrated environmental and geodynamic monitoring system based on offshore drilling platforms. The major components of the monitoring subsystem included satellite sensors, marine radar, and LIDAR. Oil spill detection and parameters estimation at distances to up 100 m from an oil platform were performed by the fluorescence LIDAR. As a result of preliminary work, it was shown that the LIDAR can also estimate the thickness of the oil film and therefore assess the volume of spilled oil. At distances exceeding 100 m, the primary tool for oil monitoring would be radar, such as the MIROS Oil Spill Detection System. Satellite sensors provide a synoptic perspective and the ability to characterize the larger environment, particularly in ice conditions. A graphic representation of the proposed multi-sensor measurement system is presented in Figure 34.

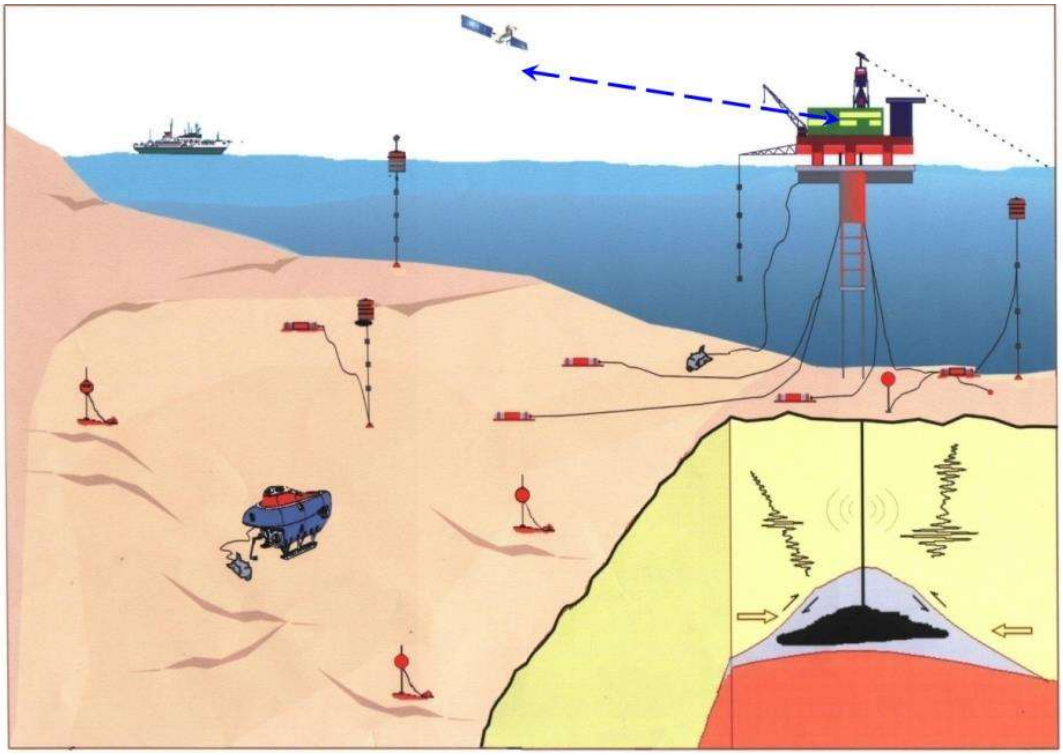

Figure 34. Multilevel multi-sensor measurement system for integrated environmental and geodynamic monitoring based on offshore drilling platforms (from Lobkovsky et al., 2009).

Moeller-Jensen (2006) proposes an oil spill identification system for offshore structures or ships. The system comprises a combination of 36 GHz and/or 90 GHz MWR and radar sensors, although other sensors could be integrated as well (e.g., UV/IR). Data collected from all sensors are transmitted to a control station for processing and analysis. Automated pattern recognition routines generate information products, which are transmitted to end users using available communication channels. Alternatively, raw images can be transmitted and subjected to operator interpretation at the control station or a remote location.

Andrews et al. (2012) describe a method for detecting oil on water using a combination of vessel or platform-mounted optical (i.e., visible and NIR) and thermal video sensors. The thermal sensor registers electromagnetic radiation in the spectral range of 7-14 µm and the sensor configuration provides a video stream monitored by an operator at a remote location. Individual frames are subjected to an analysis of temperature contrast, spectral contrast and thickness contrast to extract potential slicks. The detection of a potential slick triggers an alarm for the operator. The approach to sensor design and interpretation follows the observations of Shih and Andrews (2008). The system may integrate data streams from other sensors, such as visible light cameras, RF sensors, chemical sensors, Raman sensors or fluorescence sensors.

7.3 Data Fusion for Application in Ice-Affected Water

Although the performance of individual oil surveillance and detection systems in ice conditions is not yet fully understood, operational monitoring for oil slicks in ice environments will likely rely on the concurrent use of multiple sensing technologies. While this would apply to above surface data from satellite, airborne and vessel or platform-based sensors currently used in open water,

data streams from submerged platforms, such as remotely operated vehicles (ROVs) and autonomous underwater vehicles (AUVs) may be deployed to perform under-ice surveillance.

Integration in a multi-sensor network for oil spill monitoring requires accurate georeferencing and co-registration of all datasets. Image co-registration is required to ensure images from different sensors over the same region align. Georeferencing ties the imagery to the geographic reference system used during a response effort and is usually achieved by GPS measurements (e.g., Svejkovsky et al., 2012). Georeferencing is necessary to use remote sensing-based products with other spatial data within a dedicated GIS platform. Even in cases where detection products are not images, they should be associated with geographic coordinates and be available in a suitable GIS-compatible format to facilitate their downstream use (e.g. Yarovenko et al., 2011).

Ideally, raw sensor output acquired by multiple surveillance systems should be converted into information products that are meaningful and easily interpreted by response personnel and decision makers. Automated generation of information products would streamline the interpretation process and minimize variability due to varying operator experience. It would also allow for generation of information from a vast amount of input data in near real-time without overwhelming an operator (Robbe and Zielinski, 2004).

Effective communication is a critical element of oil spill response, especially with respect to the rapid transmission and dissemination of spill information products. Maritime communications largely relies on geostationary communications satellites orbiting the earth above the equatorial line (e.g., INMARSAT). While the theoretical coverage of such systems extends to 81°N, signal instability can occur at latitudes as low as 70°N due to the satellite's low elevation angles and the associated susceptibility to signal attenuation. In practice, at latitudes higher than 75°N, satellite communications is essentially restricted to using IRIDIUM satellite telephony. Over shorter distances, LOS communication via VHF is possible, as are HF and MF, albeit with significant bandwidth limitations.

The ICEMAR initiative (Hall, 2012) aims to address the issue of limited communications bandwidth and demand on resources from multiple users by implementing intelligent delivery of information content to vessels operating in the Arctic (Andrew Fleming, British Antarctic Service, per. comm., 2012). The ICEMAR system uses user location, area of interest and data compression together with available communications channel bandwidth to deliver information efficiently. ICEMAR is being developed primarily for ice-related information, but once operational it can be used to delivery any type of spatial information product, including spill reconnaissance products, in a wide range of data formats (e.g., SIGRID-2, S-57, GEOTIFF, JPEG, NETCDF, etc.). The ICEMAR architecture is presented in Figure 35.

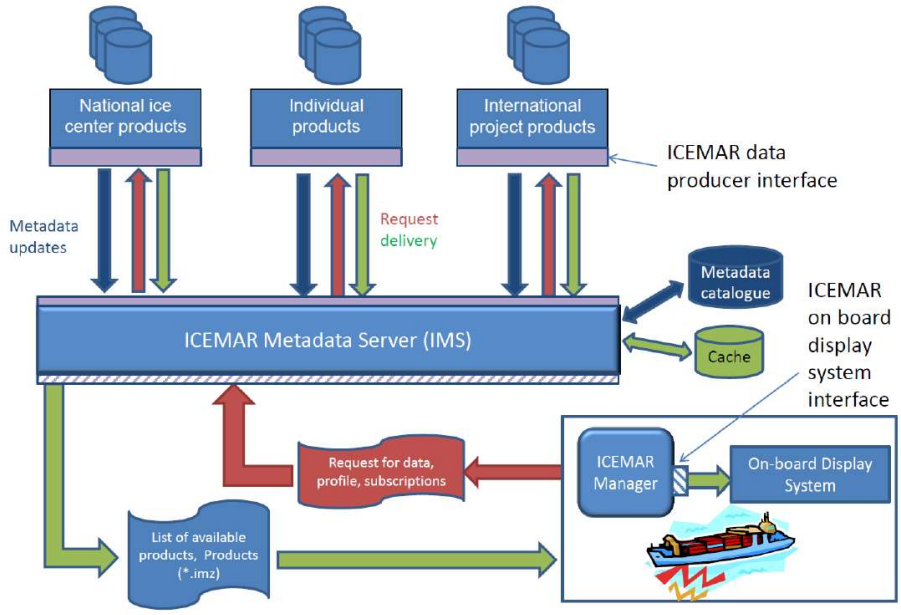

Figure 35. ICEMAR architecture. From Hall (2012)

Across the Arctic and other ice-affected areas, national ice services rely routinely on satellite imagery to generate ice information products in NRT. While the primary data source for ice charting is SAR imagery, data from optical satellites are used as well to aid interpretation, especially if radar images are not available. For spill response in ice-affected areas, satellite imagery can provide useful information on ice conditions and provide situational awareness. Depending on sea state and illumination conditions, it can also provide a synoptic view of major spill events (e.g., Leifer et al., 2012). A number of satellite systems acquire data systematically (e.g., LANDSAT, MODIS and AVHRR). Automated systems can be implemented to download and georeference all available imagery for a given area of interest. An example is presented in Figure 36 showing the online database operated by the Danish Meteorological Institute (DMI) for satellite images for the coastal zone of Greenland.

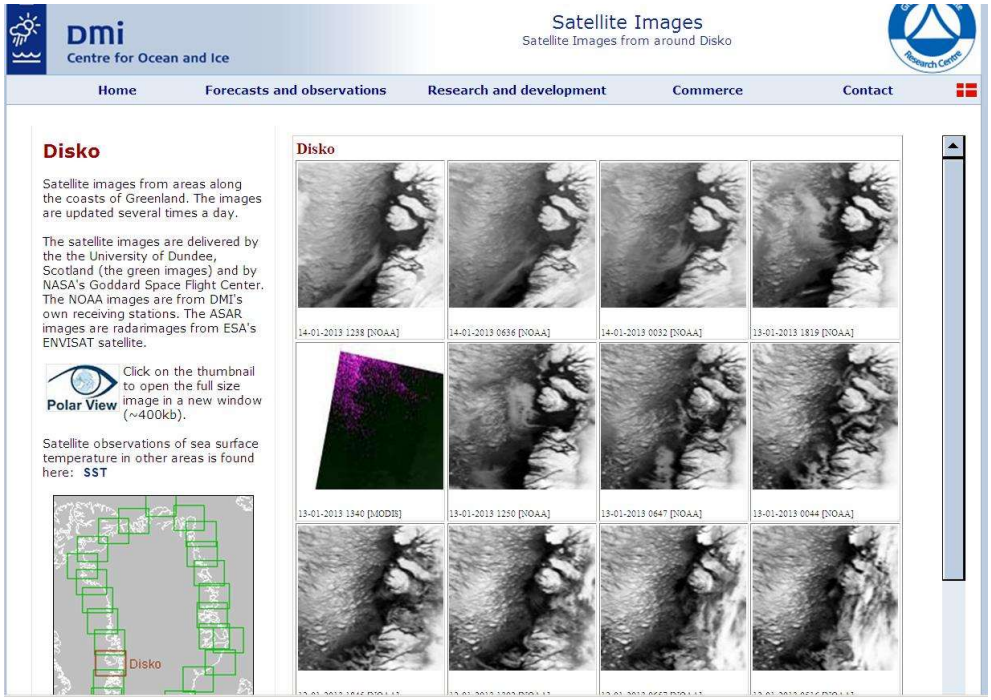

Figure 36. Online database of satellite images for the Disko Bay area, Greenland (DMI, 2013)

Ongoing acquisition of satellite imagery can be useful during response activities, since a search for imagery would not be required and the data are already readily available in a GIS compatible format. The future European satellite missions SENTINEL-1 (SAR) and SENTINEL-2 (optical) will be designed to collect data systematically and will be available in NRT via online archives. A steady stream of optical satellite imagery could also be exploited by developing nested approaches to extrapolate high-resolution observations from ship-borne or aerial sensors to the larger spatial footprint of a satellite image.

CHAPTER 8. EVALUATION AND RECOMMENDATIONS

This section summarizes the comparison of remote sensing technologies, describes the qualitative evaluation and outlines recommended near term priorities for research, development and operationalization of oil spill remote sensing in ice-affected waters. The most promising technologies are hyperspectral, laser-based, and microwave radiometer. It is recommended to proceed in two stages. The first, which can be performed in the laboratory or in specialized facilities, includes measurement and analysis of the hyperspectral signature and MWR images for oil in conditions appropriate to the Arctic marine environment to find the best suitable sensors (UV, VIS, IR, and laser-based). The second stage should be testing the selected sensors in the field in various ice and visibility conditions.

8.1 Technology Evaluation

A qualitative evaluation of the technologies described in the preceding sections was conducted using the scenarios and expected performance levels given in Table 6.

Table 6. Performance Scenarios and Expected Performance Levels

Performance Scenarios	**Description**
Detection of Oil among Pack Ice	Ice concentration < 30%: At sea ice concentrations less than 30%, oil is generally considered to be unaffected by the presence of ice; the performance of detection technologies is expected to be similar to open water conditions
	Ice concentration of 30% to 60%: The movement of oil and the ability to detect it are affected by the presence of sea ice
	Ice concentration > 60%: The oil is expected to move with the ice; oil is present in between ice floes and is mixed with slush and brash ice
Detection of Oil on Ice	The oil is present on the ice surface or on melt ponds
Detection of Oil under Ice, Snow or Encapsulated in Ice	The oil is under the ice, encapsulated within the ice or on the ice surface covered by snow
Detection of Oil in Low Visibility	Darkness
	Blowing snow
	Rain or fog
Expected Level of Performance	
The technology is proven and fully validated, its performance and limitations under the current scenario are well understood	
The technology is potentially applicable, partial validation may have taken place, but the technology has not been comprehensively validated for performance under the given scenario	
The likely performance of the technology is not known; it has never been tested under the given scenario	
The technology is not applicable to the given scenario	

Each technology was assigned an expected performance level for each ice condition and visibility scenario. The result of the evaluation is summarized in Figure 37. The assignment of colours corresponds to the performance levels described in Table 6, where green is assigned to cases where the technology is expected to perform well under a given scenario, yellow denotes

a potential for application, white indicates that the performance is unknown and cannot be estimated from available data and red designates cases where technologies are not applicable to the current scenario.

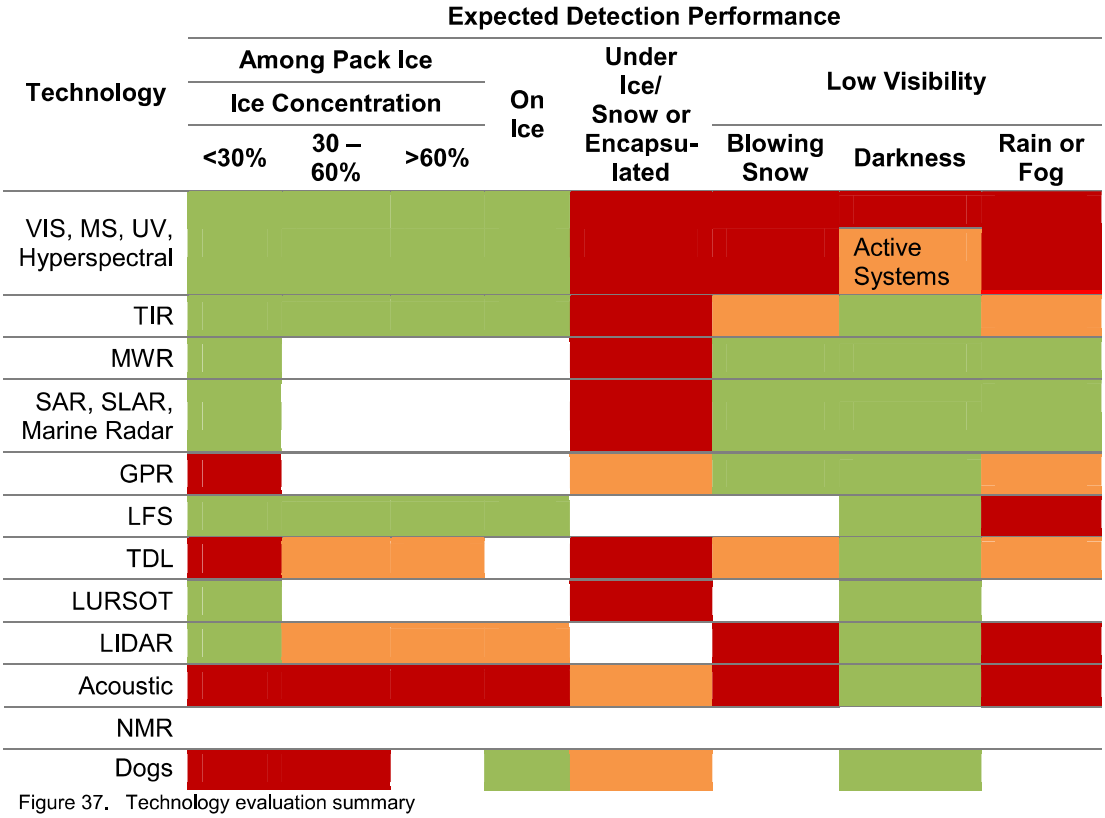

Figure 37. Technology evaluation summary

Optical (visible, multispectral and UV) and TIR sensors are routinely used in oil spill monitoring, and visual interpretation of still and video camera output remains an important element of operational surveillance. Oil spills may be easily confused with other phenomena, especially if the interpretation is not made by trained operators. A significant body of knowledge exists to describe the use of visible instruments to map and characterize oil on water, but there is little validated information available to describe their use in different ice conditions. A weakness of optical systems is their reliance on good visibility, which will be limited in Arctic conditions, while TIR has fewer visibility limitations. Capabilities of optical systems in darkness can be improved using illumination (active systems). A variety of imaging systems are available, many of which can be used on airborne platforms, as well as mounted on vessels or oil platforms. Recent studies demonstrate the utility of hyperspectral imagery, although at present the interpretation of hyperspectral datasets requires specialized expertise.

Microwave radiometers are being used primarily for pollution control and enforcement. Their performance in ice conditions is unknown.

Airborne laser fluorosensors have the unique ability to detect oil on different surfaces, including ice, with a high degree of certainty, classify oil type and determine the thickness of thin slicks. Despite these advantages, LFS systems are not widely used in pollution control. LFS instruments require dedicated aircraft and are restricted to relatively low flying altitudes and correspondingly narrow spatial coverage due to power limitations. Non-UV LIDAR sensors have

shown promise for detecting oil, with generally lower costs and increased availability with respect to LFS systems.

Tunable diode laser technologies are capable of oil detection, however, they may face two major challenges in ice environments, including the need for deployment in the field and expected time delay between spill occurrence and sensor deployment. As a result, this study does not consider them a priority for further research.

The LURSOT concept to extract oil thickness from an array of multiple lasers was successfully demonstrated. However, the development of the initial experimental system was not continued, and there is no LURSOT system in operation today.

Although radar sensors are routinely being used in the detection and monitoring of oil spills on water, their utility for detecting oil under ice conditions is likely limited. However, satellite, airborne and field-based radar systems are extremely useful in characterizing and mapping the general ice environment, tracking movement of ice and guiding deployment of surveillance equipment. In addition, they do not rely on solar illumination to operate, and in the case of satellite-based imagery the dependence on weather conditions is minimal. Therefore, radar sensors should be considered a critical element of any suite of sensing technologies deployed for spill response in ice-affected waters.

The application of GPR to detect oil under ice and snow is a relatively recent development, although initial research was undertaken as early as the 1980s. The use of ground-based units for detecting oil under ice is now considered operational, while research continues on airborne systems with frequency modulated continuous wave architecture.

Acoustic sensors have been investigated in the past for detecting oil under ice, although the initial research was not continued. In principle, it may be possible to detect oil under ice, but acoustic sensors require contact with the ice surface and therefore need to be deployed in-situ. In addition to logistical challenges, the interpretation of the acoustic signal is not trivial due to inhomogeneities in the ice cover that may affect detection.

NMR was recently proposed as a means to detect oil under ice. Present work is focused on improving the operational maturity of the technology including developing a helicopter-based system and improving SNR of the detected signal.

Trained dogs are capable of detecting oil buried in soil and under snow, but their performance in ice has not been evaluated yet. Since the use of dogs requires field deployment, their application has potential for areas near local communities.

8.2 Potential Technologies for Detecting Oil in Ice and Low Visibility

This section highlights the most appropriate confirmed and potential technologies for application in different ice and visibility scenarios to help focus research and development activities over the next 18-24 months.

8.2.1 Pack ice Concentration < 30%

The utility of the following technologies in open water conditions is well documented and they are therefore expected to perform well in low concentrations of sea ice:

- Optical imagery, including visible, multi-spectral, UV, and hyper-spectral sensors;
- Thermal infrared scanners and FLIR sensors;
- Microwave radiometers;
- Laser fluorosensors and LIDAR; and

- SAR, SLAR, and marine radar.

8.2.2 Pack ice Concentration 30 to 60%

Sensor technologies anticipated to perform well under intermediate ice cover conditions include the following systems:

- Optical imagery, including visible, multi-spectral, UV and hyper-spectral sensors;
- Thermal infrared scanners and FLIR sensors;
- Microwave radiometers; and
- Laser fluorosensors and LIDAR.

Given the widespread use of radar sensors, it would be useful to benchmark the potential of SAR, SLAR and marine radar technologies to detect oil at moderate concentrations of sea ice. This would include an estimation of the boundary parameters to generate Bragg scattering as well as consider the measurement of conductivity using SAR polarimetry.

8.2.3 Pack Ice Concentration > 60%

At high ice concentrations, the following sensing technologies are expected to be applicable for detecting oil between ice floes:

- Optical imagery, including visible, multi-spectral, UV and hyper-spectral sensors;
- Thermal infrared scanners and FLIR sensors; and
- Laser fluorosensors and LIDAR.

8.2.4 Detecting Oil on Ice

The following sensors offer potential for detecting oil present on the surface of sea ice or on melt ponds:

- Optical imagery, including visible, multi-spectral, UV and hyper-spectral sensors;
- Thermal infrared scanners and FLIR sensors;
- Laser fluorosensors and LIDAR; and
- Dogs.

8.2.5 Detecting Oil under Ice or Snow, or Encapsulated in Ice

Detecting oil under ice or snow is currently possible with the following technologies:

- GPR;
- Acoustic sensors;
- Dogs; and
- Drilling.

Active research is being undertaken using airborne and NMR systems, and it is anticipated that field testing of NMR will become available within two years.

LFS can potentially be used to detect oil under smooth ice and should be considered for further evaluation.

8.2.6 Detection in Darkness

Only passive optical systems, including visible, UV, and hyper-spectral sensors require sunlight to operate. Other systems, including active optical systems, can be used in darkness.

It should be noted that thermal infrared sensors require a measurable temperature difference between oil and the surrounding water or ice, and this differential is initiated by the absorption of

solar irradiation. At night, the temperature between oil and the surrounding area will equalize, and thermal imaging will become less applicable as the temperature difference decreases.

8.2.7 Detection in Blowing Snow

Operation of the following technologies would be possible in blowing snow:

- SAR, SLAR, Marine Radar;
- Thermal and FLIR ;
- GPR;
- Microwave radiometers; and
- Acoustic.

Thermal and FLIR systems as well as optical systems would have decreased visibility due to blowing snow, however, when the system is deployed on the platform operating within a short distance from the surface these systems may provide meaningful information. Radar systems (e.g. SAR) can operate in snow, however, detecting oil spills will be limited in high sea states.

8.2.8 Detection in Fog or Rain

Performance of IR and FLIR cameras in fog and rain depends on three factors:

- Atmospheric conditions (category of fog or rain);
- The type of IR sensor (its wave range); and
- Properties of the observed oil spill including size, temperature difference to water or ice background and oil type.

Performance of optical systems is significantly limited by fog and rain. Oil spill detection capabilities in open water by SAR and SLAR systems are also be affected by rain, as rain changes the ocean surface roughness in a similar way that oil spills dampen capillary waves. The following technologies can operate in rain and fog:

- SAR, SLAR, Marine Radar;
- GPR;
- Thermal and FLIR;
- Microwave radiometers; and
- Acoustic.

8.3 Recommendations for Research

This section presents recommendations and further considerations for operationalizing remote sensing technologies for Arctic oil spill detection and monitoring. Recommended actions include validating and testing the currently operational technologies in ice conditions, embedding trained oil observers in ongoing operations, developing and implementing integrated multi-sensor systems and automated data processing algorithms and working towards standardized products and processes for remote sensing of oil in ice environments. A list of potential suppliers and research partners is provided in Appendix A.

8.3.1 Validation of Currently Operational Technologies for Application in Ice

Presently research is ongoing on GPR and NMR technologies, which showed potential for detecting oil under ice and snow. There is little research available to describe the performance of other remote sensing technologies for detecting and monitoring oil in ice-affected marine environments. It is therefore recommended to investigate the performance in ice conditions for technologies currently used to monitor oil in open water. Hyperspectral sensors, which include UV, visible, and IR wave ranges have great potential and should be explored further. Active

hyperspectral, laser based systems (LIDAR, LFS), and microwave radiometers should be considered due to their ability to operate in low visibility conditions.

A ***first stage*** would comprise preliminary experiments conducted in laboratories, specialized test facilities, and if possible, in the field. For each sensor, this research would be focused on understanding the underlying physical mechanisms for oil detection in different ice regimes as well as other conditions specific to the Arctic marine environment.

8.3.1.1 Hyperspectral Sensors

Hyperspectral sensors measure the reflected electromagnetic (EM) signal at tens to hundreds wavelength bands, including UV, visible, and infrared. Hyperspectral data provide complete spectral information to identify the hyperspectral signature for oil. Therefore, it is recommended initially to use hyperspectral sensors in the laboratory or field experiments to measure the EM spectrum for oil in good visibility conditions in an environment similar to the Arctic. These experiments may include tests for different types of oil in water and various ice conditions at ambient temperatures present in the Arctic. Knowledge of the hyperspectral signature of Arctic oil will demonstrate which bands are most suitable for discriminating between oil and the ice/ocean background. The results will be used as a baseline to prioritize which parts of the spectrum from visible to IR merit further research. These specific spectral bands may be further explored using off-the-shelf sensors, which are already being used to detect oil in open water.

It is of particular interest to test active hyperspectral systems in low-visibility conditions (hyperspectral sensor with illumination). There are several sources of illumination suitable for this purpose (multi-wavelength hyperspectral LIDAR systems, white laser and Xenon search light). Experiments can be performed with laboratory instruments similar to the one described in Section 2.3.

8.3.1.2 Laser Systems

Laser fluorosensors can be used to probe oil on various surfaces (e.g., snow, ice and water). The optical attenuation coefficients for some ice types may allow laser illumination to penetrate through ice covers. Past research suggests that this approach works well with snow-free ice up to about 1 m thick.

LIDAR systems can be used for oil detection with airborne and ship-based systems which operate in the visible and IR ranges. Past results demonstrate that reflected laser beams from the oiled water has a detectable difference in intensity, which is important for detecting oil in water with low ice concentrations. The ability to detect oil on the ice/snow surface can be investigated in laboratory or field experiments. Research on hyperspectral systems, recommended in Section 8.3.1.1, would provide useful input to determine the appropriate wavelength of the LIDAR system.

8.3.1.3 Microwave Radiometers

MWRs are capable of detecting, measuring, and mapping oil layers (in open water) with a thickness in the range from 0.05 to 3 millimeters. The benefit of this system is the ability to operate in low visibility conditions caused by precipitations and darkness. It would be useful to analyze potential of this technology for oil detection in various ice regimes and Arctic conditions.

8.3.2 Testing of Validated Technologies

The ***second stage*** would estimate the applicability of the validated sensors in different scenarios in the field, including oil in varying concentrations of pack ice as well as on fast ice or large ice floes. The performance of the optical (UV and hyperspectral) sensors for detecting oil

in slush and brash ice is unknown. Additional testing under field conditions is required to determine the capabilities of these sensors for detecting oil in a variety of ice conditions (i.e., oil on ice and snow, oil between ice floes, etc.).

The second validation stage would serve to identify the deployment platforms appropriate for the different sensors. Field experiments can be aligned with the JIP's Field Research Working Group for maximum efficiency.

Satellite, airborne and marine radar imagery will be an important element of all response activities in ice-affected waters. In areas where environmental conditions allow for radar-based oil spill detection, satellite images can be subjected to analysis and extraction of potential spill areas. If environmental conditions are not suitable for spill monitoring, satellite radar data will still be valuable for providing ice information to responders and operators in near real-time, and provide a general synopsis of the area of interest. Radar systems should be benchmarked during field trials to determine the range of ice conditions over which oil slick detection is likely (e.g., varying concentrations of pack ice).

8.3.3 Integrated Networks of Multiple Sensors

As no single technology will likely fulfill the needs of all aspects of oil detection in ice environments, a suite of multiple sensors is required to improve detection performance. Recommended sensors should not be used in isolation, but integrated within a suitable architecture to achieve effective data acquisition, information product generation and product dissemination to other stakeholders. Depending on the needs of the individual operations, the sensor networks may include different sensors mounted on a single drilling rig (e.g., radar, optical and TIR), or multiple sensors on multiple platforms, including rigs, vessels, satellites, aerial platforms and underwater vehicles.

The data streams from all sensors should be integrated using accurate geopositioning and accessible from one or more central interfaces (e.g., on the bridge of a vessel, incident command post). Ideally the generation of value-added information products (e.g., spill location, thickness estimates) should be accomplished in an automated fashion with limited quality control to facilitate the dissemination of products in real time over existing communication channels and allow response personnel without specialized knowledge of the sensors involved to interpret output products. Automated detection algorithms may need to be customized for specific geographic areas due to differing environmental conditions (e.g., sediment load, water depth, algae, etc.).

As the number of satellites used for remote sensing is steadily growing, new and emerging satellite sensors should be incorporated in ongoing research activities. Of particular interest are the future C-Band SAR missions SENTINEL-1 and RADARSAT Constellation Mission (RCM). The contribution of optical satellite missions should also be considered. For example, the currently operational Disaster Monitoring Constellation (DMC) provides LANDSAT-type multispectral imagery at 30 m and 20 m resolution and a maximum swath width of 600 km, resulting in near daily global repeat coverage. SENTINEL-2, scheduled for launch in 2014, will have near daily coverage at high latitudes with multispectral data provided at a spatial resolution ranging from 10 m to 60 m. The hyperspectral mission ENMAP, expected to be launched in 2016, will collect hyperspectral imagery from 420 to 2450 nm at a spatial resolution of 30 m and a swath width of 30 km. The investigation of satellite imagery should also include the utility of nested approaches to scale-up airborne or in-situ observations to the larger spatial coverage provided by satellite sensors.

Presently, there are several successful examples (e.g., OSSAS, DISMAR) of automated or semi-automated systems being used operationally for multisource data fusion and analysis to simplify the work of analysts in oil spill monitoring. Consequently, developing algorithms and software to support implementation of the potential sensors and systems has to be one of the final steps for operationalizing oil detection and mapping in the Arctic environment.

8.3.4 Standardized Products and Processes

Sensor evaluation and development of information extraction processes should be preceded by comprehensive analysis of the information requirements of response personnel and decision makers. Emphases should be placed on information content (e.g., outline of total area affected, outline of recoverable oil only, map of oil types/emulsions, etc.), data format and delivery mechanisms required at different stages of response and mitigation activities. This analysis should be carried out by involving a broad sample of representative stakeholders concerned with spill response in ice conditions. The output of this analysis would shape guidelines for best practices, which could evolve into globally accepted standards in the future.

Having well defined information requirements and product specifications will also make it easier to evaluate technical solutions provided by service providers and developers in the future, as there will be an accepted set of standards and performance benchmarks. Established standards would also facilitate future implementation of integrated systems in plug-and-play architectures designed to accept any compatible technology.

8.3.5 Trained Observers Embedded in Operations

Visual interpretation of oil slicks remains a key element of oil spill monitoring. Accordingly, existing programs to train oil spill observers should be augmented by elements focusing specifically on detecting and monitoring oil in different ice conditions using principles of visual interpretation of optical, TIR and radar imagery.

Trained observers also play a key role in the early characterization of spills. To avoid a significant time lag between the spill occurrence and the arrival of trained observers, it is suggested to embed trained observers in ongoing operations. One possibility is to extend existing ocean or sea ice observation and forecast activities to include oil spill monitoring. Having trained oil spill observers on-site or near-site could limit uncertainties in response decisions early in a spill situation. Quick boarding of such trained operators on aircraft of opportunity with hand-held sensors or with deployment of suitable devices may be useful.

8.3.6 Automation of Data Analysis

Operational application of monitoring systems based on multiple sensors or sensors with challenges in data analysis and interpretation requires development of automated tools for data analysis. For example, hyperspectral sensors can contain hundreds of spectral bands and automation is needed to simplify work of the analyst. Automating the information extraction process will make it easier to integrate hyperspectral and other sensor outputs into operations for the following reasons:

- Rapid interpretation/flagging of data allowing the analyst to spend more time focusing on interpreting results instead of viewing large data streams;
- Generation of informative products from complicated data sets (e.g., multi-spectral or hyperspectral imagery).

Interpretation of GPR data acquired over sea ice with inclusions can be challenging due to the complex backscatter process that results in variations of signal magnitude and phase.

Application of laser-based system (LIDAR and LFS) can be simplified with the development of signal processing and analysis software for automated detection of the oil reflected signal.

CHAPTER 9. ACKNOWLEDGEMENTS

We would like to acknowledge the reviewers from JIP Remote Sensing In Situ Burn technical work group for their suggestions and recommendations to the draft report. During the project period, C-CORE has contacted the following leading experts in the area of oil monitoring: David Dickens, Ron Goodman, Merv Fingas, Tim Nedwed, and Ed Saade; and we would like to acknowledge them for their constructive advices and suggestions.

REFERENCES

Adalsteinsson, D.; Camassa, R.; Harenberg, S.; Lin, Z.; McLaughlin, R. M.; Mertens, K.; Reis, J.; Schlieper, W.; and White, B. (2011), "Subsurface trapping of oil plumes in stratification: Laboratory investigations, in Monitoring and Modeling the Deepwater Horizon Oil Spill: A Record-Breaking Enterprise" Geophysical Monograph Series, 195, pp. 1-7.

Ahmed, S.; Gilerson, A.; Oo, M.; Zhou J.; Chowhardy J.; Gross, B. and Moshary, F. (2006) "The polarization properties of reflectance from coastal waters and the ocean-atmosphere system", in the Proceedings of SPIE Vol. 6360 Remote Sensing of the Ocean, Sea Ice, and Large Water Regions 2006.

Alawadi, F. (2011) "Airborne/spaceborne oil spill determining system." US patent # 2011/0101225 A1.

Allen, A.A. (2008) "Oil Spill Response Planning for Shell Shell's Offshore Exploration Program in s the Alaskan Beaufort Sea." Alaska Forum on the Environment, Anchorage, Alaska, February, 2008.

Alimov S. V.; Kosachev, D. V.; Danilov, O. B.; Zhevlakov, A. P.; Kashcheev, S. V.; Mak, A. A.; Petrov, S. B. and Ustyugov, V. I. (2009) "Aviation Raman LIDAR with ultraspectral resolution", Journal of Optical Technology 76(4), pp. 199 – 207.

Andrews, A.; Clayton, M.; Mullins, O.; Shih, W.-C. (2012) "Method and Apparatus for Oil Spill Detection," Patent # EP 2372352 A (US8124931).

Andrew, Fleming British …per comm., 2012

APTOMAR. (2012) "The SECurus System," Brochure at http://www.aptomar.com/wp-content/uploads/2010/09/SECurus-brochure-PDF.pdf (available on 20.12.2012).

Armstrong, L.; Fast, O.; Schneider, H.A.; Abrahamsson, A.H. (2008) Integration of Airborne AIS Brings a New Dimension to the Detection of Illegal Discharge of Oil Spills. International Oil Spill Conference: IOSC 2008. International Oil Spill Conference Proceedings: May 2008, Vol. 2008, No. 1, pp. I-XXIII.

ASL. (2012). Semi-Automated Classification of Oil slicks at sea using RADAR and Optical imagery (SACORO), PR-717.

ATMARIL-3 Pamphlet of the Institute of Atmospheric Optics SB RAS, Russia, http://www.sbras.nsc.ru/dvlp/eng/pdf/059.pdf (available on 20.12.2012)

Babichenko, S. (2008) Laser Remote Sensing of the European Marine Environment: LIF Technology and Applications. In: Barale, V. and Gade, M. (eds.) Remote Sensing of the European Seas. Springer Science+Business Media B.V. 2008

Babiker, M.; Kloster, K.; Sandven, S. and Hall, R. (2010) "The Utilization of Satellite Images for the Oil in Ice Experiment in the Barents Sea", SINTEF Materials and Chemistry, SINTEF, Oil in Ice – JIP, Report No. 29.

Baschek, B. (2007) "Multi-Sensor Oil Spill Surveillance Program", presented at the International Oil & Ice Workshop, Anchorage AK.

Bobra, A. M. and Fingas, M. F. (1986) "The Behaviour and Fate of Arctic Oil Spills", Water Science and Technology, 18, pp. 13-23.

Brobrovnikov, S. M.; Serikov, I. B.; Arshinov, Y. F.; Sakovich, G.; Vorozhtsov A. and Eisenreich, N. (2008) "Remote detection of leaks in gas pipelines with an airborne Raman LIDAR", in Strategic Insights, Vol. 7 (Center for Contemporary Conflict, Moterey).

Bogdanov, A. Robbe, N., Wald, L. and Cauneau, F (2005) Data Integration System for Marine Pollution and Water Quality. Final Report on Multi-Source Data fusion and Algorithms. DISMAR Report 16, 68 pp.

Bonn Agreement (2009) "Bonn Agreement Aerial Operations Handbook."

Bradford, J. H.; Liberty, L. M. and Dickens, D. F. (2008) "Locating Oil Spills Under Sea Ice Using Ground-Penetrating Radar", The Leading Edge, 27(11), pp. 1424-1435.

Bradford, J. H.; Dickins, D. F. and Brandvik, P. J. (2010) "Assessing the potential to detect oil spills in and under snow using airborne ground-penetrating radar", Geophysics, 75(2), pp. G1-G12.

Brandvik, P. J. and Buvik, T. (2009) "Using dogs to detect oil hidden in snow and ice – Results from field training on Svalbard April 2008", SINTEF Materials and Chemistry, SINTEF, Oil in Ice – JIP, Report No. 14.

Brandvik, P. J. and Johansen, J. (2007) “Comments to Shell’s Methane Measurements at Svea April 2007”, SINTEF Materials and Chemistry, SINTEF, Oil in Ice – JIP, Report No. 5.

Brekke, C. and Solberg, A.H.S. (2005) Oil spill detection by satellite remote sensing. Remote Sensing of Environment, Vol. 95 (1), pp. 1-13.

Buffagni, M.; and Aiello, G.; Bjørnbom, E.; Hansen, O.; and Foldnes, G.E.; Thorbjørnsen, S.; Engen, F. (2012) “Coastal Oil Spill Preparedness Improvement Programme (COSPIP) and Memorandum of Understanding - Comprehensive Joint & Industrial Project Focusing on Coastal Oil Spill Challenges,” International Conference on Health, Safety and Environment in Oil and Gas Exploration and Production, 11-13 September 2012, Perth, Australia.

Buist, I. A.; Potter, S. G. and Dickins, D. F. (1983) “Fate and behaviour of water-in-oil-emulsions in ice”. In Proceedings of the 6th Arctic Marine Oilspill Program Technical Seminar, Environment Canada, Ottawa, pp. 263-279.

Brown, C. E. (2011) “Laser Fluorosensors”. In Fingas, M. F. (Ed.), Oil Spill Science and Technology: Prevention, Response, and Clean-up (New York, Elsevier).

Brown, C. E. and Fingas, M. F. (2003a) “Review of the development of fluorosensors for spill application”, Marine Pollution Bulletin 47, pp. 477 - 484.

Brown, C. E. and Fingas, M. F. (2003b) “Development of airborne oil thickness measurements”, Marine Pollution Bulletin 47, pp. 485 - 492.

Brown, C. E.; Fingas, M. and Marois, R. (2005) “Laser Fluorosensor Demonstration Flights around the Southern Coast of Newfoundland”, presented at the 2005 International Oil Spill Conference.

Campbell, J. B. and Wynne, R. H. (2011) Introduction to Remote Sensing, 5th Edition (New York, The Guilford Press).

Clark, R. N.; Swayze, G. A.; Leifer, I.; Livo, E.; Kokaly, R.; Hoefen, T.; Lundeen, S.; Eastwood, M.; Green, R. O.; Pearson, N.; Sarture, C.; McCubbin, I.; Roberts, D.; Bradley, E.; Steele, D.; Ryan, T.; Dominguez, R. and the Airborne Visible/Infrared Imaging Spectrometer (AVIRIS) Team (2010) “A Method for Quantitative Mapping og Thick Oil Spills Using Imaging Spectroscopy”, U.S. Geological Survey, Reston, Virginia, Open-File Report 2010-1167.

Cocks, T.; Jenssen, R.; Stewart, I.; Willson, I.; and Shields, T. (1998) “The HyMap(TM) airborne hyperspectral sensor: The system, calibration and preformance.” In Proceedings 1st EARSeL workshop on imaging spectroscopy, 6-8 October, 1998. Zürich, Switzerland, pp. 37-42.

CRREL. (2012) "Detecting oil in sea ice using Ground-penetrating radar: Developing a new airborne system," The Cold Regions Research and Engineering Laboratory (CRREL). Test Report.

Deslauriers, P. C.; Martin, S.; Morson, B. and Baxter, B. (1977) “The physical and chemical behaviour of the Bouchard No. 65 oil spill in the ice-covered waters of Buzzards Bay”, National Oceanic and Atmospheric Administration (NOAA), Environmental Research Laboratory, Boulder, CO, 185 p.

Dick, R., Fruhwirth, M., Fingas M., and Brown, C. (1992) “Laser fluorosensor work in Canada.” pp. 223–236 in Proceedings of the First Thematic Conference: Remote Sensing for Marine and Coastal Environments.

D. F. Dickins Associates Ltd.; Shell Global Solutions (US) Inc. and Polaris Applied Sciences Inc. (2005) “New and Innovative Equipment and Technologies for the Remote Sensing and Surveillance of Oil in and Under Ice”, prepared for the United States Department of Interior, Minerals Management Service, Herndon, Virginia, USA.

Dickins, D. F. (Ed.) (2010) “Project P5: Remote Sensing Summary Report”, SINTEF Materials and Chemistry, SINTEF, Oil in Ice – JIP, Report No. 30.

Dickins, D. F. (2011) “Behavior of Oil Spills in Ice and Implications foe Arctic Spill Response”, presented at the Arctic Technology Conference, Houston, Texas, USA.

Dickins, D. and Andersen, J. H. (2009) “Remote Sensing Technology Review and Screening”, SINTEF Materials and Chemistry, SINTEF, Oil in Ice – JIP, Report No. 22.

Dickins, D.F. and Andersen, J.H. (2010) “Evaluation of Airborne Remote Sensing Systems for Oil in Ice Detection.” SINTEF Oil-in-Ice final report No. 28, Trondheim, 2010.

Dickins, D. and Buist, I. (1981) “Oil and gas under sea ice”, Dome Petroleum Ltd. For COOSRA, Report CV-1, Vol I and II.

Dickins, D. F. and Buist, I. (1999) “Countermeasures for ice covered waters”, Pure and Applied Chemistry, 71(1), pp. 173-191.

Dickins, D. Brandvik, P. J.; Faksness, L.-G.; Bradford, J.; and Liberty, L. (2006) “2006 Svalbard Experimental Spill to Study Spill Detection and Oil Behavior in Ice,” report prepared for the U.S. Department of Interior, Minerals Management Service, contract number 1435-0106-CT-3925.

Dickins, per. Comm., 2013

DMI. (2013). http://ocean.dmi.dk/arctic/modis.uk.php, accessed January 14, 2013

Domargård, A. (2012) “Airborne Maritime Surveillance Systems.“ Presentation of Interspill, London, UK, 13-15th March 2012.

Dong, X.; Xi, B.; Crosby, K.; Long, C. N.; Stone, R. S.; and Shupe, M. D.; (2010) A 10 year climatology of Arctic cloud fraction and radiative forcing at Barrow, Alaska, J. Geophys. Res., 115, D17212,

Ed Saade, Fugro, pers. Comm.., 2012

Egset, C. N. and Nøst, E. (2007) “Oil Spill Detection System Based on Marine X-Band Radar”, Sea Technology magazine.

Environment Canada (2007) “Protecting Canada’s Coasts: Using Laser Remote Sensing to Detect and Track Oil Spills”, retrieved from the Environment Canada website: www.ec.gc.ca/scitech

Environment Canada (2013) “Blowing Snow,” Public Alerting Criteria, Environment Canada, (http://www.ec.gc.ca/meteo-weather/default.asp?lang=En&n=D9553AB5-1#blowingsnow (available on 15.03.2013)

Ferraro, G., Baschek, B., de Montpellier, G., Njoten, O., Perkovic, and M., Vespe, M. (2010) On the SAR derived alert in the detection of oil spills according to the analysis of the EGEMP. Marine Pollution Bulletin 60 (2010) 91–102

Fingas, M. F. (2011) “Introduction to Spill Modeling”. In Fingas, M. F. (Ed.), Oil Spill Science and Technology: Prevention, Response, and Clean-up (New York, Elsevier).

Fingas, M. F. and Brown, C. E. (1997) “Review of Oil Spill Remote Sensing”, Spill Science and Technology Bulletin, 4(4), pp. 199-208.

Fingas, M. and Brown, C. (2000) “A Review of the Status of Advanced Technologies for the Detection of Oil in and with Ice”, Spill Science and Technology Bulletin, 6(5/6), pp. 295-302.

Fingas, M. and Brown, C. E. (2011) “Oil Spill Remote Sensing: A Review”. In Fingas, M. F. (Ed.), Oil Spill Science and Technology: Prevention, Response, and Clean-up (New York, Elsevier).

Fingas, M. F.; Brown, C. E. and Gamble, L. (1999) “The Visibility and Detectibility of Oil Slicks and Oil Discharges on Water”, presented at the 22nd Arctic and Marine Oilspill Program (AMOP) Technical Seminar.

Fingas, M. F. and Hollebone, B. P. (2003) “Review of behaviour of oil in freezing environments”, Marine Pollution Bulletin, 47, pp. 333-343.

Fingas pers.comm., 2012

Gade, M.; Alpers, W.; Bao, M.; and Hühnerfuss, H. (1996) Measurements of the radar backscattering over different oceanic surface films during the SIR-C/X-SAR campaigns, Proceed. Intern. Geosci. Remote Sens. Sympos. (IGARSS)'96, IEEE, Piscataway, NJ, USA, 860-862.

Gade, M., and B. Baschek, (2013) “The German Operational Monitoring System in the Baltic Sea: Sensors, Methods and Example Data, in Oil Pollution in the Baltic Sea,” Kostianoy, A.G. and. Lavrova, O.Yu. (Eds.), Hdb Env Chem, DOI 10.1007/698_2011_130, Springer, Heidelberg, in press.

Gangeskar, R. (2004) Automatic oil-spill detection by marine X-band radars. Sea Technology, 45, pp. 40–45.

Goodman, R.H.(1978) "Review of ice movement buoys for tracking oil spills." Canada, ON, Environment Canada, 38 p.

Goodman, R. H. (1989) “Application of the Technology in North America”. In Lodge, A. E. (Ed.), The Remote Sensing of Oil Slicks (John Wiley and Sons, Toronto).

Goodman, R. (1994) “Overview and future trends in oil spill remote sensing”, Spill Science and Technology Bulletin 1, pp. 11 – 21.

Goodman, R. (2008) “Oil under Ice Detection: What is the State-of-the-Art?” In Davidson, W. F.; Lee, K. and Cogswell, A. (Eds.), Oil Spill Response: A Global Perspective (Springer).

Goodman, R. (2009) “Oil under Ice Detection,” Exploration and Production Oil and Gas Review. Touch Brifiengs, Vol. 7, No. 2, p. 142-147.

Hall, R. (2012) “ICEMAR,” presented at the 13th Meeting of the International Ice Charting Working Group (IICWG), Thirteenth IICWG Meeting, October 15-19, 2-012, Tromsø, Norway.

Hänninen, S. and Sassi, J. (2010) “Acute Oil Spills in Arctic Waters - Oil Combating in Ice.” Research report VTT-R-03638-09. VTT.

Halse, M. E.; Coy, A.; Dykstra, R.; Eccles, C.; Hunter, M.; Ward, R.; Callaghan, P.T.; (2006) A practical and flexible implementation of 3D MRI in the Earth’s magnetic field, Journal of Magnetic Resonance. Vol. 182 (1), pp. 75-83.

Hirst, W. and O’Connor, S. (2007) “Measurements of Methane Emissions from Oil Spill Experiments at Svea Test Site, Svalbard, April 2007”, report prepared for SINTEF JIP (Project 5) by Shell Exploration and Production, Rijswijk, Netherland and Shell Global Solutions, Thornton, Chester, England.

Hover, G. L. and Plourde, J. V. (1994) “Evaluation of Night Capable Sensors for the Detection of Oil on Water.” Report of COAST GUARD WASHINGTON DC OFFICE OF RESEARCH AND DEVELOPMENT. 83 p.

Hurford, N. and Buchanan I. (1989) “Results of the 1987 forties crude oil trial in the North Sea.” International Oil Spill Conference Proceedings: February 1989, Vol. 1989, No. 1, pp. 525-532.

Huppunen, J.; Putula, K.; Tenhu, H. and Helkala, T. (2012) “Soil Investigation with a Trained Dog”, presented at 4th Nordic Joint Meeting on Remediation of Contaminated Sites, Oslo, Norway.

Jensen, H.V.; Andersen, J.; Gyltnes, S. (2012) Norwegian oil spill response technology development," Presentation of Interspill, London, UK, 13-15th March 2012.

Jha, M.N.; Levy, J.; Gao, Y. (2008). “Advances in Remote Sensing for Oil Spill Disaster Management: State-of-the-Art Sensors Technology for Oil Spill Surveillance”, Sensors 2008, 8, pp. 236-255.

Johnson, B.; Joseph, R.; Nischan, M.L.; Newbury, A.B.; Kerekes, J.P.; Barclay, H.T.; Willard, B.C., Zayhowski, J.J., (1999) "Compact active hyperspectral imaging system for the detection of concealed targets." Proc. SPIE 3710, Detection and Remediation Technologies for Mines and Minelike Targets IV, 144 (August 2, 1999).

Knoll, J. (1985) "Visible fluorescence from ultraviolet excited crude oil," Applied Optics, Vol. 24, Issue 14, pp. 2121-2123.

Kozintsev V.I.; Orlov V.M.; Belov M.L.; Gorodnichev V.A.; Strelkov B.V. (2002) Optiko-elektronnye sistemy ekologicheskogo monitoringa prirodnoi sredy [Optical-electronic systems of environmental monitoring of the natural environment]. Moscow, Bauman MSTU Publ. 528 p. (in Russian)

Kudryavtsev, A. B. and Linert, W. (1996) Physico-Chemical Applications of NMR: A Practical Guide (New Jersey, World Scientific).

Lääperi, A. and Nyfors, E. (1983) “Experimental results from oil thickness measuremens with the microprocessor controlled microwave radiometer”, in the Proceedings of the International Geoscience and Remote Sensing Symposium, San Francisco, California, USA.

Legchenko, A. V.; Shushakov, O. A.; Perrin, J. A. and Portselan, A. A. (1995) “Noninvasive NMR Study of Subsurface Aquifers in France”, presented at SEG Annual Meeting, Houston, Texas.

Leifer, I.; Lehr, W. J.; Simecek-Beatty, D.; Bradley, E.; Clark, R.; Dennison, P.; Hu, Y.; Matheson, S.; Jones, C. E.; Holt, B.; Reif, M.; Roberts, D. A.; Svejkovsky, J.; Swayze, G. and Wozencraft, J. (2012) “State of the art satellite airborne marine oil spill remote sensing: Applications to the BP Deepwater Horizon oil spill”, Remote Sensing of Environment 124, pp. 185-209.

Liberty, L. M.; Bradford, J. H. and Brosten, T. R. (2006) “Acoustic imaging through sea ice”, presented at the SEG/New Orleans Annual Meeting, New Orleans, LA, USA.

Lobkovsky, L.; Kopelevich, O.; Kovachev, S. (2009) “Use of offshore oil platforms for environmental and geodynamic monitoring of the oil and gas reservoirs.” The 4th Norway – Russia Arctic Offshore Workshop on Joint Research and Innovation for the Petroleum industry working in the Arctic, Oslo, Norway, 17th – 18th June, 2009.

Lumex Ltd. (2012), “Optical detector of oil films,” Internet pamphlet (in Russian) at http://www.lumex.ru/equipment.php?id=43 (available on 20.12.2012).

McMahon, O. B.; Murphy, T. J. and Brown, E. R. (1997) “Remote measurement of oil spill thickness”, presented at the 4th International Conference on Remote Sensing for Marine and Coastal Environments, Orlando, Florida, USA.

MacNeill, M.R. and Goodman, R.H. (1987) "Oil monitoring during lead closure." Environmental Studies Research Fund, Report No. 053, National Energy Board, Calgary, AB, 13 p.

Minchew, B.; Jones, C.E.; Holt, B. (2012) "Polarimetric Analysis of Backscatter From the Deepwater Horizon Oil Spill Using L-Band Synthetic Aperture Radar," IEEE Transactions on Geoscience and Remote Sensing, vol.50, no.10, pp.3812-3830.

Miros (2012), “Oil spill surveillance by marine radar: Miros OSD - Oil Spill Detection System” www.miros.no/dynamisk/ftp/dokumenter/DB114ApplicationNoteOSD_S_utenmerker.pdf (available 20.12.2012)

MMS, Minerals Management Service, U.S. Department of the Interior, (2009) "Arctic Oil Spill Response Research and Development Program: A Decade of Achievement." WESTERN GRAY WHALE ADVISORY PANEL (WGWAP), 9th Meeting 4-6 December 2010.

Moeller-Jensen, P. (2006) “Method and apparatus for monitoring and measuring oil spills,” Patent # EP 1639387 A2 (US2004257264).

National Snow and Ice Data Center (NSIDC). (2012) Arctic Climotology and Meteorology: clouds. http://nsidc.org/arcticmet/factors/clouds.html (available 20.12.2012).

National Snow and Ice Data Center (NSIDC). (2013) Arctic Climotology and Meteorology: Precipitationhttp://nsidc.org/cryosphere/arcticmeteorology/factors_affecting_climate_weather.html#precipitation (available 12.03.2013).

Nedwed, T.; Srnka, L.; Thomann H. (2008) “Remote Detection of Oil Spilled under Ice and Snow using Nuclear Magnetic Resonance”, Proceedings of the AMOP Technical Seminar on Environmental Contamination and Response, Environment Canada, pp. 693 – 702.

Nedwed, pers. Comm. 2013

Nischan, M.L.; Joseph, R.M.; Libby, J.C.; and Kerekes, J.P. (2003) "Active Spectral Imaging." Vol. 14, No. 1, LINCOLN LABORATORY JOURNAL.

NOAA (2012) Open Water Oil Identification Job Aid for Aerial Observation with Standardized Oil Slick Appearance and Structure Nomenclature and Codes. Version 2, updated July 2012

NOFO (2009) NOFO Standard. Requirements for oil recovery vessels on the Norwegian Continental Shelf. Norwegian Clean Seas Association for Operating Companies 27 pp.

NORCOR Engineering Research Ltd. (1975) “The interaction of crude oil with arctic sea ice”, Beaufort Sea Project, Department of the Environment, Beaufort Sea Technical Report No. 27, Victoria.

O’Neil, R. A.; Neville, R. A. and Thompson, V. (1983) “The Arctic Marine Oilspill Program (AMOP) Remote Sensing Study”, Environment Canada Report EPS 4-EC-83-3.

OPTIMARE Product Sheet (2013) “MWR. Microwave Radiometer.” www.optimare.de/cms/fileadmin/PDF/GB_FEK/optimare_product_fek_mwr_120515pt.pdf (available on 01.03.2013)

Payne, J.R.; McNabb. Jr. G. D.; Clayton. Jr. J. R. (1991) "Oil weathering behavior in Arctic environments." In Sakshaug. E.. Hopkins. C. C. E. & Britsland. N. A. (eds.): Proceedings of the Pro Mare Symposium on Polar Marine Ecology. Trondheim. 12-16 May 1990. Polar Research (2), pp. 631-662.

Pelyushenko, S. A. (1995) “Microwave Radiometer System for the Detection of Oil Slicks”, Spill Science and Technology Bulletin, 2, pp. 249 – 254.

Plaza, J.; Pérez, R.; Plaza, A.; Martinez, P. and Valencia, D. (2005) “Mapping oil spills on sea water using spectral mixture analysis of hyperspectral image data”, in the Proceedings of SPIE Vol. 5995, Chemical and Biological Standoff Detection III.

Przybylak, R. (2003) "The Climate of the Arctic," Kluwer Academic Publishers, Norwell, MA, USA, 270 p.

Pohl, C.; Van Genderen, J. L.; (1998): Review article Multisensor image fusion in remote sensing: Concepts, methods and applications, International Journal of Remote Sensing, 19:5, pp. 823-854.

Potter, S.; Buist, I.; Trudel, K.; Dickins, D.F.; and Owens, E.H. (2012) Spill Response in the Arctic Offshore American Petroleum Institute and Joint Industry Programme on Oil Spill Recovery in Ice, 157 pp.

Robbe, N. (2012) Airborne Oil Spill Monitoring. Interspill2012 Spill Industry Seminar, London, UK, March 13th, 2012.

Robbe, N. and Hengstermann, T. (2008) "Airborne oil spill remote sensing: why multi-sensor technology is key for maritime surveillance," Hydro International, 12(3), pp. 10-13.

Robbe, N. and Zielinski, Z. (2004) "Airborne remote sensing of oil spills – analysis and fusion of multispectral near-range data" Journal of Marine Science & Environment. No. C2.

Robinson, J. N.; Coy, A.; Dykstra, R.; Eccles, C. D.; Hunter, M. W. and Callaghan, P. T. (2006) "Two-Dimensional NMR spectroscopy in Earth's magnetic field", Journal of Magnetic Resonance 182, pp. 343 – 347.

Safer, A. (2011). "Specialized Radar for Ice and Oil Spill Detection", Marine Technology Reporter, January/February 2011, pp. 14-17.

Salem, F. and Kafatos, M. (2001) "Hyperspectral Image Analysis for Oil Spill Mitigation," presented at the 22nd Asian Conference on Remote Sensing, Singapore.

Salem, F.; Kafatos, M.; El-Ghazawi, T.; Gomez, R.; and Yang, R.; (2002) "Hyperspectral Image Analysis for Oil Spill Detection," in Proceedings NASA/JPL Airborne Earth Science Workshop, Pasadena, CA, 2002.

Salisbury, J. W.; D'Aria, D. M; and Sabins, F. F. (1993) Thermal Infrared Remote Sensing of Crude Oil Slicks. Remote Sensing of Environment. 45, pp. 225-231.

Samberg A. (2007) "The state-of-the-art of airborne laser systems for oil mapping." Canadian Journal of Remote Sensing, 33(3): 143-149.

Shih, W. -C. and Andrews, A.B. (2008) "Infrared contrast of crude oil covered water surfaces," Optics Letters, 33(24): 3019-3021.

Skjelten, H.; Gutvik, C.; Solberg L.G.; (2011) "Ship based oil spill monitoring, a new integrated system for thickness estimation and operational overview," SETAC Europe 21st Annual Meeting. Ecosystem Protection in a Sustainable World: A Challenge for Science and Regulation.

Skou, N. (1986) "Microwave radiometry for oil pollution monitoring", IEEE Transactions in Geoscienec and Remote Sensing GE-24, pp. 360 – 367.

Ross, S.L. and Dickins D.F. (1987). Field Research Spills to Investigate the Physical and Chemical Fate of Oil in Pack Ice, Environmental Studies Revolving Funds Report No. 062.

SL Ross Environmental Research Ltd., DF Dickins Associates LLC., Envision Planning Solutions Inc. (2010) Beaufort Sea Oil Spills State of Knowledge Review and Identification of Key Issues. Environmental Studies Research Funds Report No. 177. Calgary. 126p.

Sobrino, J. A.; Jiménez-Muñoz, J. C.; Zarco-Tejada, P. J.; Sepulcre-Cantó, G.; de Miguel, E.; Sòria, G.; Romaguera, M.; Julien, Y.; Cuenca, J.; Hidalgo, V.; Franch, B.; Mattar, C.; Morales, L.; Gillespie, A.; Sabol, D.; Balick, L.; Su, Z.; Jia, L.; Gieske, A.; Timmermans, W.; Olioso, A.; Nerry, F.; Guanter, L.; Moreno, J.; and Shen, Q. (2009) "Thermal remote sensing from Airborne Hyperspectral Scanner data in the framework of the SPARC and SEN2FLEX projects: an overview," Hydrol. Earth Syst. Sci., 13, 2031-2037

Solberg, A.H.S. (2012) "Remote Sensing of Ocean Oil-Spill Pollution," *Proceedings of the IEEE*, vol.100, no.10, pp.2931-2945.

Solberg, A.H.S.; Storvik, G.; Solberg, R.; Volden, E. (1999) "Automatic detection of oil spills in ERS SAR images," IEEE Transactions on Geoscience and Remote Sensing vol.37, no.4, pp.1916-1924.

Solberg, A.H.S. (2006). "Data fusion for remote sensing applications", C.H. Chen (Ed.), *Signal and Image Processing for Remote Sensing*, CRC Press, Boca Raton, FL, pp. 515–537.

Solberg, A. H. S.; Brekke, C. and Hursøy, P. O. (2007) "Oil Spill Detection in Radarsat and Envisat SAR Images", IEEE Transactions on Geoscience and Remote Sensing, 45, 0196-2892.

Sørstrøm, S.E.; Brandvik, P.J.; Buist, I.; Daling, P.; Dickins, D.; Faksness, L.; Potter, S.; Rasmussen, J.F.; Singsaas, I. (2010) "Joint industry program on oil spill contingency for Arctic and ice-covered waters – Summary Report", SINTEF Materials and Chemistry, SINTEF, Oil in Ice – JIP, Report No. 32.

Svejkovsky, J. and Muskat, J. (2009) “Real-time Detection of Oil Slick Thickness Patterns with a Portable Multispectral Sensor.” Final Report for U.S. Minerals Management Service Contract 0105CT39144, 37 P.

Svejkovsky, J.; Lehr, W.; Muskat, J.; Graettinger, G.; Mullin, J. (2012). “Operational Utilization of Aerial Multispectral Remote Sensing during Oil Spill Response: Lessons Learned During the Deepwater Horizon (MC-252) Spill.” Photogrammetric Engineering and Remote Sensing 78(10), pp. 1089-1102.

Tarchi, D. (2005) Detecting and deterring illicit discharges. Satellite Monitoring and Assessment of Sea-based Oil Pollution, Istanbul, 13-14 June 2005

Tennyson, E.J. (1985) "Shipborne radar as an oil spill tracking tool," Proc. of the 11th Arctic and Marine Oilspill Program, Technical Seminar. Environment Canada, Ottawa, ON. p.385-390.

Topouzelis, K. N. (2008) “Oil Spill Detection by SAR Images: Dark Formation Detection Feature Extraction and Classification Algorithms”, Sensorsm, 8, pp. 6642 – 6659.

Trieschmann, O.; Hunsänger, Th.; Harjenbruch, U. (2001) “A multiple remote sensor system for the aerial surveillance of the north sea and Baltic sea”, presented at the 5th International Airborne Remote Sensing Conference, San Francisco, California, USA.

Tufte, L.; Trieschmann, O.; Hunsänger, T.; Kranz, S.; Barjenbruch, U. (2004) Using air- and spaceborne remote sensing data for the operational oil spill monitoring of the German north sea and Baltic Sea, XXth ISPRS Congress Technical Commission VII, ISPRS, July 12-23, 2004 Istanbul, Turkey, Archives – Volume XXXV Part B7.

Turner Designs Inc. (2012) “Application Note: Crude Oil”, retrieved from Turner Designs Inc. website: http://www.turnerdesigns.com/t2/doc/appnotes/S-0079.pdf

Van Zyl, J. and Kim, Y. (2011) Synthetic Aperture Radar Polarimetry (New Jersey, John Wiley & Sons).

Veprik, A.; Riabzev, S.; Avishay, N.; Oster, D. and Tuitto, A. (2012) “Linear cryogenic coolers for HOT infrared detectors”, in the Proceedings of SPIE Vol. 8353 Infrared Technology and Applications XXXVIII.

Wang, K.; Leppäranta, M.; Gästgifvars, M; Vainio, J. and Wang, C. (2008) “The drift and spreading of the Runner 4 oil spill and the ice conditions in the Gulf of Finland, winter 2006”, Estonian Journal of Earth Sciences, 57(3), pp. 181-191.

Wang, Z.; Stout, S. (2006) Oil Spill Environmental Forensics : Fingerprinting and Source Identification. Burlington, MA, USA: Academic Press. p 428.

Wang, X.; Key, J.; Liu, L.; Fowler, C.; Maslanik, J.; and Tschudi, M.; (2012) “Arctic Climate Variability and Trends from Satellite Observations,” Advances in Meteorology, vol. 2012, Article ID 505613, 22 pages.

Yapa, P. D. and Zheng, L. (1997) “Simulation of oil spills from underwater accidents I: Model development”, Journal of Hydraulic Research, 35(5), pp. 673-687.

Yapa, P. D.; Zheng, L. and Nakata, K. (1999) “Modeling Underwater Oil/Gas Jets and Plumes”, Journal of Hydraulic Engineering, 125(5), pp. 481-491.

Yarovenko, N. V.; del Carmen, M.; de la Cruz, M.; Vilas, L. G.; Zhang, B.; Perrie, W.; Li, X.; and Pichel, W. (2011) Oil Pollution Using Shipborne LIF/LIDAR. 5thEARSeL Workshop on Remote Sensing of the Coastal Zone 94 Prague, Czech Republic, 1st – 3rd June, 2011

Zhang, J. (2010) “Multi-source remote sensing data fusion: status and trends,” International Journal of Image and Data Fusion, 1:1, 5-24

APPENDIX A – SUPPLIERS AND STAKEHOLDERS

Company	Contact person	Contact Information	Expertise
Akvaplan Niva	Lionel Camus and Alexei Bambulyak	lc@akvaplan.niva.no; ab@akvaplan.niva.no	Satellite remote sensing, sampling with remotely operated vehicles, in-situ deployment of passive and integrating chemical and sedimentary sampling devices, video and camera data collection methods
APTOMAR	Magne Østby and Lars Solberg	magne.ostby@aptomar.com lars.solberg@aptomar.com	Softwares (SECurus) for detection, thickness measurement, exact plotting and drift estimate of the oil spill. SECurus system combines advanced stabilized long range and highly sensitive IR and digital video cameras
Blue Water Satellite	Tali Berzins	<http://www.linkedin.com/e/-j42pcd-h1tlityh-1x/pra/74362089/I134130788_50/EML_inml_rec_reply/?hs=false&tok=1B1pZXBpNDPIc1>	satellite imaging technology capable of detecting surface and sub-surface oil
C-CORE	Charles Randell	charles.randell@c-core.ca Phone: 709.864.8354 | Fax: 709.864.4706 Captain Robert A. Bartlett Building, Morrissey Road, St. John's, NL, Canada, A1B 3X5 www.c-core.ca	SAR/ optical satellite image processing for ice detection and classification, algorithm development for oil detection on water based on SAR.
CEDRE	Francois Merlin	francois.merlin@cedre.fr	Providing advice and expertise to the authorities responsible for responding to accidental pollution on national-level
CLS – Collect Localisation Satellites	Alexandre Salman	http://www.cls.fr; a.salman@es-pas.com	Oil slick detection using SAR images
Det Norske Veritas	Ole Øystein Aspholm and Tor Jensen	Ole.Oystein.Aspholm@dnv.com Tor.Jensen@dnv.com	Oil spill risk management
Environment Canada	Carl Brown and Bruce Hollebone	Carl.Brown@ec.gc.ca, Bruce.Hollebone@ec.gc.ca	Offers a wide rage of publications related to oil spills and pollution prevention

Company	Contact person	Contact Information	Expertise
Fugro EarthData, Inc	Edward Saade	Edward Saade President/Marketing Director Fugro EarthDate,Inc 7320 Executive Way, Frederick, MD 21704 +1 301 948 8550 +1 301 963 2064 (FAX) +1 858 945 5360 (cell) esaade@fugro.com www.fugroearthdata.com	Radar imaging from aircraft, processing satellite imagery
GAMMA Remote Sensing Research and Consulting AG		gamma@gamma-rs.ch	Provide consulting and processing services in the field of microwave remote sensing
Horizon GeoImaging, LLC		info@hgimaging.com	Provide digital imaging processing and analysis services
Itres		info@itres.com	Develops high-performance airborne hyperspectral and thermal imaging systems
Kongsberg Maritime	Oddbjørn Malmo	km.support@kongsberg.com	Provide acoustic products to monitor oil spills / distribution of oil flow, provide oil spill simulators
Kongsberg Satellite Services - KSAT	Richard Hall	Richard@ksat.no	Use SAR from satellite for detection of oil spills
Laser Diagnostic Instruments International Inc	Alexandre Vorobiev	vorobiev@ldi3.com	Provides Fluorescent LIDAR Systems (FLS) for airborne detection of oil Pollution
Liquid Robotics	Suneli Thomas or Scott Willcox	suneil.thomas@liquidr.com scott.willcox@liquidr.com	Oil spill detection, monitoring for post-oil-spill remediation
Lockheed Martin Corp	Douglas J. Dreyer	doug.dreyer@lmco.com	Supports data gathering over the oil spill using air borne platforms (P-3 Orion), which consist of SAR, IR and accoustic sensors
MDA	Bob Dams	Tel: +1 613-727-1087 xt. 248 BDAMS@mdacorporation.com Mob: +1 613-797-3415	Detect, quantify a track maritime oil spills using RADARSAT data and automated algorithms.

Company	Contact person	Contact Information	Expertise
MIROS AS	Mikael Rydberg	mr@miros.no	Use digitized sea surface images from standard marine X-band radars to detect oil spills. MIROS OSD (Oil Spill Detection) system is capable of automatic oil spill detection, with oil spill location, area and drift
Nansen Environmental and Remote Sencing Center - NERSC	Stein Sandven or Hanne Sagen	hanne.sagen@nersc.no	Conduct researchers on detection of oil spills using sattelite based SAR
NEOS Geosolutions	Dr. Alfredo Prelat	aprelat@neosgeo.com; 281-733-4095	Use ultra high-resolution images collected by fixed-wing aircrafts to detect the presence, extent and concentration of oil, as well as its effect on plants, soil and water quality.
NORBIT	Peter Koldgaard Eriksen	email: pke@norbit.no Phone: +1 (805)7083877	Use wide-band multibeam imaging echosounder to detect oil in the water volume; the sensor is designed to fit on a multitude of different platforms both stationary and moving.
Norconsult	Jørn Harald Andersen	jsa@norconsult.no	Provides consultancy services for oil detection
Norwegian Polar Institute	Dallmann Winfried	dallmann@npolar.no	Performing scientific research, mapping and environmental monitoring in the Arctic and Antarctica
Ocean Imaging	Jan Svejkovsky	Jan@oceani.com	Provides multispectral/thermal aerial oil mapping system to map oil distribution and thickness
Optimare		info@optimare.de	Provide airborne oil spill monitoring services, manufactures Airborne IR/UV line scanners and laser fluorosensors
Polaris	Ed Owens/Greg Challenger	eowensocc@aol.com	Provide technical and scientific support for oil spills. Aerial reconnaissance and videotape surveys and mapping, Cleanup and treatment guidelines and recommendations.
Poseidon Group AS	Jan Olav Hallset	jan.hallset@poseidon-subsea.com	Protection of Marine Environment and Preventing Marine Pollution, Collection of Marine Pollutants and Cleaning including oil spills
Prince William Sound Oil Spill Recovery Institute	Scott Pegau	wspegau@pwssc.org	Support research, education, and demonstration projects designed to respond to and understand the effects of oil spills in the Arctic and sub-Arctic marine environments

Company	Contact person	Contact Information	Expertise
Raytheon		products@raytheon.com	Develops versatile airborne radar (SeaVue) that offers inverse SAR imaging which is capable of oil spill detection. It also can be connected with unmanned aerial vehicles (UAV).
Reson	Peter Koldgaard Eriksen	pke@reson.com Mobile: +1 805 708 3877	Produces high resolution multi-beam sonar systems
Rutter Technologies Inc	Brian Johnston	bjohnston@rutter.ca	Detecting oil on water using microwave radar, Detecting Oil Using combined Radar and Infrared Sensors by Aptomar, Detecting Offshore Oil Spills with Rutter Technologies' Sigma S6 Radar Technology
Sea Consulting	Ann Hayward Walker	ahwalker@seaconsulting.com	Support oil spill management teams in Command, Operations, Planning (Environmental, Situation and Resource Tracking Units), Safety, Liaison, and Information Officer ICS functions.
Sea Hawk Navigation	Per-Arne Isaksen	postmaster@sea-hawk.no	Develop high performance polarimetric radars for oil spill detection.
SeaDarQ		info@seadarq.com	The SeaDarQ software can detect and monitor oil spills on the ocean surface by using a high resolution marine X-band radar.
Sintef	Per Daling/Per Johan Brandvik/ Alf G. Melbye	Alf.G.Melbye@sintef.no; Per.Daling@sintef.no; PerJohan.Brandvik@sintef.no	A research organization having high level of competence in variety of oil spill research areas
SLR International Corp	Lydia Miner	lminer@slrconsulting.com	International environmental consultancy that performs oil spill response and contingency planning
SL Ross	Steve Potter	Steve@slross.com	Spill related oil testing and oil spill modeling
SSC Airborne Systems	Olov Fast	olov.fast@sscspace.com Tel. 46 8 627 62 08	Develops MSS 6000 Airborne Maritime Surveillance System capable of detecting and tracking oil spills. MSS 6000 includes, IR/UV scanner provides high-resolution imagery of oil spills, A Laser Flourosensor, Microwave radiometer measures the extension and distribution of the oil, and a SLAR.

Company	Contact person	Contact Information	Expertise
SpecTIR	Conrad Wright	conrad@spectir.com	Provides airborne hyperspectral imaging sensors in SWIR and VNIR range (eg; AisaDUAL) as well as high performance thermal airborne hyperspectral sensors
Surrey Satellite Technology Limited (SSTL)		info@sstl.co.uk	Provides high performance space-borne SAR systems for oil spill monitoring (e.g., NovaSAR-S)
U.S. Army Corps of Engineers, Cold Regions Research and Engineering Laboratory (CRREL)	Leonard Zabilansky P.E. Research Civil Engineer	Cold Regions Research and Engineering Laboratory 72 Lyme Rd Hanover, NH 03755 Ph: 603-646-4319 FAX: 603-646-4477 Leonard.J.Zabilansky@usace.army.mil	Detection of oil under ice using airborne GPR and ice surface based GPR
Vissim	Knut Kildal Hansen	knutkh@vissim.no	Automatic oil spill detection based on raw video from commercial X-band marine radar
WET Labs, Inc., Narragansett, RI	Michael Twardowski	mtwardo@wetlabs.com	Produces fluorometers, scattering sensors